ONCOGENE INDUCED SENESCENCE via THE TYROSINE KINASE RECEPTOR ERBB2: CHARACTERISATION BY mRNA EXPRESSION ANALYSIS AND RAMAN MICRO-SPECTROSCOPY

DISSERTATION

ZUR ERLANGUNG DES AKADEMISCHEN GRADES DES DOKTORS DER NATURWISSENSCHAFTEN (DR. RER. NAT.) DER CHEMISCHEN FALKULTÄT DER TECHNISCHEN UNIVERSITÄT DORTMUND

VORGELEGT VON
LINDSEY MACCOUX, MSc.
AUS DEN USA

DORTMUND, GERMANY 2009

1. Gutachter: Prof. Dr. J.G. Hengstler
2. Gutachter: Prof. Dr. C.M. Niemeyer

SELBSTSTÄNDIGKEITSERKLÄRUNG

Hiermit erkläre ich, die vorliegende Dissertation selbstständig und ohne unzulässige fremde Hilfe angefertigt zu haben. Es wurden keine anderen Quellen genutzt als jene, die im Literaturverzeihnis angeführt sind. Sämtliche Textstellen, die wörtlich oder sinngemäß aus veröffentlichten oder unveröffentlichten Schriften entnommen wurden, sind als solche kenntlich gemacht. Ferner sind alle von anderen Personen bereitgestellten Materialien oder Dienstleistungen als solche gekennzeichnet. Ich versichere, nicht die Hilfe eines Promotionsberaters in Anspruch genommen zu haben. Zudem hat keine Person von mir geldwerte Leistungen für Arbeiten erhalten, die im Zusammenhang mit dem Inhalt der vorgelegten Dissertation stehen. Diese Arbeit wurde bisher weder im Inland noch im Ausland in gleicher oder ähnlicher Form einer Prüfungsbehörde zum Zwecke einer Promotion vorgelegt. Ich habe keine früheren erfolglosen Promotionsversuche unternommen.

Dortmund, 3.12.09

Lindsey J. Maccoux

I. Table of Contents

II. List of Figures

III. List of Tables

IV. List of Abbreviations

ACTB	β-actin
AR	Amphiregulin
bp	Base pair
BSA	Bovine Serum Albumin
BTC	Betacellulin
cDNA	complementary DNA
Ct	Cycle threshold
CCNB2	Cyclin B2
CCND1	Cyclin D1
CCNE1	Cyclin E1
CYCS	Cytochrome *c*, somatic
d	Day(s)
Dox	Doxycycline
DTT	2,3-Dihydroxy-1,4-dithiobutane
EGF	Epidermal growth factor
EPR	Epiregulin
ErbB-	Epidermal growth factor receptor family
ErbB1, EGFR, HER1	Epidermal growth factor receptor 1
ErbB2, HER2, Neu	Epidermal growth factor receptor 2
ErbB3, HER3	Epidermal growth factor receptor 3
ErbB4, HER4	Epidermal growth factor receptor 4
ERK	Extracellular signal-regulated kinases
FAM	6-carboxyfluorescein
FCS	Foetal calve serum
FRET	Fluorescence resonance energy transfer
g	Gram(s)
x g	gravitational force
HDM2	Human-MDM2
h	Hour(s)
HP-EGF	Heparin-binding epidermal growth factor receptor
l	Liter(s)
M-value	Endogenous reference gene stability measure
MAPK	Mitogen-activated protein kinase
MCF7	Human breast carcinoma cell line
MCF7/NeuT	Human breast carcinoma cell line transfected with ErbB2 rat-homolog NeuT
MCF7/EGFP	Human breast carcinoma cell line transfected with EGFP
MEK	Mitogen-activated protein kinase, kinase
min	Minute(s)
mRNA	Messenger RNA
NTC	No template control

NRG	Neuregulin
PI3K	Phosphoinositide-3-kinase
PIP2	Phosphatidylinositol-4,5-bisphosphate
PIP3	Phosphatidylinositol-3,4,5-trisphosphate
PKC	Proteinkinase C
PTTG1	Pituitary tumour transforming gene 1
PVDF	Polyvinyldifluoride
Raf	*Ras*-activator factor
Ras	Oncogene discovered in rat sarcoma
RT-qPCR	Real time-quantitative PCR
rtTA	Reverse tetracycline transactivator
SDS-PAGE	SDS-polyacrylamide gel electrophoresis
s	Second(s)
TaqPol	Thermo stable DNA polymerase
TBP	TATA binding protein
TEMED	N,N,N',N',-Tetramethylethylenediamine
TET	Tetracycline
TGF-α	Transforming growth factor-α
TRE	Tetracycline responsive element
UBC	Ubiquitin C
V-value	Pair-wise variation

V. Abstract

English Version:

Oncogenic-induced senescence is considered to be a primary fail-safe mechanism in tumourigenesis of breast cancer. The induction of senescence leads to many structural and metabolic changes as well as cell cycle arrest. Here, we investigated underlying changes that occur as proliferating cells enter senescence through upregulation of the receptor tyrosine kinase ErbB2. To study these changes, NeuT, an oncogenic rat homolog of the receptor tyrosine kinase ErbB2, was transfected into the breast carcinoma cell line MCF7 using a vector based on the Tet-ON system. Upon incubation of the MCF7/NeuT cells with the antibiotic doxycycyline, upregulation of ErbB2/NeuT was achieved.

We investigated the signalling pathways that are involved in driving cells into a senescent state including their downstream effects on cyclins in cell cycle regulation. The results presented in this thesis show that upon ErbB2 upregulation significant changes in the cyclin dependent kinase inhibitor p21 occurred along with changes in the tumour suppressor genes p53 and PTEN and a cell cycle regulator, cyclin B2. Additionally, the knockdown of p21 in the presence of overexpressing ErbB2 reconfirmed that the MCF7 cells were able to maintain a proliferating state and escape senescence. This was determined by the upregulation of cyclin B2.

Moreover, a newly discovered oncogene was investigated for a potential role in senescence since it is suggested by literature to be involved in cell cycle arrest pathways. This oncogene, pituitary tumour transforming gene 1 (PTTG1) was found to be downregulated in overexpressing ErbB2 samples. When PTTG1 expression was tested in p21 knockdown samples it revealed an upregulation in expression, indicating that PTTG1 may have a role in senescence and p21 regulation.

Finally, the novel technique Raman micro-Spectroscopy was used to gain further insight into oncogene-induced senescence. Raman micro-Spectroscopy revealed changes in cytochrome *c* expression upon ErbB2 overexpression which was then reconfirmed by immunofluorescence and Western blotting where a higher level of cytochrome *c* expression was also detected in ErbB2 overexpressing cells.

In conclusion, the data presented in this thesis identified the up- or downregulation in expression of known senescent and cell cycle biomarkers which can be used to characterise the MCF7/NeuT cells in a senescent cell model. It also reconfirmed the involvement of p21 in senescence through gene knockdown studies by analysing cell cycle biomarker expression changes and also the effects of p21 on a newly discovered oncogene PTTG1. Finally, the novel technique, Raman micro-Spectroscopy, proved to detect changes between non-senescent and senescent cells indicating its use for further investigation into cancer diagnostics and research.

German Version:

In der Tumorgenese des Brustkrebses wird die Onkogen-induzierte Seneszenz als fail-safe Mechanismus betrachtet. Die Induktion der Seneszenz führt zu zahlreichen strukturellen und metabolischen Veränderungen sowie zum Zellzyklus-Arrest der Zelle.
Es wurde untersucht, welche zellulären Veränderungen auftreten, wenn nach ErbB2-Überexpression eine proliferierende Zelle in den seneszenten Zustand übergeht.
Um diese Veränderung zu untersuchen, wurde die onkogene ErbB2-Variante NeuT in die Mammakarzinom-Zelllinie MCF7, unter Verwendung des Doxyzyklin-regulierbaren TET-On-Systems und den Konstrukten zur TET-induzierbaren Co-Expression von NeuT und EGFP exprimiert. Diese onkogene Form des ErbB2 trägt eine Punktmutation in der transmembranen Region, was zur Folge hat, dass es zu einer Liganden-unabhängigen Rezeptordimerisierung kommt und ErbB2/NeuT nach Doxyzyklin-Gabe überexprimiert wird.

In dieser Arbeit wurden Signalwege untersucht, die an dem zellulären Phänomen der Seneszenz beteiligt sind. Der Fokus wurde hier auf die Zellzyklus-regulierenden Cykline gerichtet.

Die Ergebnisse dieser Arbeit zeigen, dass nach ErbB2-Überexpression es zu einer signifikanten Expressionsveränderung von p21, ein cyklin-abhängiger Kinaseinhibitor (CDKI) kommt. Dies geht einher mit einer Veränderung der Tumorsuppressorgene p53 und PTEN, sowie dem Zellzyklus-Regulator, Cyclin B2. Des Weiteren wurde beobachtet, dass durch den gezielten Knockdown von p21 bei gleichzeitiger ErbB2-Überexpression die Zellen die Seneszenz umgehen und weiter proliferieren.
Darüber hinaus wurde beobachtet, dass dem neu entdeckten Onkogen PTTG1 (pituitary tumour transforming gene 1) eine potenielle Rolle in der ErbB2-induzierten Seneszenz zugeschrieben werden kann. Da es bei überexprimiertem ErbB2 zu einer Herunterregulation von PTTG1 kommt. Dagegen wurde beim Knockdown von p21 eine Hochregulation von PTTG1 detektiert. Diese Beobachtung lässt den Schluss zu, dass PTTG1 an der Seneszenz und der p21 Regulation beteiligt ist.

Zusätzlich wurde die Technik der Raman-Mikrospektroskopie eingesetzt, um weitere Einblicke in die Onkogen-induzierte Seneszenz zu bekommen. Mittels der Raman-Mikrospektroskopie wurden Unterschiede in der Cytochrom c Expression nach ErbB2 Überexpression detektiert. Diese Beobachtung wurde auch mit der Western Blot-Analyse und mit immunhistologischen Färbungen bestätigt.

Zusammenfassend, die in der Arbeit präsentierten Daten zeigen eine Hoch- oder Herunterregulation der Expression von bekannten Seneszenz und Zellzyklus-Marker nach ErbB2-Überexpression. Diese Marker dienen zur Charakterisierung der MCF7/NeuT-Zellen im seneszenten Zustand. Durch Knockdown-Studien von p21 konnte eine Expressionsveränderung der Zellzyklus-Marker gezeigt werden. Zusätzlich wurde die Raman-Mikrospektroskopie-Technik genutzt, um Veränderungen zwischen nicht seneszent und seneszenten Zellen näher zu charakterisieren.

CHAPTER ONE:
INTRODUCTION

1.0 Introduction

1.1 Epidermal Growth Factor Receptor Family

1.1.1 Development of the ErbB- Family

The epidermal growth factor (EGF) was isolated in 1962 by Stanley Cohen from the mouse submaxillary gland. It was named EGF because of it's ability to stimulate epithelial cells[1]. In 1975, the presence of a specific binding site for EGF was determined and the EGF-receptor (EGFR) was discovered by showing that EGF binds to the surface of fibroblasts[2]. Later, in 1978, EGFR was identified as a 170kDa protein that demonstrated an increase in phosphorylation when bound to EGF in the A431 squamous cell carcinoma cell line. It was not until the discovery in 1980, that the transforming protein of Rous sarcoma virus had tyrosine phosphorylation activity that led to the conclusion that EGFR is a tyrosine kinase activated by EGF[1]. ErbBs are considered to be typical receptor tyrosine kinases whose normal function is to mediate cell-cell interactions in organogenesis and adulthood[3]. Following the discovery of EGFR, three other receptors were discovered. Currently, the ErbB family consists of EGFR or ErbB1/HER1, ErbB2/HER2/Neu, ErbB3/HER3 and ErbB4/HER4. The ErbB family is found to be overexpressed in many cancer cell types that range from overproduction of ligands and receptors, or constitutive activation of receptors[4].

1.1.2 ErbB Family Receptor-Ligand Binding

Each 170kDa ErbB family receptor consists of three functional domains; an extracellular ligand-binding domain, a transmembrane domain and an intracellular tyrosine kinase domain (Figure 1)[5]. The extracellular ligand-binding domain has affinity to specific ligands for each ErbB receptor. The ErbB ligands can be classified into three groups: (1) ligands which specifically bind to ErbB1(EGF, amphiregulin (AR) and TGF-α); (2) ligands which bind to both ErbB1 and ErbB4 (betacellulin (BTC), heparin-binding EGF (HB-EGF) and epiregulin (EPR)); and (3) the neuregulins which bind to ErbB3 and ErbB4 (neuregulins 1 and 2 bind to ErbB3 and ErbB4 and neuregulins 3 and 4 bind to

ErbB4)[6]. No direct ligand has been found to bind to ErbB2. Studies suggest that the primary function of ErbB2 is to act as a coreceptor. ErbB2 is considered to be the preferred heterodimerisation partner for all other ErbB family members[7]. ErbB ligands generally act over short distances as autocrine or paracrine growth factors.

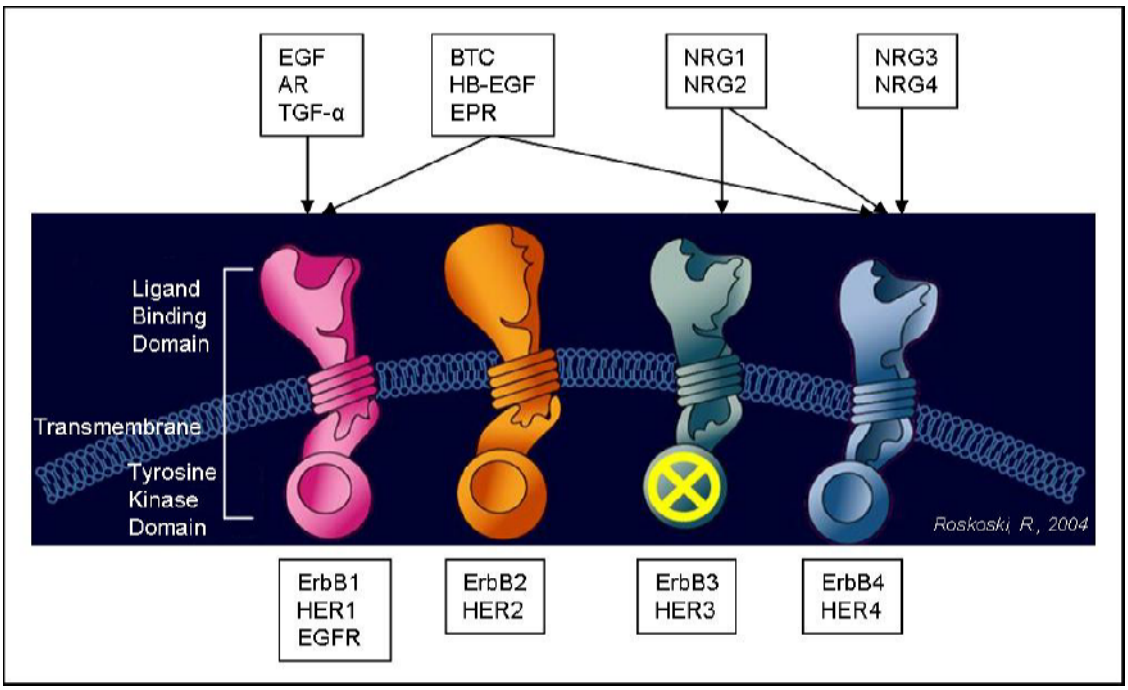

Figure 1: ErbB family receptors and their preferred ligands. Receptor activation domain consists of the ligand binding domain, the transmembrane domain and the tyrosine kinase domain. EGF, amphiregulin (AR) and TGF-α bind to ErbB1. Betacellulin (BTC), heparin-binding EGF (HB-EGF) and epiregulin (EPR) bind to ErbB1 and ErbB4. Neuregulins 1 and 2 (NRG1, NRG2) have affinity towards ErbB3 and ErbB4 and neuregulins 3 and 4 (NRG3, NRG4) bind to ErbB4 (picture derived from [5, 6]).

Crystallography studies of the extracellular domain revealed how dimerisation and activation is promoted by ligand binding[8]. Dimerisation occurs through ligand-induced receptor-receptor interactions using a 'dimerisation arm' in the cystine rich domain II at the dimer interface[9]. In the resting receptor (unliganded), the dimerisation arm is blocked intramolecularly by interacting with domain IV and thereby auto-inhibiting receptor dimerisation[10]. When the ligand becomes activated two distinct binding sites on the receptor bridge together (domains I and III) and induce domain rearrangement in the extracellular region of the receptor. This bridging of binding sites leads to homo- or heterodimerisation and trans-autophosphorylation of the intracellular tyrosine kinase domain (Figure 2)[11].

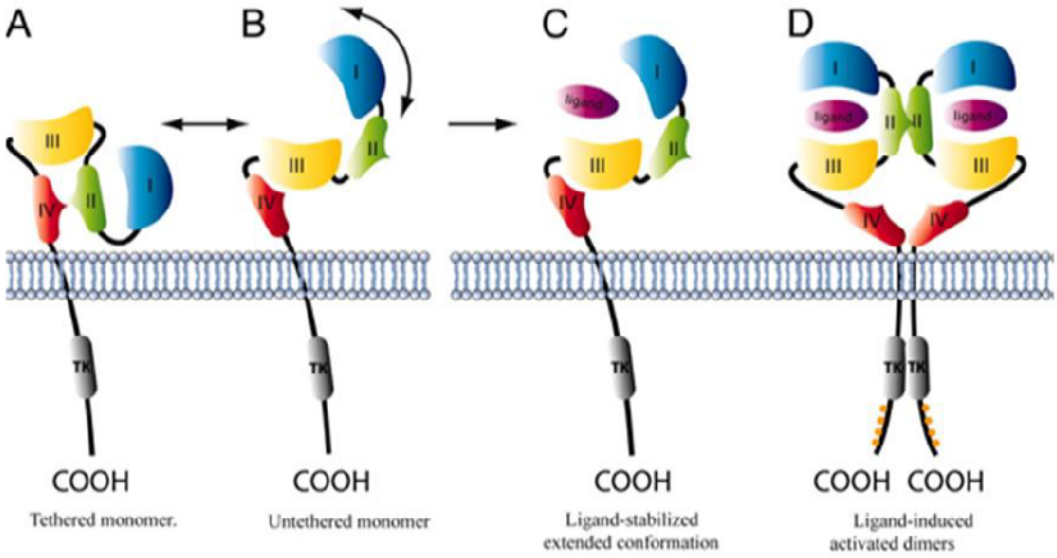

Figure 2: Ligand induced conformational changes in the EGF receptor extracellular domain. A) Unliganded EGFR exists in a tethered conformation where domains II and IV form an intramolecular interaction or tether, B) Unliganded molecules intramolecular interaction or tether is broken leaving EGFR to adopt an 'untethered' conformation, C) Ligand binds to specific untethered molecules and interacts simultaneously with domains I and III, stabilising the extended form and exposing domain II, D) Dimerisation is receptor mediated and dominated by domain II interactions. In the intracellular kinase domains the dimer-complex cross-phosphorylates residues in the C-terminal receptor tail (picture taken from [12]).

ErbB dimers formed are dictated by the ligand itself and the cell's balance of ErbB receptors[6]. Heterodimerisation of receptors follows a strict hierarchical principle with ErbB2 being the preferred dimerisation partner[4]. Figure 3 depicts the dimerisation combinations between all four of the receptors. ErbB3 homodimerisation leads to an inactive receptor due to an impared kinase on its tyrosine kinase domain. Homodimerisation of ErbB4 or ErbB1 leads to weak signalling. ErbB2 containing heterodimers exhibit increased ligand affinity that is associated with prolonged activation of downstream signalling pathways[13]. Signal diversification from the ErbB family members occurs by the differential transphosphorylation of a specific receptor in distinct ErbB dimers.

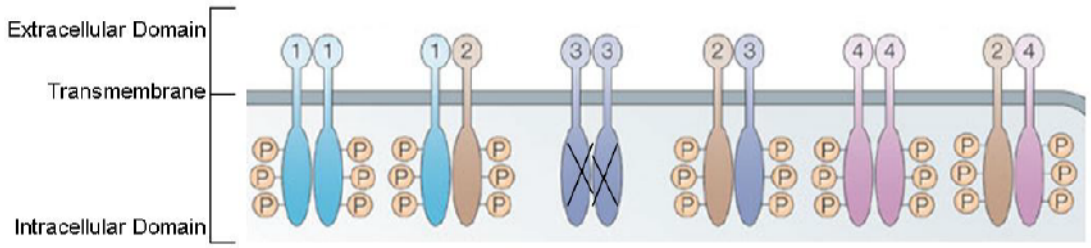

Figure 3: ErbB family receptor dimerisation partners. Ligand binding to ErbB receptors induces formation of receptor homo- and heterodimers and the activation by phosphorylation of specific tyrosine residues in the intracellular domain. ErbB3 has impared kinase activity, homodimerisation of ErbB1 or ErbB4 produce weak signalling while heterodimerisation of ErbB2 with the other receptor members produces strong signalling and is the preferred partner (picture taken from [14]).

1.2 Signalling Pathways of ErbB- Family Members

The signalling pathways of ErbB family receptors can be divided into three layers: (1) input layer; (2) signal processing layer; and (3) output layer (Figure 4). The input layer, is the ligand-receptor binding process where upon ligand binding the tyrosine kinase domains within the intracellular area of the receptor become phosphorylated. The sites to be phosphorylated on the kinase domain are determined by the identity of the ligand and the dimer partners. This phosphorylation marks the beginning of the signal processing layer. The signal processing layer begins with the activation of the adaptor/enzyme proteins such as Shc, Grb, and SOS this depends on the phosphorylation site on the tyrosine kinase domain. Next, activated adaptor/enzyme proteins stimulate multiple kinase pathways through *Ras* activation. The *Ras* activation leads to simultaneous activation of linear cascades such as protein kinase C, Akt and MAPK pathways where they converge to the nucleus and then diverge into distinct transcriptional messages. These distinct transcriptional messages are then relayed to the output layer. The output layer provides information for the cell that ranges from cell division and migration to adhesion, differentiation and apoptosis. This again all depends on the specific ligand and dimer-dimer formation. For example, the ErbB2-ErbB3 heterodimer increases cell motility[15] and transformation[16].

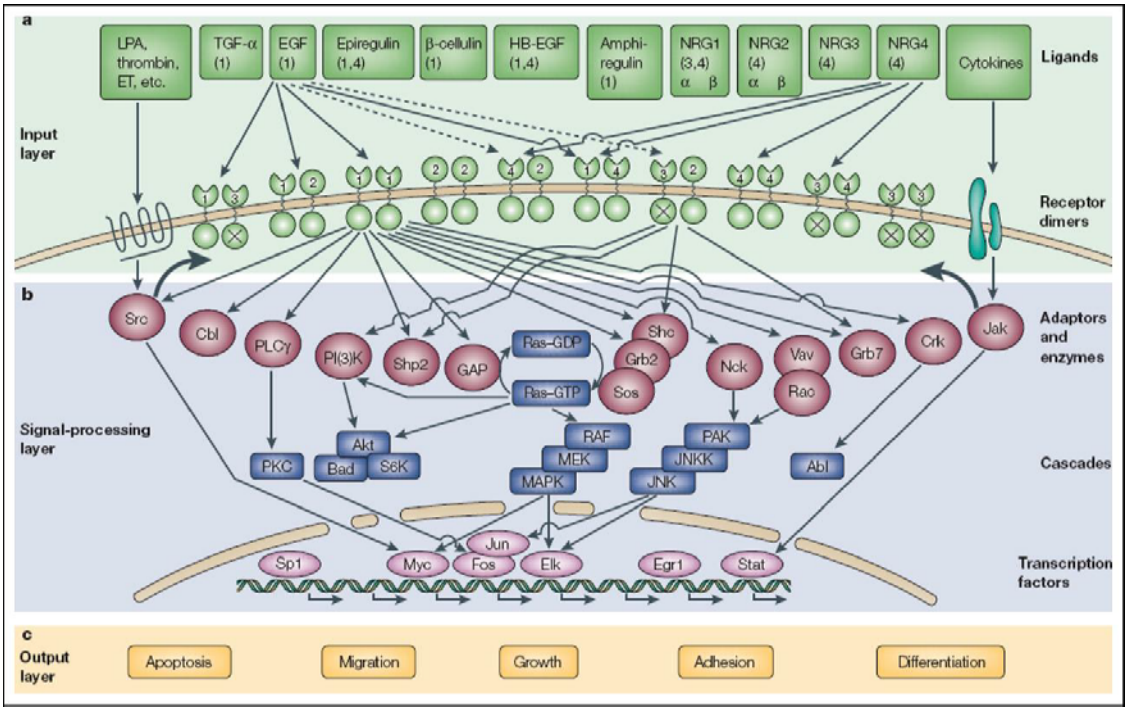

Figure 4: ErbB family receptor signalling network. The signalling network can be divided into three layers; 1) Input layer, 2) Signal-processing layer, and 3) Output layer. A) Ligands and the ten dimeric receptor combinations which comprise the input layer. Ligand affinity depends on the dimer-dimer combination. B) Signalling to the adaptor/enzyme layer is the first step in signal processing this then leads to kinase cascade activation and eventually activation of multiple transcription factors. C) The input and signal processing is then translated into the output layer which could lead to a combination of cell division and migration to adhesion, differentiation and apoptosis. Output response is dependent on initial input from the ligand-receptor activation. Raf-MEK-MAPK and PAK-JNKK-JNK shown here are two cascades of serine/threonine kinases that regulate a number of transcription factors (picture taken from [4]).

1.3 Tyrosine Kinase Receptor ErbB2/HER2 (NeuT)

The tyrosine kinase receptor, originally called Neu was derived from rat neuro/glioblastoma cell lines in 1985[17] encoding a tumour antigen, p185, which was found to be related to EGFR. In the same year, a potential cell surface receptor of the tyrosine kinase gene family was identified and characterised by cloning the gene[18]. The sequence was very similar to that of the human EGFR. Therefore, due to this close similarity, the authors named the gene HER2. ErbB2 is localised to chromosome 17q21.1. In 1986, Akiyama and colleagues raised antibodies against a synthetic peptide that corresponded to 14 amino acid residues at the carboxyl terminus of a protein suspected to be derived from the ErbB2 nucleotide sequence[19]. They were then able to

precipitate ErbB2 gene product from adenocarcinoma cells, revealing the ErbB2 protein to be 185kDa with tyrosine kinase activity.

After the discovery of the gene and protein, ErbB2's function was assessed. In 1989, it was discovered that ErbB2 played a role in breast and ovarian cancer which combined account for one-third of all cancers in woman and approximately one-quarter of cancer related deaths in females[20]. In 1997, evidence showed that HER2 may be involved in chemotherapy resistance in breast and ovarian cancer[21]. Besides its involvement in cancer, ErbB2, has been found to be involved in neuromuscular junction development[22], muscle regeneration[23] and cardiomyopathy[24]. An activated mutant form of ErbB2 is rarely found in human cancers. Although important in development and cell proliferation and generation, the wildtype ErbB2 is overexpressed and/or amplified in 30% of breast cancers correlating to chemoresistance and poor prognosis. Recently, a new trend in ErbB2 overexpression studies is its involvement in oncogenic-induced senescence as a premature fail-safe mechanism where upon *Ras* activation drives breast cancer cells into senescence rather than proliferation[25].

1.4 ErbB2 Signalling Cascade

Upon ligand binding and dimerisation of ErbB2, tyrosine residues in the intracellular domain of the receptor are phosphorylated. This then leads to multiple signalling cascades within the cytoplasm and nucleus (Figure 5). As mentioned above, the recruitment of the adapter proteins Shc, Grb and SOS to the phosphorylated tyrosine kinase domains lead to recruitment and activation of *Ras* this then leads to the phosphorylation of other proteins eventually leading to transcription and translation of proteins involved in cell proliferation and differentiation, and apoptosis. Aside from *Ras* recruitment and activation, a second pathway is also activated upon phosphorylation of the tyrosine kinase domain. The phosphoinositide-3-kinase (PI3K) is also recruited to the phosphorylated site of the tyrosine domain and in turn activates the Akt pathway which leads to cell adhesion and migration. The following two subsections will discuss the activation of these two pathways.

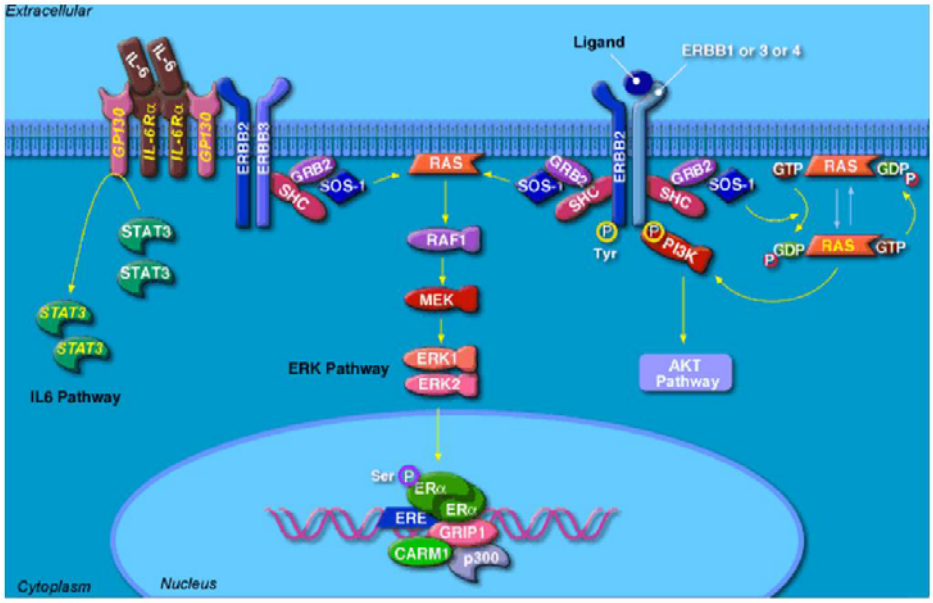

Figure 5: ErbB2 signalling pathways upon activation. Phosphorylation of the tyrosine kinase domain in the intracellular portion of the receptor leads to two main signalling cascades, the *Ras*/MAP and PI3K/Akt pathways which lead to cell proliferation, differentiation, adhesion and migration (picture taken from www.nci.gov).

1.4.1 *Ras*-MAP Signalling Pathway

The *Ras* signalling pathway is a very potent cell signalling pathway. It is considered to be more mitogenic than any other oncogene and the prevalence of *Ras* mutations is seen in approximately 20% of all tumours[26]. Activation begins by the binding of the adapter protein complex Grb2-SOS to the phosphotyrosine on ErbB2 (Figure 6). This then activates the small G-protein *Ras* by facilitating the exchange of guanosine diphosphate (GDP) for guanosine triphosphate (GTP), creating a conformational change in *Ras* allowing *Ras* to bind to Raf-1 recruiting it from the cytosol to the cell membrane where Raf-1 activation takes place. Multiple processes need to occur for Raf-1 activation, the dephosphorylation of inhibitory sites by protein phosphatise 2A (PP2A) as well as the phosphorylation of activating sites by PAK, Src and other unknown kinases. Once Raf-1 is activated it phosphorylates and activates MEK (MAPK) kinase which then phosphorylates and activates extracellular-signal-regulated kinase (ERK). This three-tiered kinase cascade is scaffolded by kinase suppressor of *Ras* (KSR). Activated ERK has many substrates within the cytosol such as phospholipase A2, tyrosine kinase

receptors, oestrogen receptors, and activator of transcription proteins[27]. ERK also has the ability to enter the nucleus to control gene expression by phosphorylating transcription factors such as Elk-1, c-myc and c-jun[28]. The activated *Ras*-MAP kinase signalling pathway is one of the main pathways for cell signalling and proliferation.

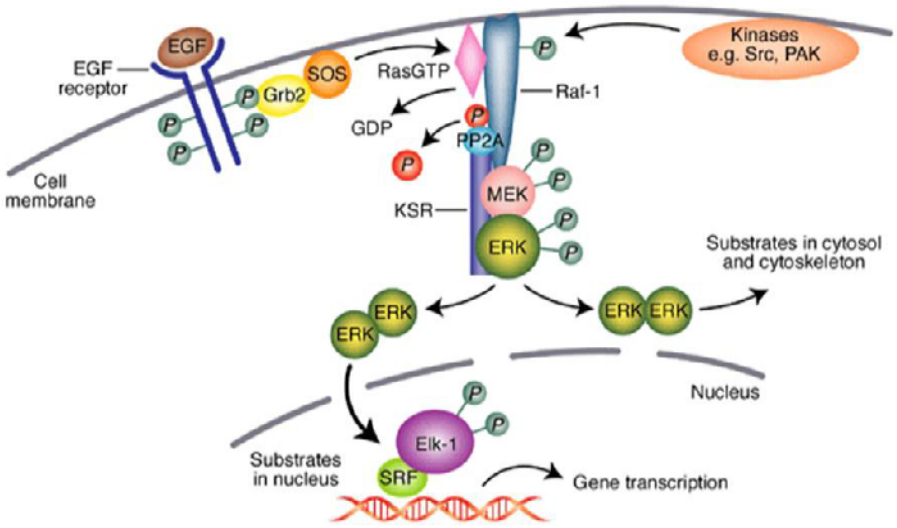

Figure 6: Ras-Raf-MEK-ERK signalling pathway. The activation of *Ras* by phophorylated residues on the tyrosine kinase domain of ErbB2 results in a highly potent signalling cascade that eventually leads to cell proliferation, differentiation or apoptosis (picture taken from [28]).

1.4.2 PI3K/Akt Signalling Pathway

Phosphatidylinositol 3-kinase (PI3K) is the second important pathway upon ErbB2 phosphorylation. PI3K/Akt signalling pathway is initiated when PI3K binds to phophotyrosine residues in the tyrosine kinase domain of ErbB2 (Figure 7). Phosphorylated PI3K, phosphorylates the lipid second messenger phosphatidylinositol 4,5- bisphosphate (PIP2) into phophatidylinositol 3,4,5-triphosphate (PIP3). PIP3 then recruits and activates phosphatidylinositol dependent kinase 1 (PDK1). PDK1 phosphorylates and activates protein kinase B (Akt/PKB). Upon Akt activation, it inhibits forkhead (FoxO) transcription factors resulting in cell proliferation and survival[29]. The tumour suppressor phosphatase with tensin homology (PTEN) negatively regulates PI3K by dephosphorylating PIP3 into PIP2. Activated Akt also inhibits tuberous sclerosis 1 and 2 (TSC1 and TSC2 respectivly) allowing for mTOR

activation and cell growth[30]. The activation of the PI3K/Akt leads to cell proliferation and is of particular interest in tumour metastasis[31, 32].

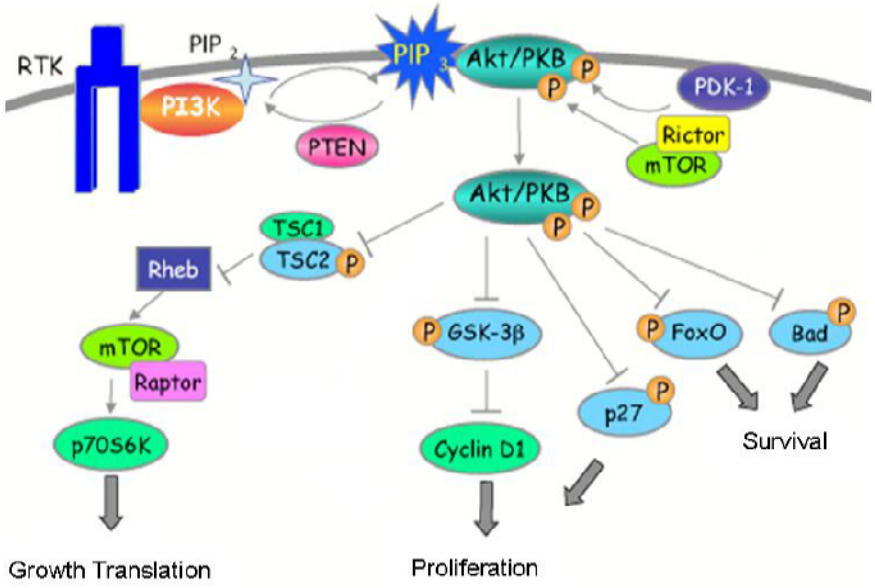

Figure 7: PI3K/Akt signalling pathway. The PI3/Akt signalling pathway begins with PI3K activation by phosphotyrosine residues on ErbB2. This activation leads to a signalling cascade which activates Akt and other cell promoting proteins.

1.5 ErbB2/HER2 (NeuT) and Cancer

The tyrosine kinase receptor ErbB2 is overexpressed in 15-30% of invasive ductal breast cancers. This overexpression correlates with tumour size, tumour spreading to lymph nodes, higher percentage of cells in the S-phase, aneuploidy and lack of steroid hormone receptors[33]. It is found to be overexpressed in multiple cancers, including breast, lung, pancreas, colon, oesophagus, endometrium and cervix. ErbB2 overexpression triggers ligand independent activation of the kinase domain resulting from spontaneous dimer formation. Although, ErbB2 undergoes spontaneous dimer formation, observations have suggested that ErbB2 cooperates with other ErbB receptors during tumour development. For example, ErbB2 has been known to associate with ErbB1 where by inhibiting ErbB2, tumour cells displaying ErbB1 autocrine activation were no longer able to proliferate[34]. Interestingly, ErbB2 overexpression is found in early forms of breast cancer relative to advanced and invasive carcinomas. This suggests that alterations in ErbB2 activity alone

are not sufficient for breast tumour progression. Many ErbB2 overexpressing tumours do not express oestrogen and progesterone receptors depicting an inverse relationship between steroid hormones and the ErbB network. An *In vitro* study has suggested that overexpression of ErbB2 shows resistance to anti-oestrogens and develops cancer cells independent of oestrogen[35]. However, oestrogen has been found to suppress transcription of the ErbB2 promoter inhibiting growth of ErbB2 overexpressing cells[36]. It can be implied then that there is a functionally linked pathway between steroids and ErbB2 pathways that warrant cell proliferation in carcinogenesis. Therapies are being developed to alleviate some of the potent effects that ErbB2 and the other family members have on tumour metastasis and development. One cancer therapy of particular interest is the antibody against ErbB2 called Herceptin®. Herceptin® works by binding to ErbB2 surface receptors to inhibit autodimerisation and also through inducing the cylin dependent kinase inhibitor p27 and its Rb-related protein p130 which reduces the number of cells in S-phase[37].

1.6 Conditional Upregulation of ErbB2 in a TET-System

Many transgenic inducible systems are currently available, the ecdysone-regulated gene switch[38, 39], the lac-operator-repressor system[40], and the inducible GAL4/UAS system[41]. However, the most widely used transgenic inducible system was developed by Gossen and colleagues in 1992[42] which is the tetracycline controlled transcriptional activation system used to investigate the function and regulation of a variety of genes under physical and pathological conditions. The inducing agent doxycycline is used to control gene expression in either a Tet-ON or Tet-OFF system. The Tet-ON system which will be discussed below is used to enhance expression of a particular gene of interest where the Tet-OFF system is used to silence a gene of interest. There are many types of inducible systems being used in research and although the components and structures are different, the principle and function of the system is contiguous. Three parts are needed for a fully functioning transgenic system; a regulatory unit, a responsive element linked to the target gene, and an inducing agent[43]. Combing these three parts

with a specific promoter, the transgenic system should be able to provide temporal and spatial control over expression of gene of interest.

1.6.1 rtTA-System (TET-ON)

The reverse tetracycline-controlled transcriptional activator system (rtTA) is generated by fusing the DNA-binding domain of a mutant tetracycline repressor which is encoded in *E.coli* with the transcription activation domain of virion protein 16 of herpes simplex virus (VP16)[42] to form rtTA. The second construct involved contains the target gene under control of a minimal promoter sequence of the human cytomegalovirus promoter IE combined with the responsive element a tet operator sequence from *E.coli*[43]. In the absence of doxycycline the continuously expressed rtTA is unable to bind to the tetracycline response element (TRE) and therefore, no target gene is transcribed (Figure 8). In the presence of doxycycline, the rtTA is able to bind to the TRE due to a conformational change of the rtTA from binding to doxycycline and in turn activates the gene of interest. The induction of the gene of interest occurs within minutes or a few hours in certain systems[43]. Due to the use of the well-understood and inexpensive inducing agent doxycycline, Tet-based systems are steadily becoming the ideal inducible transgenic system of choice.

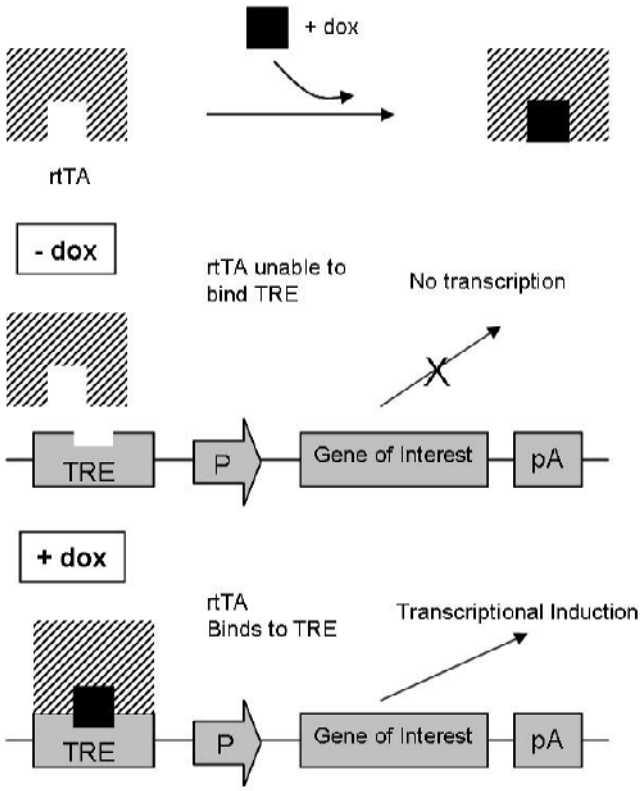

Figure 8: A Tet-ON Tetracycline-controlled transcriptional regulation system. The continuously expressed reverse tetracycline-controlled transcriptional activator (rtTA) makes a conformational change in the presence of doxycycline (dox) enabling the rtTA to bind to the tetracycline response element (TRE) activating the gene of interest.

1.7 Oncogene-induced Senescence via Ras Activation

As mentioned above, the oncogene *Ras* represents the 'Gold Standard' for oncogenes and when activated is more oncogenic than any other oncogene[44]. *Ras* mutations in human tumours represent approximately 20% of all tumours. The oncogene *Ras* is at a pivotal point for most mitogenic extracellular stimuli. As extracellular signals activate *Ras* and multiple intracellular signals diverge from *Ras*. This divergence allows *Ras* to activate signalling pathways that are implicated in cell proliferation and survival[45]. However, *Ras* is a double-edge sword, in that it can initiate cell proliferation but it can also initiate cell cycle arrest. Initial effect of oncogenic *Ras* in normal cells is to promote proliferation but aberrant proliferation is not sustained and after a few doublings, cells enter a premature cell cycle arrest with senescence characteristics[46]. *Ras* induced

senescence is accompanied by the upregulation of $P16^{INK4a}$ and $P19^{ARF}$ (human form is $P14^{ARF}$) and as a result activates Rb and P53 which then stimulates $P21^{Cip1}$ expression driving the cells into cell cycle arrest[47-50]. A neoplastic transformation by *Ras* supersedes only when the balance between senescence and proliferation is broken. Interestingly, murine fibroblasts deficient in $P16^{INK4a}$ and $P19^{ARF}$alone, or P53 showed direct transformation by *Ras*[51]. This induction of senescence via oncogenic *Ras* upregulation indicates that senescence is a programmed cellular response which is triggered by proliferative stresses and not accumulation of cell doublings reinforcing that senescence may have an anti-tumourigenic role. These next few sections will discuss three known pathways triggered by *Ras* which regulate cellular senescence or immortalisation. This includes the PTEN/$P27^{Kip1}$, $P16^{INK4a}$/Rb, and $P14^{ARF}$/P53/$P21^{Cip1}$ pathways [44, 52, 53].

1.7.1 PTEN/$P27^{Kip1}$ Pathway

PTEN is a newly discovered tumour suppressor. It was defined as a tumour suppressor when researchers began to realise its influence on PI3 kinases (PI3K)[54]. PTEN is a phosphatase that catalyses the conversion of 3,4,5-trisphosphate (PIP_3) into PIP_2 which opposes the effects of PI3K. PI3K phosphorylates PIP_2 into PIP_3 which goes on to phosphorylate and activate Akt/PKB increasing cell proliferation. The overexpression of PTEN results in the upregulation of the cyclin dependent kinase inhibitor $P27^{Kip1}$ (Figure 9). The upregulation of $P27^{Kip1}$ was found to be a response to decreased PIP_3 levels and occurs by protein stabilisation[55]. $P27^{Kip1}$ is destabilised by phosphorylation and recognition of an ubiquitin ligase in which Akt/PKB could be responsible for the phosphorylation and destabilisation[44]. Interestingly, Tresini et al found that human fibroblasts treated with PI3K inhibitors reduced the lifespan of cells giving rise to early onset of senescence[56] which correlated with the notion that upon PI3K depletion $P27^{Kip1}$ becomes elevated. However, it still remains to be established if this is a direct refection of the balance between PTEN and PI3K. The significance of the PTEN/$P27^{Kip1}$ pathway makes it of important interest when investigating senescence and its relation to tumourigenesis.

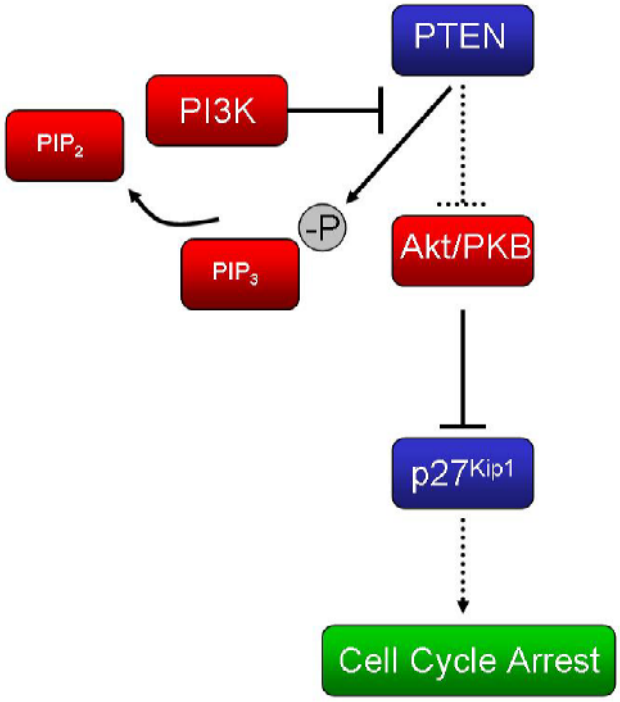

Figure 9: The PTEN/P27^{Kip1} pathway. PTEN catalyses the conversion of PIP_3 into PIP_2 inhibiting the activation of Akt/PKB and increasing expression of P27 ^{Kip1}.

1.7.2 P16^{INK4}/Rb Pathway

The retinoblastoma tumour suppressor protein (Rb) in its unphosphorylated form associates with multiple transcription factors involved in cell proliferation silencing their transactivation abilities. In particular, the transcription factor family of E2F proteins which are important for cell cycle progression where upon release from Rb activate the upregulation of cyclins E and A through DNA synthesis[57]. To maintain Rb in its unphosphorylating and cell cycle arresting state, the INK4 cyclin dependent kinase inhibitor P16 inhibits cyclin dependent kinases 4 and 6 (CDK4-6) as CDK 4-6 phosphorylates Rb allowing for the release of cell cycle promoting transcription factors (Figure 10). CDK 4-6 binds to and activates cyclin D1 which is essential for progression from the G0- to G1-phase leading up to the S-phase in the cell cycle. When the P16 ^{INK4a}/Rb pathway is lost or inhibited cyclin D1 was found to be overexpressed[58]. Altogether, the establishment of cell cycle arrest through P16 ^{INK4a} activation requires Rb[44]. This pathway is found to be deregulated in multiple human tumours.

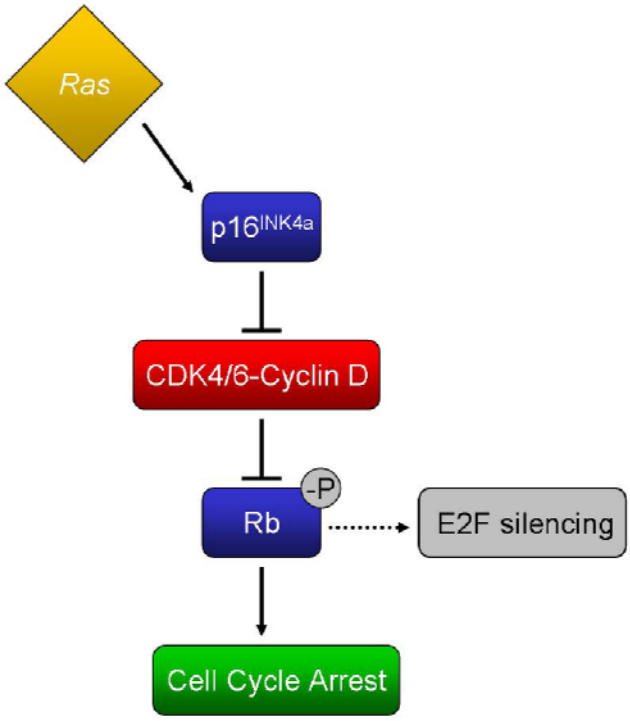

Figure 10: The $P16^{INK4a}$/Rb pathway. Upregulation of the cyclin dependent kinase inhibitor $P16^{INK4a}$ allows for Rb to remain in its unphosphorylated state bound to the transcription factor E2F preventing cell cycle progression.

1.7.3 $P14^{ARF}$/P53/$P21^{Cip1}$ Pathway

It is widely known that the tumour suppressor P53 is inactivated in approximately half of all human cancers and is involved in multiple cellular functions ranging from cell migration and proliferation to cell cycle arrest and apoptosis. Activation of P53 requires post-translational modifications which include phosphorylation and acetylation resulting in a half-life of hours and a conformation suitable for DNA binding and transactivation[59]. There are several downstream targets of P53; Fas and Bax which are involved in apoptosis and PAI which is involved in metastasis and angiogenesis inhibition and also of particular interest in senescence, $P21^{Cip1}$. The $P14^{ARF}$/P53/$P21^{Cip1}$ pathway is of particular interest in oncogene-induced cellular senescence as with the inhibition of P53 or $P21^{Cip1}$ cells do not enter senescence[25, 60]. The pathway is initiated upon *Ras* activation by an external stimulus such as tyrosine kinase activation. *Ras* then activates $P14^{ARF}$ which inhibits the ubiquitin ligase E3-type enzyme, HDM2

(MDM2 is the mouse form) from degrading P53 protein. Therefore, the overexpression of $P14^{ARF}$ allows for the stabilisation of P53 and the progression of upregulating downstream targets. $P21^{Cip1}$ is then activated by P53 and blocks cyclin dependent kinase 2 expression which is responsible for the activation of cyclin E1 for cell cycle progression from the G1- to the S-phase. This block in progression to the S-phase leads then to cyclin B2 downregulation which is involved in carrying the cell cycle from G2- to M-phase and eventually arrests cells in a senescence-like state (Figure 11). In summary, the induction of cell cycle arrest by $P14^{ARF}$ requires the functional activity of P53, having $P21^{Cip1}$ as one of its main targets, when either of these proteins are inactive tumour development persists.

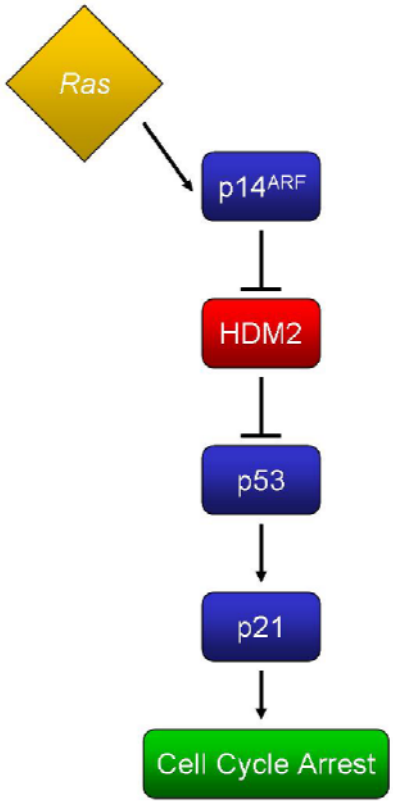

Figure 11: $P14^{ARF}$ /P53/ $P21^{Cip1}$ pathway. Upregulation of the cyclin dependent kinase inhibitor $P14^{ARF}$ results in upregulation of P53 which targets upregulation of multiple genes including $P21^{Cip1}$.

1.8 Pituitary Tumour Transforming Gene 1 (PTTG1) and Cancer

The pituitary tumour transforming gene 1 (PTTG1) was first isolated from rat pituitary tumour cells in 1997 by Pei and Melmed[61] and was later identified as a vertebrate securin that regulates sister-chromatid separation[62]. PTTG1 functions in cell replication[62], cell cycle control[63], DNA damage/repair[64], cell transformation[65] and cellular senescence[66]. It is considered an oncogene because of its effects on tumour development and growth. PTTG1 is expressed in multiple cancer cell lines such as colorectal adenocarcinoma cells SW480, lung carcinoma cells A549 and hepatoma cells HepG2[67] as well as breast cancer cells MCF-7[68]. Multiple mechanisms have been proposed for PTTG1 involvement in cancer development. As a transcription factor it can directly and indirectly induce expression of genes involved in regulating tumourigenesis[69]. PTTG1 has been found to interact with P53 by inducing its expression[70] which was confirmed in MCF-7 cells[71]. The PTTG1-P53 interaction thereby has the possibility to affect downstream targets of P53 such as P21. Chesnokova and colleagues found that upon P21 depletion PTTG1 expression is restored indicating a connection between P21 overexpression and PTTG1 regulation[66]. Interestingly, Chesnokova also found that mice double negative to PTTG1 had higher levels of P21 expression compared to mice expressing PTTG1[72] when entering senescence. Evidence is continually suggesting that PTTG1 may be a biomarker in cancer metastasis and treatment outcome warranting further investigation into the role of PTTG1 at both the transcription and epigenetic levels.

1.9 Aims

Oncogenic induced senescence is a well known phenomenon. However, the mechanisms leading up to senescence and its purpose in cancer are not well understood. Using a Tet-ON system transfected into the breast carcinoma cell line MCF7 to overexpress the rat-homolog of ErbB2, NeuT; this work will attempt to characterise senescent signalling pathways by investigating select senescent biomarkers over a time course study. Inhibition of the P53 downstream target P21 will also be analysed and downstream cyclin targets of P21 will be examined. Additionally, the newly discovered tumourigenesis

biomarker PTTG1 will be investigated to determine its role in oncogene induced senescence. Finally, a novel technique, Raman micro-Spectroscopy will be explored to analyse cytochrome *c* expression in oncogene-induced senescence via NeuT overexpression.

CHAPTER TWO:
MATERIALS AND METHODS

2.0 Materials and Methods

2.1 Materials

2.1.1 Chemicals

Acrylamide 30%	Carl Roth
Ammonium chloride	Roth
Ammonium persulfate, for electrophoresis	Sigma
Bromophenol blue, ACS	Carl Roth
BSA (Albumin Fraction V)	Carl Roth
Buffer Concentrate A and K, for electrophoresis	Carl Roth
2,3-Dihydroxy-1,4-dithiobutan (DTT)	Carl Roth
DMEM, high glucose, culture medium	PAN BioTech
Doxycycline hyclate	Sigma Aldrich
Ethanol, absolute	Carl Roth
FCS, tetracycline-free	PAN BioTech
Formaldehyde	Roth
Glycerol, for electrophoresis	Carl Roth
Glycine, for electrophoresis	Carl Roth
Hydrochloric acid, molecular grade	Carl Roth
Isopropanol, absolute	Carl Roth
2-Mercaptoethanol	Carl Roth
Methanol, HPLC gradient grade	Carl Roth
Opti-MEM® I medium	Invitrogen
Phenylmethanesulphonylfluoride (PMSF) 98.9%	Carl Roth
Penicillin (10^4U/ml)/Streptomycin (10mg/ml)	PAN
Polyoxoethylene (20) sorbitan monolaurate (Tween 20)	Carl Roth
Ponseau S	Carl Roth
Sodium dodecyl sulphate (SDS), ultra grade	Carl Roth
N,N,N',N'-Tetramethylethylenediamine (TEMED)	Carl Roth
Tris-(hydroxymethyl-)aminomethane (Tris)	Carl Roth

Triton X-100	Carl Roth
Trypsin/EDTA (0.05/0.02% w/v)	PAN BioTech

2.1.2 Commercial Kits

innuPREP RNA Mini Kit	AnalytikJena
RNeasy Micro Kit	Qiagen
QiaShredder	Qiagen
Stealth siRNA Tranfection Kit	Invitrogen
BCA™ Protein Assay Kit	ThermoScientific
RNase-Free DNase Set	Qiagen
High-Capacity© cDNA Reverse Transcription Kit	Applied Biosystems

2.1.3 Antibodies

2.1.3.1 Primary Antibodies

anti-β-actin, from mouse (WB)	Sigma
anti-Cytochrome *c*, from rabbit (WB)	Cell Signalling
anti-Cytochrome *c*, from mouse (IHC)	Abcam
anti-c-ErbB2/Neu/p185^{Her-2}, from mouse (FACS)	Biosource
anti-p21, from rabbit (FACS)	Cell Signalling

2.1.3.2 Secondary Antibodies

anti-mouse HRP (WB)	Sigma
anti-rabbit HRP (WB)	Cell Signalling
anti-mouse-APC, from rat (FACS)	BD Pharminogen
anti-rabbit-Cy3, from goat (FACS)	JacksonImmunoResearch
anti-mouse-Cy3, from donkey (IHC)`	JacksonImmunoResearch

2.1.4 Consumables

75cm^2 Cell Culture Flasks	GreinerBio
24-well Culture Plates	Corning
Cell Scrapers	Sarstedt
PVDF-Membrane Transfer Paper	Perkin-Elmer
Whatman® Paper 3MM	Schleicher & Schuell

2.1.5 Buffers and Solutions

2.1.5.1 Commercial Buffers and Solutions

5x Loading Buffer	Bio-Rad
10x RT Buffer	Applied Biosystems
10x RT Random Primers	Applied Biosystems
25x dNTP Mix (100mM)	Applied Biosystems
BD Cytofix/Cytoperm™	BD Biosciences
Buffer HS	AnalytikJena
Buffer LS	AnalytikJena
Buffer RDD	Qiagen
Buffer RLT	Qiagen
Buffer RPE	Qiagen
Buffer RW1	Qiagen
DNase I	Qiagen
Lipofectamine™ RNAiMAX	Invitrogen
Luminol Solution	Perkin Elmer
MultiScribe™ Reverse Transcriptase	Applied Biosystems
Perm/Wash™ Buffer	BD Biosciences
Phosphotase Inhibitor	Invitrogen
Protease Inhibitor	Invitrogen
Stripping Buffer	ThermoScientific
TaqMan® Universal PCR Master Mix	Applied Biosystems

2.1.5.2 Prepared Buffers and Solutions

Buffer/Solution	Contents	Amount
Anode Buffer	Buffer Concentrate A	10%
	Methanol	20%
	Distilled Water	70%
APS Buffer	Ammonium persulphate	10% in distilled water
Blocking Solution (IHC)	BSA	3%
	PBS	1x
	Tween 20	0.1%
Blocking Solution (WB)	Non-fat Milk Powder	5% (w/v)
	TBS	1x
	Tween 20	0.1%
	BSA	5% (w/v)
	TBS	1x
	Tween 20	0.1%
Cathode Buffer	Buffer Concentrate K	10%
	Methanol	20%
	Distilled Water	70%
5x Loading Buffer	Tris/HCl, pH 6.8	2.25 mL
	Glycerol	5 mL
	SDS	0.5 g (10% (w/v))
	Bromophenol blue	5 mg
	DTT	2.5 mL (1M)
10x PBS, pH 7.4	NaCl	8%
	KCl	0.2%
	Na_2HPO_4	0.9%
	KH_2PO_4	0.2%
PMSF	PMSF	200 mM in Isopropanol
Ponseau S Buffer	Triclorite acetic acid	3% (w/v)
	Ponseau S	0.1% (w/v)
2x RIPA Buffer	NaCl	150 mM
	Tris/HCl, pH 7.4	50 mM

	NP-40	1%
	Sodium deoxycholate	1%
	EDTA, pH 7.4	1 mM
	SDS	0.1%
1x Running Buffer	10x Running Buffer	10%
10x Running Buffer, pH 8.3	Tris Base	3.03% (w/v)
	Glycine	14.4% (w/v)
	SDS	1% (w/v)
SDS Buffer	Sodiumdodecylsulphate	10% (w/v) in distilled water
Separation Buffer	Tris/HCl, pH 8.8	3M
Sodium Fluoride	NaF	200 mM in distilled water
Stacking Buffer	Tris/HCl, pH 6.7	0.47M
10x TBS, pH 7.4	Tris	1.2%
	NaCl	5.3%
TBS-T	TBS	1x
	Tween 20	0.1%

2.1.6 Equipment

ABI 7500® Sequence Detection System	Applied Biosystems
Bio-Rad Mini-PROTEAN© Tetra Electrophoresis System	Bio-Rad
Centrifuge Rotina 35R	Heraus
CO_2 Incubator	ThermoScientific
Confocal Laser Scanning Microscope FV1000	Olympus
Eppendorf-microcentrifuge	Eppendorf
Confocal Fluorescent Microscope	Olympus
Fastblot© B34	Biometra
Laminar Flow Hood for Cell Culturing	Heraus
NanoDrop® ND-1000 UV/Visible Spectrophotometer	ThermoScientific

Raman confocal micro-Spectroscopy Imaging Set-Up	WiTec
UV/Visible Spectrophotometer	Jasco

2.1.7 Cell Lines

MCF7/NeuT (Trost, et al., 2005)[25]

The human breast carcinoma cell line MCF7 was transfected with the expression plasmid pcDNA3Neo/rtTa and a second bidirectional plasmid pINSpBI-EGFP/NeuT (Figure 12). Using the tetracycline ON (Tet-ON) system, ErbB2/NeuT and EGFP can be conditionally expressed with the use of the antibiotic doxycycline (dox).

MCF7/EGFP (Trost, et al., 2005)[25]

The human breast carcinoma cell line MCF7 was also transfected with the expression plasmid pcDNA3Neo/rtTa and a second bidirectional plasmid pBI-EGFP (Figure 12). Using the tetracycline ON (Tet-ON) system, EGFP can be conditionally expressed with the use of the antibiotic doxycycline (dox).

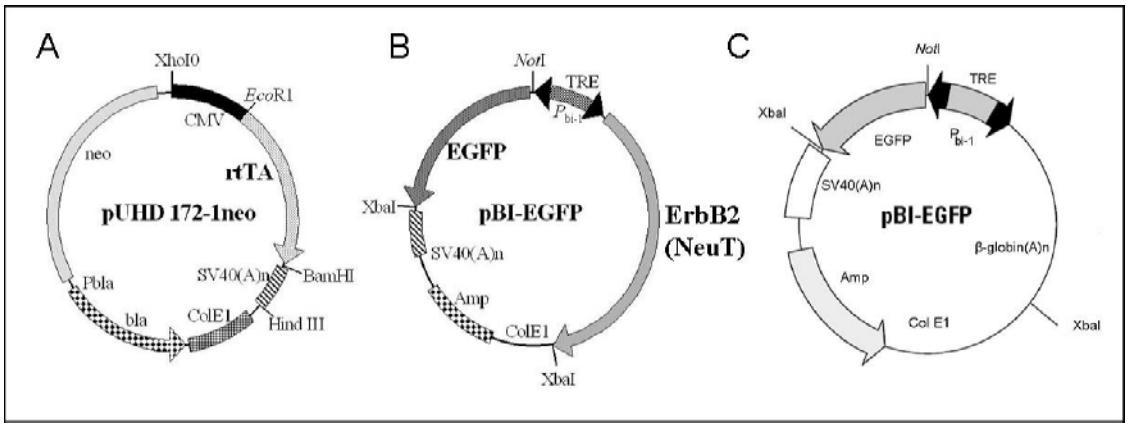

Figure 12: MCF7/NeuT cell transfection constructs (Trost, et al., 2005). MCF7 cells were transfected with the expression plasmid pcDNA3Neo/rtTa (A) and a second bidirectional plasmid either pINSpBI-EGFP/NeuT (B) or pBI-EGFP (C). Cells transfected with vectors A and B became MCF7/NeuT cells and those transfected with A and C became MCF7/EGFP cells.

2.2 Methods

2.2.1 Cell Culture

The MCF7/NeuT and MCF7/EGFP cell lines were continuously cultured in high glucose Dulbecco's Modified Eagle's Medium containing 1% Penicillin/Streptomycin and 10% tetracycline-free Fetal Bovine Serum in 37°C, humidified air at 5% CO_2. For all experiments, MCF7/NeuT and MCF7/EGFP cells were seeded onto their respective culture dishes for each experiment and allowed to adhere for a minimum of 24 hours before beginning dox incubation (treated) or media replacement (non-treated). A non-cytotoxic final concentration at 1 μg/mL of dox was added to complete growth media after the adhesion period for all treated samples.

2.2.2 Total RNA Collection

2.2.2.1 Time Dependent Study Total RNA Extraction

Total RNA was extracted from MCF7/NeuT and MCF7/EGFP samples at each specified time point (Results Section 3.2.2.2) using the AnalytikJena innuPREP© RNA Mini Kit. Cells were cultured as stated above (Section 2.2.1) in 75 cm^2 culture flasks at the specified time points so that they reached a confluence of 70-90% at the time of RNA collection. In order to lyse the cells, culture media was removed from the 75 cm^2 culture flasks and cells were washed twice with 1x PBS. Cells were then trypsinised in 2 mLs of Trypsin/EDTA (PAN Biotech) and resuspended in 20 mLs of media to stop the trypsinisation. The suspension was then placed into 50 mL falcon tubes and centrifuged at 400 x g for 5 minutes creating a cell pellet. Supernatant was removed from the falcon tube so that no growth media was left in the falcon tube. 400 μL of RL lysis buffer (AnalytikJena) was then added to the pellet and gently mixed by pipetting up and down to disrupt the cell pellet. The suspension was then incubated for 5 minutes at room temperature and resuspended half-way through the incubation period. To insure complete disruption of the cells the falcon tube was briefly vortexed before continuing on to the RNA isolation steps. Next the supernatant was placed into Spin Filter D (AnalytikJena) and centrifuged at 10,000 x g for 4 minutes in order to separate protein

and genomic DNA from RNA taking care that all of the supernatant passed through the filter into the collection tube. An equal volume of 70% ethanol (approx. 400 µL) was gently mixed into the filtrate by pipetting up and down. The mixed filtrate was then transferred to Spin Filter R (AnalytikJena) and centrifuged at 10,000 x g for 4 minutes to bind the total RNA to the silicon filter. Filtrate was discarded. An on-column DNase digestion was performed on each sample to remove any remaining DNA. 250 µL of buffer HS (AnalytikJena) was added to the spin column of Spin Filter R and centrifuged at 10,000 x g for 2 minutes and filtrate was discarded. Using the RNase-Free DNase Set (Qiagen), 10 µL of DNase I stock solution (Qiagen) was added to 70 µL of buffer RDD (Qiagen) in a micro-centrifuge tube, mixed gently by inverting the tube and centrifuged briefly to pull residual liquid down. Each sample received 80 µL of DNase I incubation mix which was placed directly onto the silicon filter of the spin column and incubated at room temperature for 15 minutes. Following incubation, 250 µL of buffer HS was added to Spin Filter R and centrifuged for 1 minute at 10,000 x g and filtrate was discarded. 750 µL of buffer LS (AnalytikJena) was added to Spin Filter R and centrifuged at 10,000 x g for 2 minutes. Filtrate was discarded and spin column was centrifuged for an additional 6 minutes at 10,000 x g to remove any residual ethanol from the silicon filter. Spin Filter R was then placed into a micro-centrifuge tube and 33 µL of RNase-free water was added to the spin column. To elute the total RNA, the spin column was incubated for 1 minute and centrifuged at 10,000 x g for 2 minutes. Spin Filter R was then discarded and the total RNA sample was stored at - 80°C until needed for further experiments. See Figure 13 for a flow chart of experimental set-up.

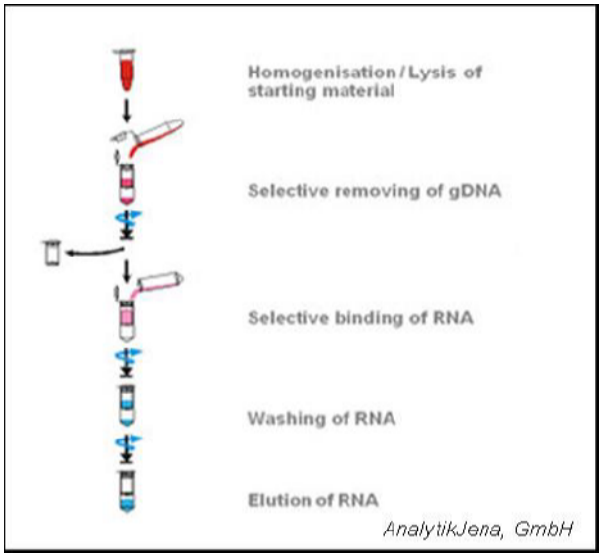

Figure 13: innuPREP RNA Mini Kit flow chart for total RNA isolation in MCF7/NeuT and MCF7/EGFP cells

2.2.2.2 siRNA Study Total RNA Extraction

Total RNA was extracted from the siRNA MCF7/NeuT samples using the RNeasy® Micro Kit (Qiagen). MCF7/NeuT cells were cultured in 24-well culture dishes in complete growth media as described above (Section 2.2.1). Cells were seeded so that they reached confluence of 70-90% at time of RNA collection. 350 µL of buffer RLT (Qiagen) containing 1% 2-Mercaptoethanol (Roth) was added directly to the culture plate wells and incubated at room temperature for 1 minute. A cell scraper was then used to disrupt the monolayer and lysate was then collected into a micro-centrifuge tube and vortexed to ensure no cell debris was visible. The lysate was then pipetted into QIAshredder® spin columns (Qiagen) to homogenise the sample by centrifuging at 10,000 x g for 2 minutes. 350 µL of 70% ethanol was added to the lysate and mixed well by pipetting up and down. This mixture was then transferred to an RNeasy® MinElute® spin column (Qiagen) and centrifuged at 10,000 x g for 1 minute. Flow-through was discarded and 350 µL of buffer RW1 (Qiagen) was added to the spin column and centrifuged at 10,000 x g for 1 minute. An on-column DNase digestion was performed on each sample to remove any remaining DNA. Using the RNase-Free DNase Set (Qiagen), 10 µL of DNase I stock solution (Qiagen) was added to 70 µL of buffer RDD

(Qiagen) in a micro-centrifuge tube, mixed gently by inverting the tube and centrifuged briefly to pull residual liquid down. Each sample received 80 µL of DNase I incubation mix which was placed directly onto the silicon filter of the spin column and incubated at room temperature for 15 minutes. Following incubation, 350 µL of buffer RW1 was then added to each RNeasy® MinElute® spin column and centrifuged for 1 minute at 10,000 x g. Flow-through was discarded and the RNeasy® MinElute® spin column was placed into a new collection tube. 500 µL of buffer RPE (Qiagen) was then added to the spin column and centrifuged at 10,000 x g for 1 minute. Flow-through was discarded and 500 µL of 80% ethanol was added to the RNeasy® MinElute® spin column and centrifuged at 10,000 x g for 2 minutes. Flow-through and collection tube were then discarded and the RNeasy® MinElute® spin column was placed into a new collection tube and centrifuged at 10,000 x g for 5 minutes to remove any residual ethanol. The RNeasy® MinElute® spin column was then placed into a micro-centrifuge tube and 14 µL of RNase-free water was added to the spin column. To elute the RNA, samples were centrifuged at 10,000 x g for 1 minute. Samples were stored at -80°C until needed for further experiments. See Figure 14 for flow chart of experimental set-up.

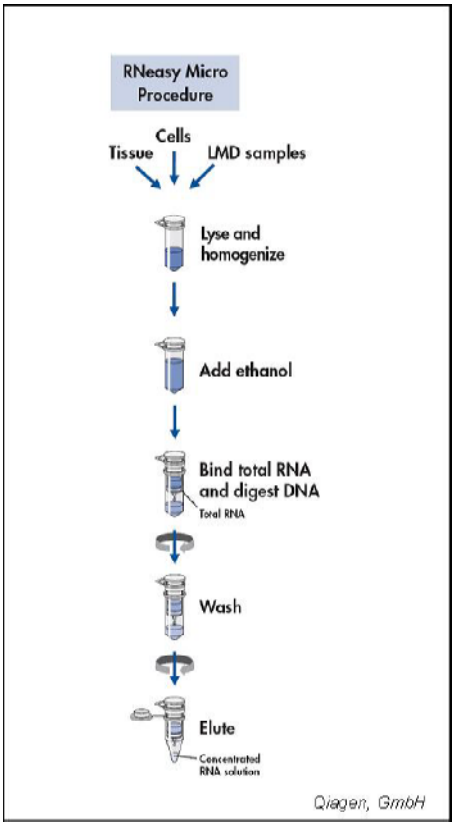

Figure 14: RNeasy® MinElute® flow chart for RNA isolation of MCF7/NeuT cells in siRNA studies.

2.2.3 Quantitative RNA Yield

RNA concentration was quantified by using a NanoDrop® ND – 1000 UV/Visible Spectrophotometer (ThermoScientific). To standardise the reading, 1.2 µL of nuclease-free water (blank control) was added to the detector. To obtain readings for the RNA samples the same procedure was repeated only using 1.2 µL of each RNA sample. To quantify the purity of the RNA samples the concentration (ng/µL) and ratio of absorbance at 260nm:280nm and 260nm:230nm were measured. A measurement of a 260nm:280nm ratio between 1.8 and 2.0 and a 260nm:230nm ratio between 1.5 and 2.0 indicated RNA purity, with respect to protein contamination. All MCF7/NeuT and MCF7/EGFP total RNA samples were subjected to this analysis (See Appendix 1).

2.2.4 cDNA Synthesis

Following RNA extraction and RNA yield quantification, complementary DNA (cDNA) was synthesised using the High-Capacity© cDNA Reverse Transcription kit (Applied Biosystems). To perform the cDNA synthesis reaction a 2X reverse transcription master mix was prepared. Prepared on ice, the 2X reverse transcription master mix contained the following; 2.0 µL 10x RT buffer, 0.8µL 25x dNTP Mix (100nM), 2.0 µL 10X RT Random Primers, 1.0 µL MultiScribe™ Reverse Transcriptase, and 4.2 µL nuclease-free water. Each cDNA synthesis reaction contained 10 µL of 2X reverse transcription master mix and 10 µL of total RNA sample. Samples were subjected to 10 minutes incubation at 25°C following 120 minutes at 37°C and 5 seconds at 85°C to stop the reaction and then held at 4°C. All RNA samples were subjected to cDNA synthesis. Proceeding cDNA synthesis, all cDNA samples were diluted in nuclease-free water to a final concentration of 2.0ng/µL.

2.2.5 Assay Primer and Probe Design for RT-qPCR

Prior to primer and probe design, mRNA sequences for each target gene and reference gene were identified. Human mRNA sequences were compiled from records at the National Centre for Biotechnology Information (NCBI). The database provided sequences that were derived from genetic transcripts. However, this database did not provide the details of exon-exon boundaries to allow for RNA specific assay design (described below). The NCBI mRNA sequences for each reference and target gene assayed in the studies were compared to the human genome on the database for the European Molecular Biology Laboratories (EMBL). This database is able to identify exon-exon boundaries (if any) within transcript sequences. The NCBI and EMBL recorded mRNA sequences were compared and analysed for consensus regions and exon boundaries within the genetic sequences of interest using the GENEDOC® software package.

For each reference and target gene, the mRNA sequences derived from the NCBI records were analysed individually to select the appropriate probe and primer sets. The NCBI mRNA sequence was scanned against the human Universal Probe Library Assay Design Centre from Roche Diagnostics (Roche). Following the Universal Probe Library Assay Design Centre search, each individual reference and target gene was then presented with a list of appropriate primer and probe sets, generated by Roche Diagnostics that can be used for RT-qPCR assays. One set of primers and probes was chosen for each reference and target gene used in the studies. The most suitable primer and probe sets were selected on the basis of a number of factors;

A) The primers and probe, if possible, should fall within a consensus region in the mRNA sequence so that both the NCBI and EMBL transcript sequence versions align to allow for a reliable transcript sequence.

B) The primers and probe, if possible should fall within certain areas in the transcript sequence so that the forward primer is homologous to one exon, the reverse primer is homologous to the adjacent exon and the probe is complementary to the sequence that crosses the exon-exon junction. This format is needed to prevent the co-amplification of genomic DNA that is irrelevant to the assays being performed and can also distort the results. When the option was not probable, care was taken to chose a primer/probe set whereby one primer lies on one exon and the probe and remaining primer lie wholly on the adjacent exon, and that the intron length was greater than 1kb. If that was not applicable, the entire primer/probe set lied entirely on one exon as close to the 3'end as possible to avoid, if any, fragmented cDNA sequences.

C) The melting temperature for the primers should be approximately between 50-60°C, with the melting temperature of the probe being at approximately 70°C.

D) The length of the amplicon should be between 50-100 base pairs.

E) The G/C percent content of the primer should be between 40-60% to avoid non-specific binding.

All probes used for reference and target gene assays were synthesized by Roche Diagnostics and primers were synthesized by Metabion. Each probe was labelled at the 5'-end with the reporter dye fluoresceine (FAM (6-carboxy fluoresceine)) and at the 3'-end with a dark quencher dye.

The primer sequences from each primer and probe set were then finally submitted to a human homology search using NCBI BLAST®. This was performed to rule-out any possibility that chosen primers may possess sequence homology to non-target genes, meaning they should only primer-extend the gene of interest. Primer sets were redesigned if found to be homologous to a human gene other than the gene of interest. The final primer/probe sets used then were all specific to the genes of interest (See Appendix 2).

2.2.6 TaqMan™ RT-qPCR

Reverse transcribed Real-time PCR (RT-qPCR) assays were conducted on an ABI 7500® (Applied Biosystems) using 96-well plates, having three replicates for each assay. Each assay well contained a 20 µL reaction volume. In the reference and target gene assays, the reaction volume in each well consisted of 10 µL 2x TaqMan® Universal PCR Master Mix (Applied Biosystems), 5µL of RNase-free water, 0.4 µL of 20 µM forward primer (Metabion), 0.4 µL of 20 µM reverse primer (Metabion), 0.2 µL of 10 µM fluorescently-labelled probe (Roche Diagnostics) and 4 µL of sample cDNA. Each assay included three no-template controls replacing cDNA with nuclease-free water. Subsequently, each PCR plate was sealed using sealing foils (Applied Biosystems) and centrifuged at 400 x g for 1 minute to remove any bubbles and pull down residual liquid. Each PCR plate was then analysed in the ABI 7500® sequence detection system. The standard amplification conditions consisted of 1 cycle at 50°C for 2 minutes to activate AmpErase® UNG, 1 cycle at 95°C for 10 minutes to initiate the AmpliTaq Gold® DNA polymerase followed by 40 cycles of 95°C for 15 seconds (DNA duplex denaturation) and 60°C for 1 minute

(strand annealing/extension). Real-time data was then analysed by using ABI 7500® standard software to determine cycle threshold values (Ct) and then relatively quantified.

2.2.7 Selection of Reference Genes for MCF7/NeuT and MCF7/EGFP Cell Lines

Following the RT-qPCR protocol as described in section 2.2.6, ideal reference genes for each cell line were selected prior to beginning gene expression studies. Using the statistical software programme geNorm developed by Vandesompele, et al. in 2002[73] the best fit reference genes were selected for the MCF7/NeuT and MCF7/EGFP cell lines. Ideal reference genes were chosen from a list of common reference genes shown in table 1.

Table 1: Common reference genes evaluated for RT-qPCR assays. Taken from [73].

Common Reference Genes Evaluated			
Symbol	**Accession Number**	**Name**	**Function**
ACTB	NM_001101	Beta-actin	Cytoskeletal structural protein
B2M	NM_004048	Beta-2-microglobulin	Beta-chain of major histocompatibility complex class I molecules
GAPDH	NM_002046	Glyceraldehyde-3-phosphate dehydrogenase	Oxidoreductase in glycolysis and gluconeogenesis
HMBS	NM_000190	Hydroxymethyl-bilane synthase	Heme synthesis, porphyrin metabolism
HPRT1	NM_000194	Hypoxanthine phosphoribosyl-transferase I	Purine synthesis in salvage pathway
RPL12A	NM_012423	Ribosomal protein L13A	Structural component of the large 60S ribosomal subunit
RPL32	NM_000994	Ribosomal protein 32	Structural component of the large 60S ribosomal subunit
SDHA	NM_004168	Succinate dehydrogenase complex, subunit A	Electron transporter in the TCA cycle and respiratory chain
TBP	NM_003194	TATA box binding protein	General RNA polymerase II transcription factor
UBC	NM_021009	Ubiquitin C	Protein degradation
YWHAZ	NM_003406	Tyrosine 3-monooxygenase/tryptophan 5-monooxygenase activation protein, zeta polypeptide	Signal transduction by binding to phosphorylated serine residues on a variety of signaling molecules

2.2.8 siRNA Transfection of Cyclin Dependent Kinase Inhibitor 1A (P21) and Pituitary Tumour-Transforming 1 (PTTG1) in MCF7/NeuT Cells

Reverse siRNA transfection was performed on the MCF7/NeuT cell line using predesigned Stealth RNAi™ siRNA duplex oligoribonucleotide sequences (See Appendix 3) for the genes cyclin dependent kinase inhibitor 1A (p21) and Pituitary Tumour-Transforming 1 (PTTG1) (Invitrogen). MCF7/NeuT cells were reverse siRNA transfected in 24-well culture dishes. Stealth RNAi™ siRNA duplex-Lipofectamine™ RNAiMAX complexes were prepared for each sample well as follows;

1) Each Stealth RNAi™ siRNA oligoribonucleotide was first diluted from a 20 µM concentration to a working concentration of 2 µM in DEPC-treated nuclease-free water (Invitrogen).
2) For every well used, 3 µL of diluted oligoribonucleotides was added to 97 µL of serum-free Opti-MEM® I Medium (Invitrogen) in a micro-centrifuge tube, pipetted into the well and mixed gently by rocking the culture plate back and forth.
3) 1 µL of Lipofectamine™ RNAiMAX (Invitrogen) was then added to each well containing the diluted siRNA oligos, mixed gently by rocking the plate back and forth and then incubated for 20 minutes at room temperature.
4) Prior to reverse siRNA transfection, MCF7/NeuT cells were cultured in 75cm^2 flasks to 90% confluency. MCF7/NeuT cells were then trypsinised and centrifuged down into a pellet and resuspended in complete growth medium without antibiotics as described above (Section 2.2.1) where 500 µL of complete media contained the following; 50,000 cells for the 0h -24h time points, 25,000 cells for the 3d time point and 10,000 cells for the 7d time point. 500 µL of cell suspension was then pipetted into each respective well containing the Stealth RNAi™ siRNA duplex-Lipofectamine™ RNAiMAX complexes and mixed gently by rocking the plate back and forth.
5) Culture plates were then incubated for 24 hours in humidified air at 37°C in 5% CO_2 to allow for the reverse transfection to occur prior to beginning the timed dox incubation experiments.

Three siRNA oligoribonucleotide sequences were tested for each gene of interest. To optimise the efficiency of the reverse transfection of the siRNA oligoribonucleotides, they were first tested at 10 nM and 30 nM concentrations in duplicate and the knockdown efficiency was measured using RT-qPCR. Beta-actin was used at the positive control. For every siRNA experiment, in order to ensure the knockdown in the gene of interest

was specific to the siRNA oligoribnucleotides, a non-sense sequence was used as a negative control and the Lipofectamine™ RNAiMAX (transfecting agent) was used as the buffer control. Cell passages were kept below 10 for each experiment which was performed 3 independent times. See plate layouts below for optimisation and experimental set-ups (Figures 15 and 16).

	1	2	3	4	5	6
A	Target Gene – Oligo A (10nM)	Target Gene – Oligo A (10nM)	Target Gene – Oligo A (30nM)	Target Gene – Oligo A (30nM)	Positive Control – β-Actin (10nM)	Positive Control – β-Actin (10nM)
B	Target Gene – Oligo B (10nM)	Target Gene – Oligo B (10nM)	Target Gene – Oligo B (30nM)	Target Gene – Oligo B (30nM)	Negative Control	Negative Control
C	Target Gene – Oligo C (10nM)	Target Gene – Oligo C (10nM)	Target Gene – Oligo C (30nM)	Target Gene – Oligo C (30nM)	Transfection Agent Only – Buffer Control	Transfection Agent Only – Buffer Control
D						

Figure 15: 24-well plate layout for optimisation of siRNA oligoribonucleotide concentrations

	Time Point A – Non-Treated			Time Point A - Treated		
	1	2	3	4	5	6
A	Target Gene 1 Oligo A	Target Gene 1 Oligo B	Target Gene 1 Oligo C	Target Gene 1 Oligo A	Target Gene 1 Oligo B	Target Gene 1 Oligo C
B	Target Gene 2 Oligo A	Target Gene 2 Oligo B	Target Gene 2 Oligo C	Target Gene 2 Oligo A	Target Gene 2 Oligo B	Target Gene 2 Oligo C
C	Negative Control	Transfection Agent Only – Buffer Control		Negative Control	Transfection Agent Only – Buffer Control	
D						

Figure 16: 24-well plate layout for siRNA timed dox incubation experiments

2.2.9 Total Protein Extraction

Total protein was extracted from MCF7/NeuT and MCF7/EGFP cell lines. Cells were grown to 90% confluency in 75cm^2 flasks in complete growth media and normal culturing conditions. Prior to extraction, 1 µL of Protease Inhibitor (Invitrogen), 10 µL of Phosphotase Inhibitor (Invitrogen) and 1 µL PMSF-serine inhibitor (Roth) was added for every millilitre of RIPA buffer to the RIPA buffer and mixed gently. On ice, 1 mL of RIPA-lysis buffer was added directly onto the cells and left to incubate for a few minutes. Using a cell scraper, cell lysate was scraped from the culture flask and pipetted into micro-centrifuge tubes. Cell lysate was then left on ice for 30 minutes. Following incubation, cell lysates were centrifuged at 15,000 x g for 15 minutes at 4°C. The supernatant containing total protein was then pipetted off and transferred to a new micro-centrifuge tube. Total protein lysates were then stored at -80°C until needed for further experiments.

2.2.10 Western Blotting

2.2.10.1 BCA Protein Assay for Protein Quantification

Protein quantification of all protein samples was determined by using the BCA™ Protein Assay Kit (ThermoScientific). 10 µL of protein sample was added to 790 µL of distilled water in micro-centrifuge tubes. 200 µL working reagent was prepared for each sample with 50 parts of reagent A and 1 part reagent B and added to the diluted protein sample. Samples were then incubated at 60°C for 30 minutes with interval shaking and then incubated at room temperature for an additional 10 minutes. The sample (1 mL) was then transferred to a sterile cuvette. Cuvette samples were placed into a UV/Visible spectrophotometer (Jasco). Protein concentrations were measured at a wavelength of 562 nm and calculated using the Jasco spectrophotometer software. Total protein concentration for each well was 30 µg. Samples were measured three times and then averaged.

2.2.10.2 SDS Gel Preparation

Gels were prepared using the Bio-Rad Mini-PROTEAN© Tetra Electrophoresis System (Bio-Rad). Glass plates needed to mould the gel were first washed with 70% ethanol, dried and then placed into casting frames with the shorter plate aligned to the front of the frame. Provided seals were placed at the bottom of the casting apparatus to insure no leakage before gel solidifies. A 10% separation gel, 1.5 mm thick, was then prepared with the following; 3.2 mL of distilled water, 2.64 mL of Acrylamide (Roth), 2.0 mL of separation buffer, 80 µL of 10% SDS, 3.2 µL of TEMED (Roth) and 80 µL of 10% APS was added to a 50 mL falcon tube and gently mixed by inverting and vortexing briefly. 7 mLs of separation gel was then pipetted between the glass plates in the casting frames and 1 mL of isopropanol was added to the top of the gel to prevent evaporation. The separation gel was then left to polymerise for approximately 20 minutes. After the gel was set and the isopropanol was removed a stacking gel was prepared. A 10% stacking gel, 1.5 mm thick, was prepared with the following; 3.6 mL of distilled water, 750 µL of Acrylamide (Roth), 600 µL of stacking buffer, 48.75 µL of 10% SDS, 3.75 µL of TEMED (Roth) and 75 µL of 10% APS was added to a 50 mL falcon tube and gently mixed by inverting and vortexing briefly. 2.5 mL of stacking gel was then pipetted between the glass plates in the casting frames and a comb to mould for the appropriate number wells was inserted into the stacking gel. The stacking gel was left to polymerise for 20 minutes. Polymerised gels were then stored by removing the glass plates containing the gel from the casting frame, wrapping in towelling, soaking with distilled water and placing it in a plastic storage bag at 4°C until needed.

2.2.10.3 SDS Gel Electrophoresis

After measuring the concentration of protein samples and preparing the gel, an SDS gel electrophoresis was performed on the samples of interest. Protein samples and bench markers were first thawed on ice. Samples were diluted using 5x Loading Buffer (Bio-Rad) based on the concentrations calculated from the BCA protein assay. Protein samples were then vortexed and heated at 95°C for 5 minutes to denature the proteins. Next the gel was mounted into the Bio-Rad Mini-PROTEAN© Tetra Electrophoresis

System and the comb was removed from the gel. 1x running buffer was then poured into the inner chamber of the apparatus and samples were loaded into the wells. Approximately 20 µL of protein sample was loaded into its respective well and 1x running buffer was loaded into any empty wells to ensure uniform electrophoresis. Wells were also designated for 10 µL of Bench Mark (Invitrogen) and 5 µL of Magic Mark XP (Invitrogen) in order to track the electrophoresis. The apparatus was connected to the power supply and initially run at 25 mA until the dye front (protein samples) moved out of the stacking gel (Approx. 30 minutes). The power was then increased to 45 mA for 90 minutes. After electrophoresis, the gel was removed from the apparatus and the orientation was marked by cutting off the top left corner of the gel. The gel was then placed in cathode buffer until needed for membrane transfer.

2.2.10.4 Membrane Transfer

To transfer the protein samples onto the immobilising membrane after electrophoresis, 16 Whatman® papers were cut to the size of the gel and a piece of PVDF-membrane transfer paper was also cut and orientation marked by cutting the top left corner off. The PVDF-membrane transfer paper was activated by briefly washing with methanol and equilibrated in anode buffer. Twelve Whatman® papers were placed in anode buffer and 4 were placed in cathode buffer for several minutes before beginning the transfer to allow the papers to equilibrate to the buffer. The Fastblot© B34 (Biometra) electro-blotting apparatus was used for transferring protein samples onto the membrane. A 'paper sandwich' was then prepared as follows from bottom up; 12 Whatman® papers, PVDF-membrane transfer paper, gel and 4 Whatman® papers. The 'paper sandwich' was then placed into the Fastblot© B34 so that all pieces were aligned. To ensure that no bubbles were present a large volume pipette was rolled over the 'paper sandwich'. The power pack was connected to the Fastblot© B34 and run for approximately 40 minutes at 200 mA per/gel. Current was calculated by dividing 5 mA into the width and length of the gel. After the transfer was complete the PVDF-membrane transfer was washed with distilled water for 5 minutes. To ensure protein was successfully transferred to the PVDF-membrane transfer paper, Ponseau S prepared in triclorite acid was used. The membrane was stained for 2 minutes with Ponseau S and then washed with distilled water

to visualise the blot. Ponseau S was then washed from the membrane by washing the membrane in 1x TBS-T for 5 minutes. The membrane was then air dried at room temperature, wrapped in aluminium foil and stored at -20°C until needed.

2.2.10.5 Antibody Incubation

To incubate the membrane with specific antibodies, the membrane was first blocked in a 5% non-fat milk or 5% BSA solution in 1x TBS-T depending on the antibody of interest, for 2 hours at room temperature. Primary antibodies were prepared in a non-fat milk or BSA solution in 1x TBS-T. Concentrations varied depending on the antibody. In a 15 mL falcon tube 7 mLs of incubation solution was added along with the appropriate concentration of antibody and then placed on a shaker to mix. The membrane was then placed into an appropriate sized plastic bag and the antibody solution was then poured into the bag, sealed and placed on a level shaker to incubate at 4°C overnight. After primary antibody incubation, the membrane was washed 6 times for 5 minutes each in 1x TBS-T. The secondary antibody was then prepared using non-fat milk or BSA solution in 1x TBS-T. Concentrations varied depending on the antibody. In a 15 mL falcon tube 10 mLs of incubation solution was added along with the appropriate concentration of antibody and then placed on a shaker to mix. The membrane was then placed into a glass cylinder bottle and secondary antibody was poured over the membrane. The bottle was then placed into a rotating incubator and spun for 1 hour at room temperature. After incubation of the secondary antibody, the membrane was washed again 6 times for 5 minutes each in 1x TBS-T. A Luminol solution (Perkin Elmer) was prepared in a Petri dish using equal volumes of solution A and B (approx. 6 mL total volume). The membrane was then placed into the Petri dish and imaged. ImageJ software was used to calculate the antibody specific protein concentration. After imaging of the membrane was complete, the membrane was washed in 1x TBS-T for 5 minutes then stripped of antibody. Membranes were stripped of antibodies after every incubation using Stripping Buffer (ThermoScientific) by incubating the membrane in the buffer for approximately 20 minutes. The membrane was then washed for 5 minutes in 1x TBS-T and to ensure complete removal of antibody, membrane was subjected a second time to the Luminol solution. If antibody was completely stripped from the membrane, it was then washed in

1x TBS-T and stored at 4°C in 1x TBS-T if further antibodies were needed to be incubated, or air dried and stored at -20°C until needed.

2.2.11 Immunofluorescence

MCF7/NeuT cells were subjected to immunofluorescence. Cells were seeded onto glass coverslips inside 24-well culture plates at a low density and cultured in conditions as stated above (Section 2.2.1). Briefly, cells were washed twice with 1x PBS and fixed with 4% Paraformaldehyde in PBS for 20 minutes at room temperature. After fixation, cells were washed twice with 1x PBS for 5 minutes. Cells were then incubated with 50 mM Ammonium chloride (NH_4Cl) in 1x PBS for 10 minutes and then washed with 1x PBS for 5 minutes. To block the cells were incubated with 3% BSA/Saponin (0.1 mg/mL) in 1x PBS for 1 hour at room temperature. Cells were then washed with 1x PBS/Saponin (0.1 mg/mL) for 10 minutes. Due to Saponin's reversibility effects on permeablisation it needs to be present at both the washing and antibody incubation steps. Therefore, cells were incubated with primary antibody for 1 hour at room temperature in 1% BSA/Saponin (0.1 mg/mL) in 1x PBS. Concentration of antibody depended on specific antibodies of interest. Cells were then washed with 1x PBS/Saponin (0.1 mg/mL) 3 times for 10 minutes. A secondary antibody was then diluted in a 1% BSA/Saponin (0.1 mg/mL) solution in 1x PBS and incubated with the cells for 1 hour at room temperature. After secondary incubation cells were washed with 1x PBS/Saponin (0.1 mg/mL) 3 times for 10 minutes. Cells were then washed 2 times in 1x PBS for 5 minutes and a DAPI stain was then performed. After the DAPI staining, cells were washed again in 1x PBS 2 times for 5 minutes then rinsed in distilled water and mounted in mounting media on glass microscope slides. Slides were then viewed immediately using a laser scanning confocal microscope (Olympus) after mounting.

2.2.12 Fluorescent Activated Cell Sorting (FACS) Cell Preparation

Fluorescent activated cell sorting (FACS) was performed on MCF7/NeuT cells to measure the efficiency of NeuT and EGFP vector protein expression using the BD FACSCalibur™ (BD Biosciences). Cells were harvested and counted where by approximately 1 x 10^6 cells were used for each antibody tested. The calculated number of cells was then transferred into a micro-centrifuge tube and centrifuged at 50 x g for 5 minutes at 4°C. Supernatant was discarded and cells were washed in 1x PBS and centrifuged again at 50 x g for 5 minutes at 4°C. Cells were next fixed by incubating in 4% Paraformaldehyde in 1x PBS at room temperature for 30 minutes and then centrifuged at 50 x g for 5 minutes at 4°C. Supernatant was discarded and the cells were washed 2 times in 1x PBS and centrifuged at 50 x g for 5 minutes at 4°C each time. After the final wash and discarding of the supernatant the cell pellet was then resuspended in 500 µL of BD Cytofix/Cytoperm™ (BD Biosciences) and incubated for 20 minutes at 4°C. 900 µL of Perm/Wash™ Buffer (BD Biosciences) was added to the micro-centrifuge tube, vortexed and centrifuged at 400 x g for 5 minutes at 4°C. Supernatant was discarded and cell pellet was resuspended in Perm/Wash™ Buffer so that 500µL equalled 1 x 10^6 cells. 500 µL of cell suspension was then transferred to a new micro-centrifuge tube and centrifuged at 400 x g for 5 minutes at 4°C. The supernatant was then discarded and 50 µL of diluted primary antibody was incubated on the cells for 1 hour at 4°C. After incubation, 1 mL of Perm/Wash™ Buffer was added to the micro-centrifuge tube and incubated for 10 minutes followed by centrifugation at 400 x g for 5 minutes at 4°C. This washing step was repeated a second time. Next the secondary antibody was added, 50 µL of diluted antibody was added to the micro-centrifuged tube and incubated for 1 hour at 4°C. After incubation of the secondary antibody, 1 mL of Perm/Wash™ Buffer was added to the micro-centrifuge tube and incubated for 10 minutes. Following the washing step, the suspension was centrifuged at 400 x g for 5 minutes at 4°C. This washing step was repeated two more times. The cell pellet was then resuspended in 500 µL of 1x PBS and transferred to a round-bottom glass tube (BD) and measured in the BD FACS Calibur™.

2.2.13 Raman Confocal micro-Spectroscopy Cell Preparation and Imaging

MCF7/NeuT cells were seeded onto quartz discs in 24-well culture dishes at a density of approximately 1 x 10^5 cells per well. Cells were cultured accordingly (Section 2.2.1) however; replacing DMEM with phenol red-free DMEM (PAN BioTech) as the dye in the media inhibits the laser from conducting accurate measurements of cell samples. After desired experimentation, media was removed from the samples and cells were washed twice with 1x PBS. Cells were then fixed in 2% formaldehyde in 1x PBS for 1 hour at room temperature. Following fixation, samples were washed once in distilled water, wrapped in aluminium foil and frozen at -80°C to inhibit auto-fluorescence until needed.

After fixation, MCF7/NeuT cells were imaged using a Raman confocal micro-Spectroscopy imaging set-up (WiTec). A laser wavelength of 514.5nm with an incident power of 20 mW was transmitted through a 100x objective. Individual cells were imaged using a spatial resolution of 0.5 μm with a step-size of 0.5. This provided 8- 10,000 spectra for each cell following raster scattering. Data was analysed by importing the spectra into CytoSpec™ software for unsupervised hierarchical cluster analysis. Image regions not containing sample were omitted using a quality test. To compensate for uneven sample thickness images were vector normalised and then clustered using D-Values and Ward's algorithm. Image clustering was carried out on individual cells taken from the Raman images and average spectra were compared.

2.2.14 Experimental Statistical Data Analysis

Statistical analysis was performed for all gene expression studies using SPSS™ 16.0 student edition. The Mann-Whitney U and Kruskall-Wallis tests were performed to determine significant differences between samples. The Bonferroni correction post-hoc test was also performed to determine global significant differences among samples. A p-value of less than or equal to 0.05 was considered to be statistically significant.

CHAPTER THREE:
RESULTS

3.0 Results

3.1 Inducible Expression of ErbB2/HER2 (NeuT): Characterisation of the Vector Cell System

To understand the mechanisms involved in the over-expression of the oncogene ErbB2 which induces cellular senescence and to study genes that are critically involved in this phenomenon the adenocarcinoma cell line, MCF7, was vector transfected to over-express ErbB2. The functionality of ErbB2 induction was controlled by a Tet-ON system using the antibiotic doxycycline to control gene expression. Therefore, to confirm the up-regulation of NeuT, mRNA and protein expression of NeuT were measured using RT-qPCR and immunoblotting technologies. The fluorescent green marker protein, EGFP, was also measured using Fluorescence Activated Cell Sorting Analysis (FACS) and fluorescent confocal microscopy.

3.1.1 Induction of mRNA Expression of NeuT

NeuT mRNA expression was detected in the MCF7/NeuT cell line treated with doxycycline. The results indicate a significant up-regulation of NeuT mRNA expression already after 10 minutes of doxycycline exposure (Figure 17). After 3 hours of doxycycline exposure, NeuT mRNA expression plateaus around a 4000-fold increase in expression compared to the non-treated MCF7/NeuT and MCF7/EGFP samples (Figure 18). These results indicate that the NeuT expression vector is functioning properly upon doxycycline treatment.

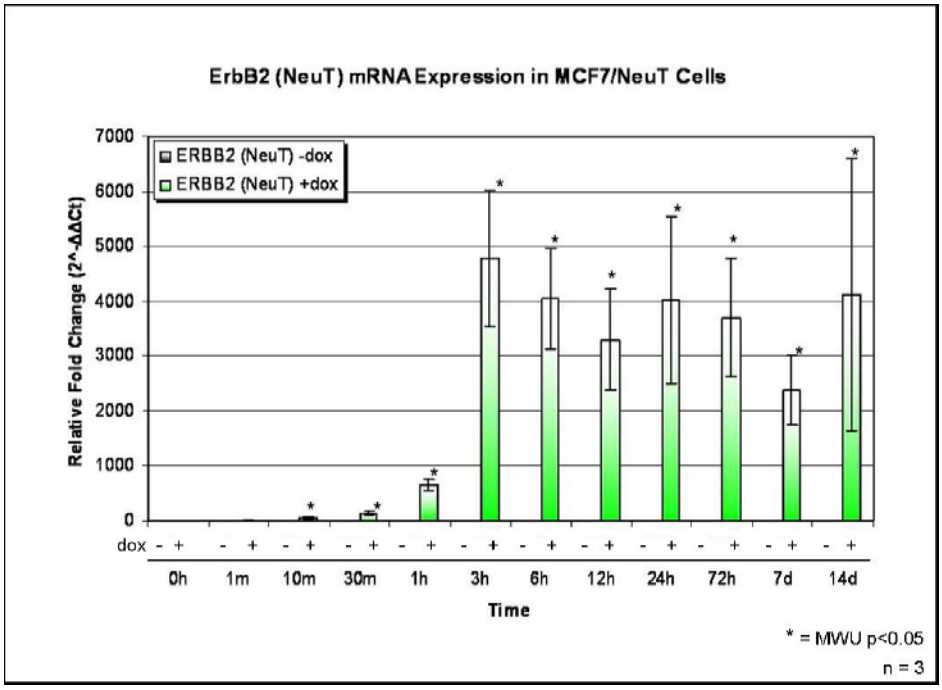

Figure 17: ErbB2 (NeuT) mRNA expression in MCF7/NeuT cells treated with or without doxycycline (dox). Data values represent the mean values of three separate experiments. RNA expression can be induced by dox in the MCF7/NeuT cell line.

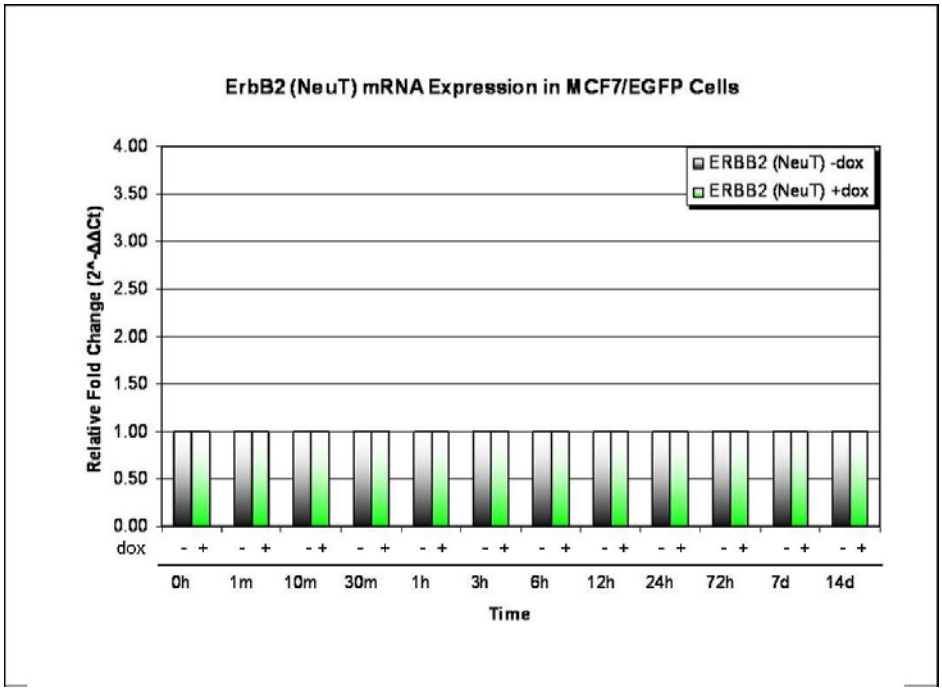

Figure 18: ErbB2 (NeuT) mRNA expression in MCF7/EGFP cells treated with or without dox. Data values represent the mean values of three separate experiments. RNA expression is not induced by dox exposure. NB: All MCF7/EGFP samples showed no detection of NeuT gene expression and were given a ΔΔCt value of 0.00 creating a value of 1.00 for 2^-ΔΔCt since all samples are relative to time point 0h they show similar levels of expression of NeuT which in this case is no expression.

3.1.2 Induction of Protein Expression of NeuT

Protein expression of NeuT was also measured in both the MCF7/NeuT (NeuT) and MCF7/EGFP (EGFP) cell lines. After 7 days of dox treatment protein expression was detected only in the MCF7/NeuT cells treated with dox (Figure 19). This indicates NeuT up-regulation is restricted to only the NeuT vector containing cells.

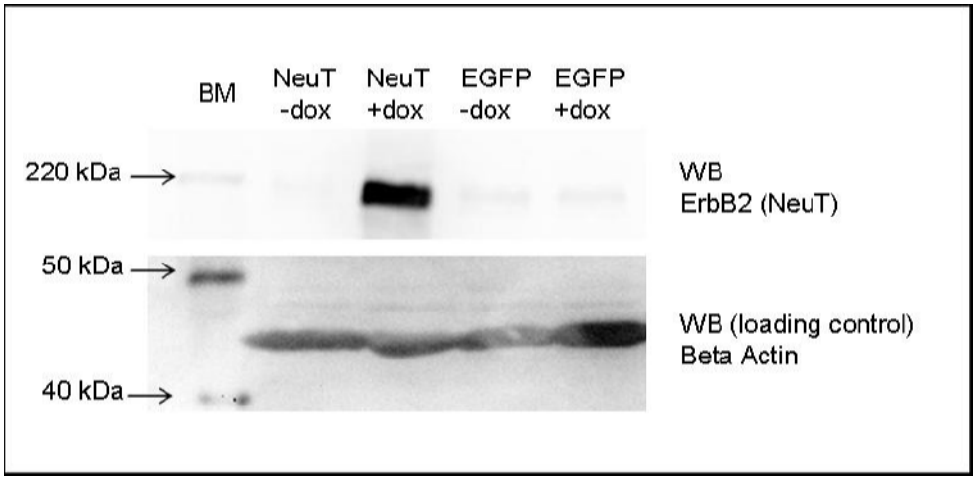

Figure 19: ErbB2 (NeuT) protein expression in MCF7/NeuT (NeuT) and MCF7/EGPF (EGFP) cells treated with (+) or without (-) dox (Day 7). Beta actin was used as loading control. Protein expression is induced by dox and is isolated in the MCF7/NeuT cell line only.

3.1.3 Fluorescence Activated Cell Sorting Analysis (FACS) of NeuT and EGFP Expression

FACS was utilised to confirm protein expression of the fluorescent green marker protein, EGFP and NeuT. Cells were treated with or without doxycycline for 7 days then fluorescent labelled anti-bodies against EGFP and NeuT were analysed using FACS. The results indicate that over 90% of the NeuT labelled non-treated cells and 99% of the EGFP labelled non-treated cells were gated into the M1 region of the histogram (Figure 20a,b; Table 2) indicating no expression of either of these proteins. Over 93% of the NeuT labelled treated cells and 97% of the EGFP labelled treated cells were gated into the M2 region of the histogram (Figure 21a,b; Table 3) indicating a shift from no expression to expression of NeuT and EGFP protein. The forward and side scatter plots also confirm these results by showing very small and condensed cells in the non-treated and very large cells in the treated which is an indication of senescence since senescencing cells increase in size (Figure 20c and 21c respectively).

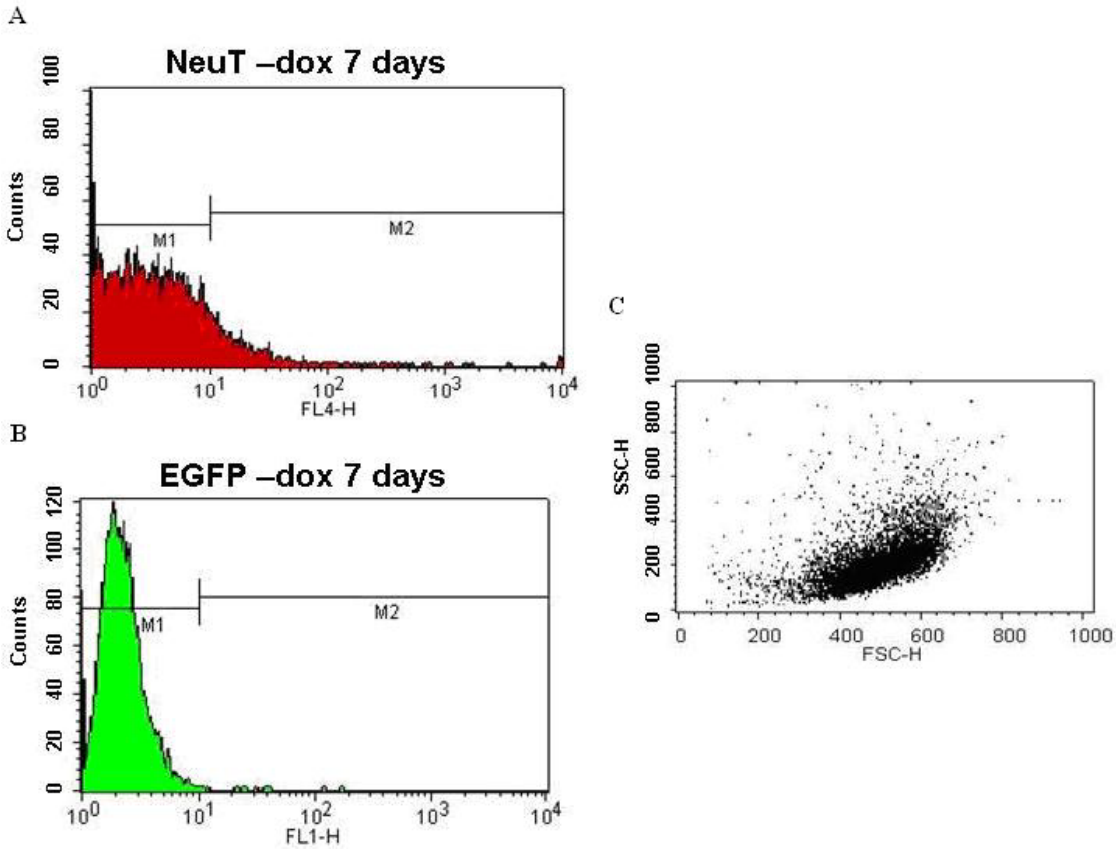

Figure 20: FACS analysis of non-treated MCF7/NeuT cells (Day 7). MCF7/NeuT cells do not respond to the fluorescent antibodies when dox is not present. The majority of cells are gated into the M1 region of the histograms (A and B). The forward and side scatter plot (C) indicates the cells are small in size by being in the lower area of the plot and similar in viability due to the cluster pattern.

Table 2: Percentage gated in FACS analysis of non-treated MCF7/NeuT cells.

NeuT Detection of MCF7/NeuT –dox (7 days)			**EGFP Detection of MCF7/NeuT –dox (7 days)**		
Marker	**Events**	**% Gated**	**Marker**	**Events**	**% Gated**
All	10000	100.00	**All**	10000	100.00
M1	9010	90.10	**M1**	9985	99.85
M2	990	9.90	**M2**	15	0.15

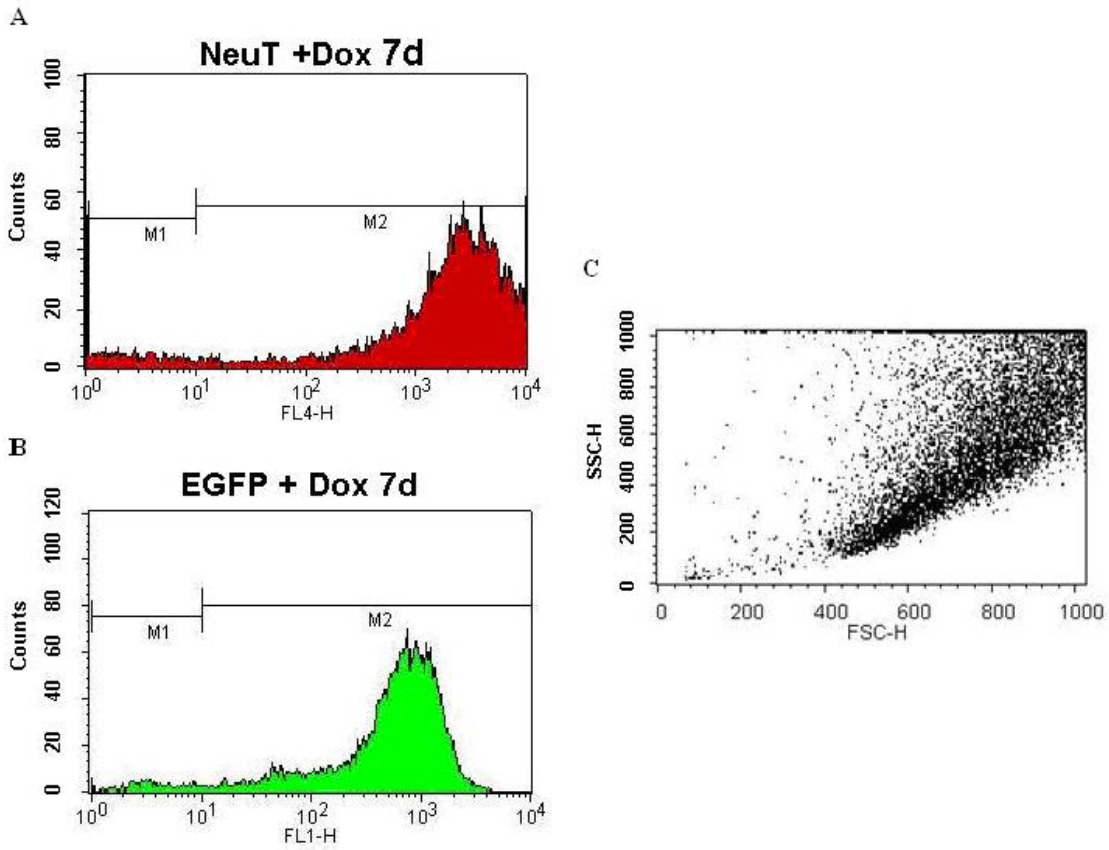

Figure 21: FACS analysis of dox treated MCF7/NeuT Cells (Day 7). MCF7/NeuT cells respond to the fluorescent antibodies when dox is present. The majority of cells are gated into the M2 region of the histograms (A and B). The forward and side scatter plot (C) indicates the cells are large in size by being in the upper area of the plot and similar in viability due to the cluster pattern.

Table 3: Percentage gated in FACS analysis of treated MCF7/NeuT cells.

NeuT Detection of MCF7/NeuT +dox (7 days)			EGFP Detection of MCF7/NeuT +dox (7 days)		
Marker	**Events**	**% Gated**	**Marker**	**Events**	**% Gated**
All	10000	100.00	**All**	10000	100.00
M1	424	4.24	**M1**	237	2.37
M2	9365	93.65	**M2**	9764	97.64

3.1.4 Fluorescent Confocal Microscopy of EGFP Expression in MCF7/NeuT and MCF7/EGFP Cells

MCF7/NeuT and MCF7/EGFP cells were subjected to fluorescent confocal microscopy to ensure the EGFP vector expressing gene is functioning. Photos were taken at a 20x objective using the FITC channel of the fluorescent microscope. Figure 22, depicts a set of images of MCF7/NeuT and MCF7/EGFP cells fluorescing the green fluorescent protein, EGFP, after 7 days of dox treatment. This indicates the vector system is able to express EGFP protein upon dox exposure.

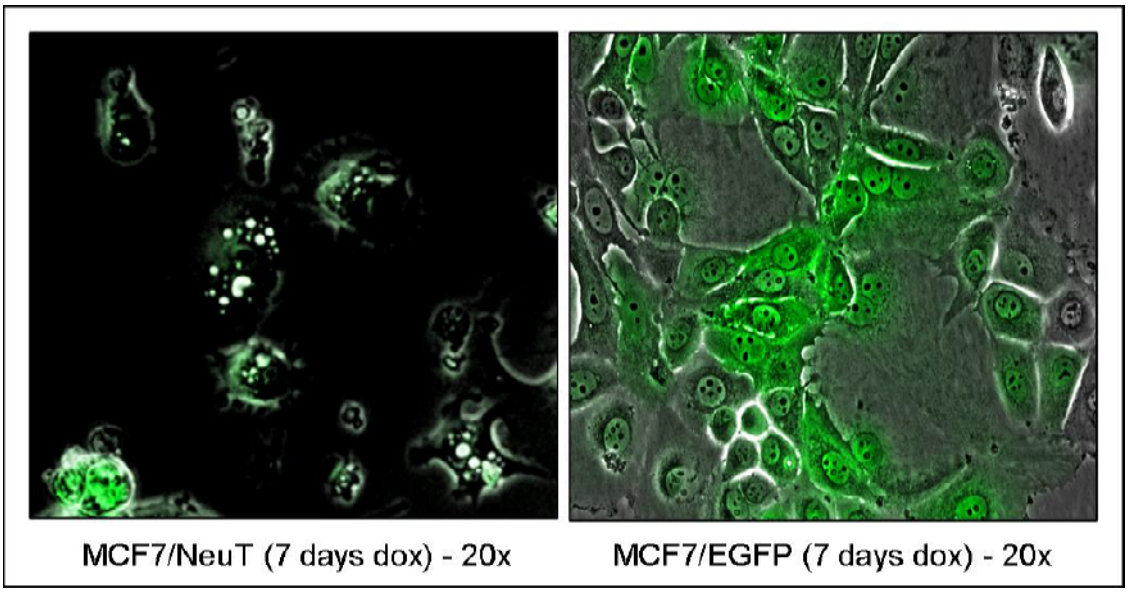

Figure 22: MCF7/NeuT and MCF7/EGFP cells expressing the green fluorescent protein, EGFP, after 7 days of dox treatment taken at 20x using the FITC channel. This indicates the vector system is able to express EGFP upon dox exposure. The images represent multiple images from each cell type.

3.2 Inducible ErbB2/HER2 (NeuT) Expression Leads to a Senescent Phenotype

Upon up-regulation of NeuT expression, the MCF7/NeuT cells begin to depict senescent like characteristics. These characteristics are a decrease in proliferation, development of vacuole structures within the cytoplasm, a centralised nucleolus, and a very large and flattened-type morphology. The phenotypic characteristics begin to occur in MCF7/NeuT cells after roughly 24 hours of over expression of NeuT. Genotypically, expression of the senescence associated marker gene, cyclin dependent kinase inhibitor 1A or better known as p21 becomes highly up-regulated. Not only p21 but other

senescent associated and cell cycle genes become up- or down-regulated as senescence progresses within a cell. These next few sections will demonstrate the characterisation of the MCF7/NeuT cell line phenotypically and genotypically as it enters senescence.

3.2.1 Senescent Morphology

3.2.1.1 Phase-contrast Confocal Microscopy of MCF7/NeuT Cells

The MCF7/NeuT cells treated with and without dox were subjected to phase-contrast microscopy after seven days of incubation with dox. The images in figure 23 depict differences between non-senescent proliferating MCF7/NeuT cells and senescent MCF7/NeuT after treatment with dox. These results portray MCF7/NeuT cells treated with dox developing senescent characteristics such as an enlarged and flattened-type morphology, a centralised nucleolus and the development of vacuole structures within the cytoplasm. From a visual observation, it can be stated that the MCF7/NeuT cell line enters a senescent state when treated with dox and in turn triggering the up-regulation of NeuT.

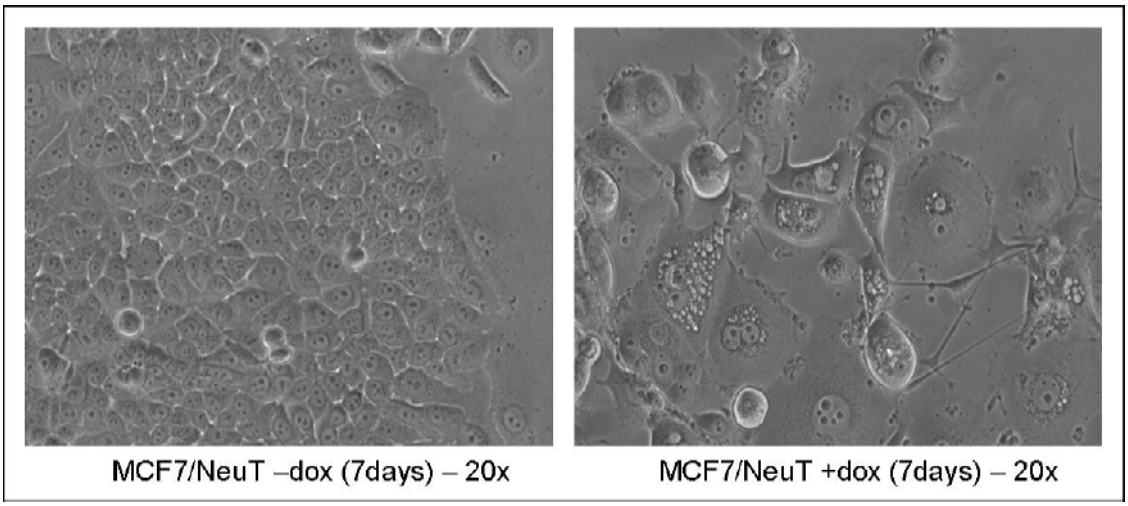

Figure 23: Phase-contrast microscopy of MCF7/NeuT cells treated with or without dox for 7 days. Dox treated cells depict senescent characteristics with low cell division, enlarged cytoplasm, development of vacuoles and a centralised nucleolus. Images represent multiple images taken of each condition.

3.2.1.2 Senescence Associated β-galactosidase Activity Measured in MCF7/NeuT Cells

To confirm the MCF7/NeuT cells are entering senescence when over-expressing NeuT, β-galactosidase activity was measured. β-galactosidase activity is known to be associated with senescence as the enzyme is highly expressed in the lysosomes of senescent cells. Figure 24 demonstrates that cells treated with dox, over-expressing NeuT, show β-galactosidase activity (shown in green), where as those not treated with dox and not over-expressing NeuT do not express any β-galactosidase activity.

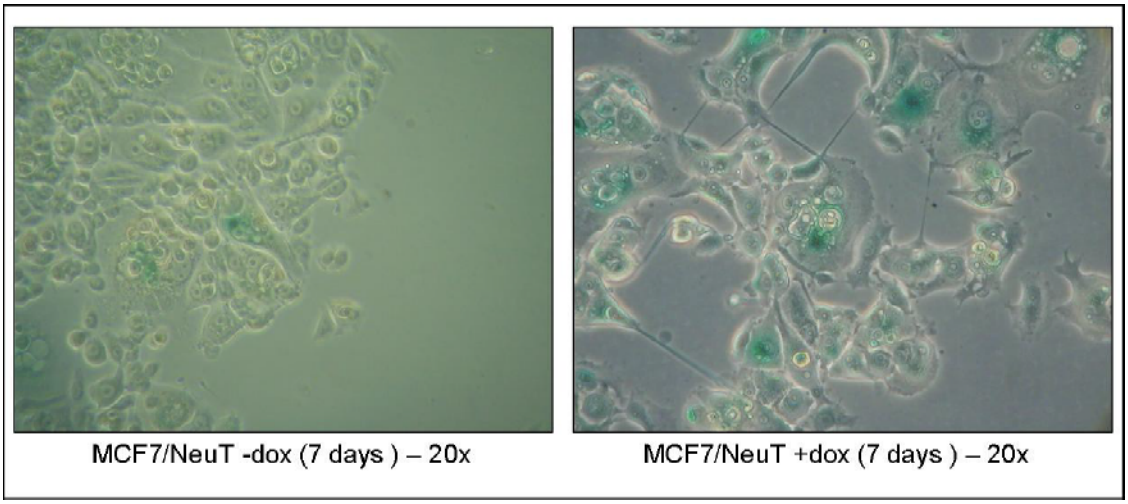

Figure 24: β-galatosidase activity (shown in green, right) detected in MCF7/NeuT cells treated with dox. The enzyme β-galactosidase is highly expressed and accumulates in the lysosomes of senescing cells.

3.2.2 Measurement of Gene Expression Activity in MCF7/NeuT and MCF7/EGFP Cells of Senescence Biomarkers and Cyclins

MCF7/NeuT and MCF7/EGFP cells were subjected to gene expression analysis to gain insight into the senescent signalling pathways utilised upon NeuT upregulation. A time course study was performed from 0h to 14 days of dox treatment in both cell lines using complete media replenishment without dox as a control. RT-qPCR using was then performed to measure mRNA expression in selected senescent biomarkers and cyclins. To measure the significance in expression a Mann-Whitney U test was performed on all samples using SPSS™ 16.0 where $p \leq 0.05$.

3.2.2.1 Reference Gene Selection for MCF7/NeuT and MCF7/EGFP Cell Lines

Prior to RT-qPCR investigation and analysis of selected senescent and cyclin biomarkers, MCF7/NeuT and MCF7/EGFP cells treated with or without dox were subjected to reference gene selection analysis using geNorm, an applet for Microsoft Excel™[73]. RT-qPCR was performed on common reference genes listed in section 2.2.7 using MCF7/NeuT and MCF7/EGFP samples treated with (7 days) or without dox. The Ct values for both cell types were calculated and entered into the geNorm programme. After analysis, geNorm provided the two most stable reference genes for the MCF7 cell line. Non-treated and treated cells were analysed and the TATA box binding protein (TBP) and Ubiquitin C (UBC) genes were chosen to be the best fit reference genes. Having a stability M-value of ≤0.15 for TBP and ≤0.32 for UBC both well below the threshold M-value of 1.50, these genes are considered to be relatively stable reference genes for normalisation of RT-qPCR assays when using the MCF7 cell line (Figures 25 and 26). Looking across the graphs, all of the selected reference genes could be considered a stable reference gene for both non-treated and treated cells since their M-values also fall below the desired threshold. However, for simplicity since TBP and UBC fell within the top 6 most stable reference genes in the majority of samples they were chosen and used for all RT-qPCR assays.

A pairwise variation was also tested using geNorm to determine the optimal number of reference genes needed for RT-qPCR normalisation. Looking at the pairwise variation graphs (Figures 27 and 28) all of the samples showed a V-value of ≤0.070 for the use of 2 to 3 reference genes for normalisation. This is well below the threshold V-value of 0.15, indicating that two reference genes are sufficient for RT-qPCR normalisation.

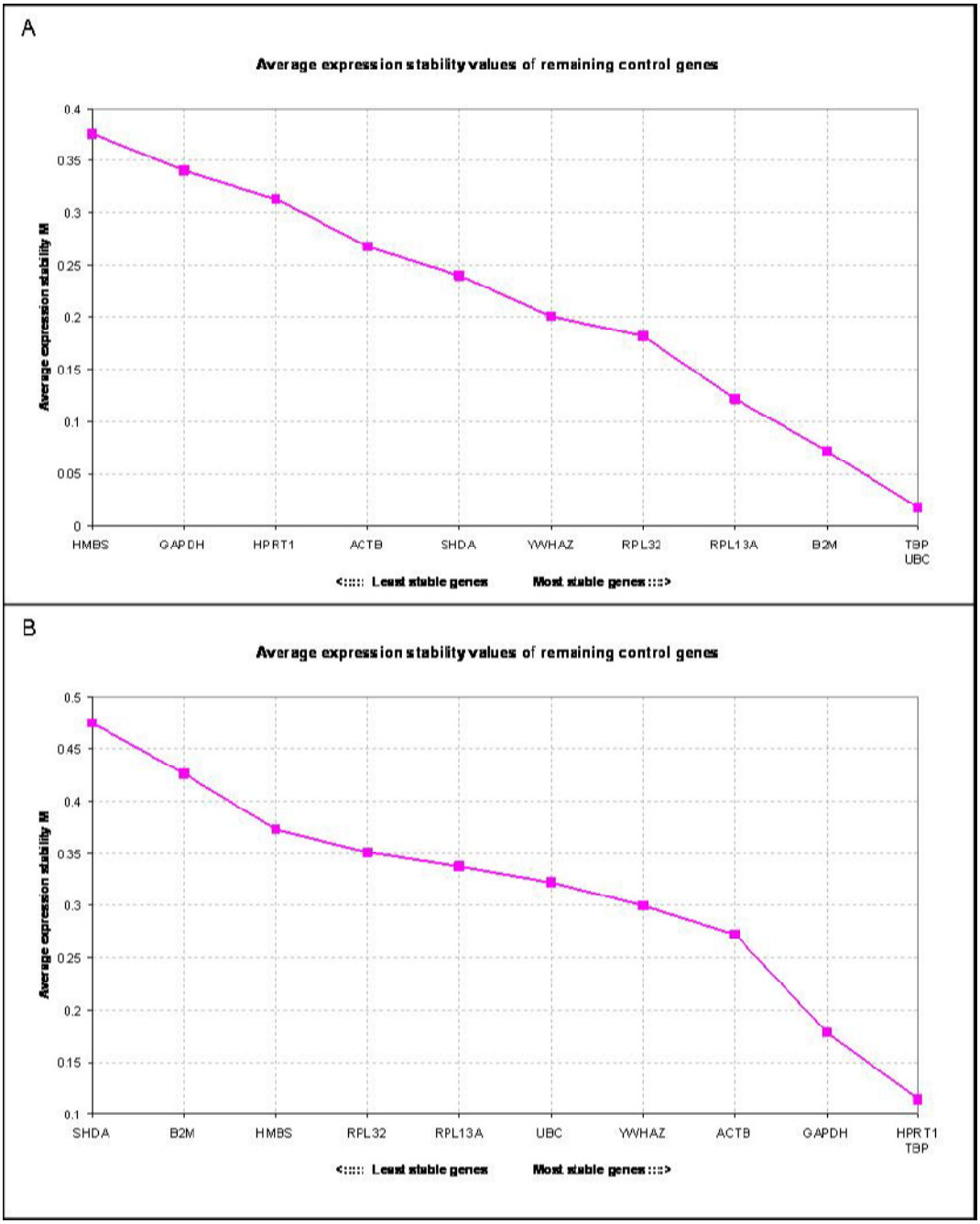

Figure 25: Average expression stability values for reference gene selection in MCF7/NeuT cells. A) expression stability values for MCF7/NeuT non-treated cells (-dox) and B) expression stability values for MCF7/NeuT cells treated (+dox, 7days). All listed reference genes are within the 1.5 M-value threshold therefore, any of these genes could be used for RT-qPCR normalisation. Values are an average of 3 independent experiments.

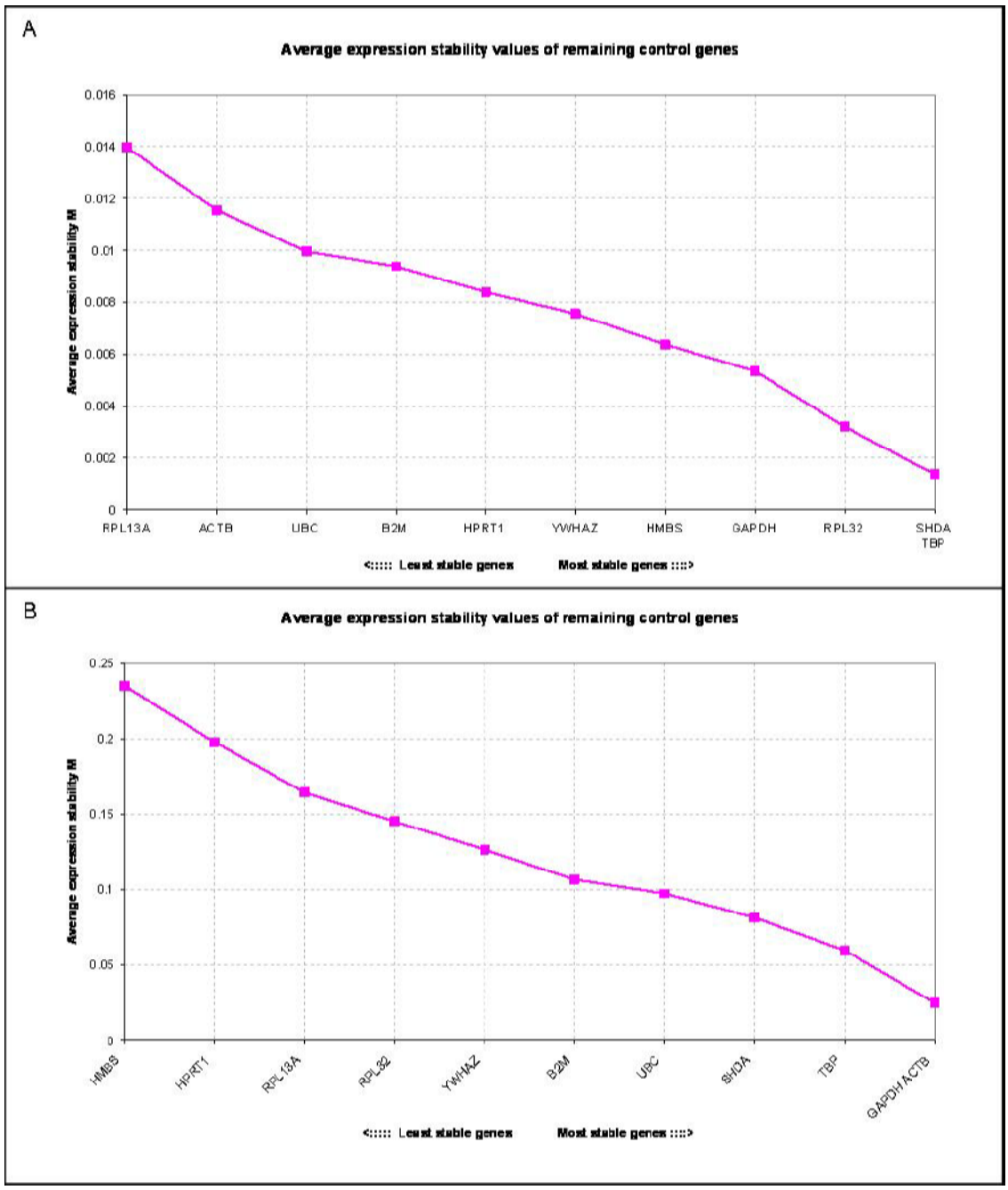

Figure 26: Average expression stability values for reference gene selection in MCF7/EGFP cells. A) expression stability values for MCF7/EGFP non-treated cells (-dox) and B) expression stability values for MCF7/EGFP cells treated (+dox, 7days). All listed reference genes are within the 1.5 M-value threshold therefore, any of these genes could be used for RT-qPCR normalisation. Values are an average of 3 independent experiments.

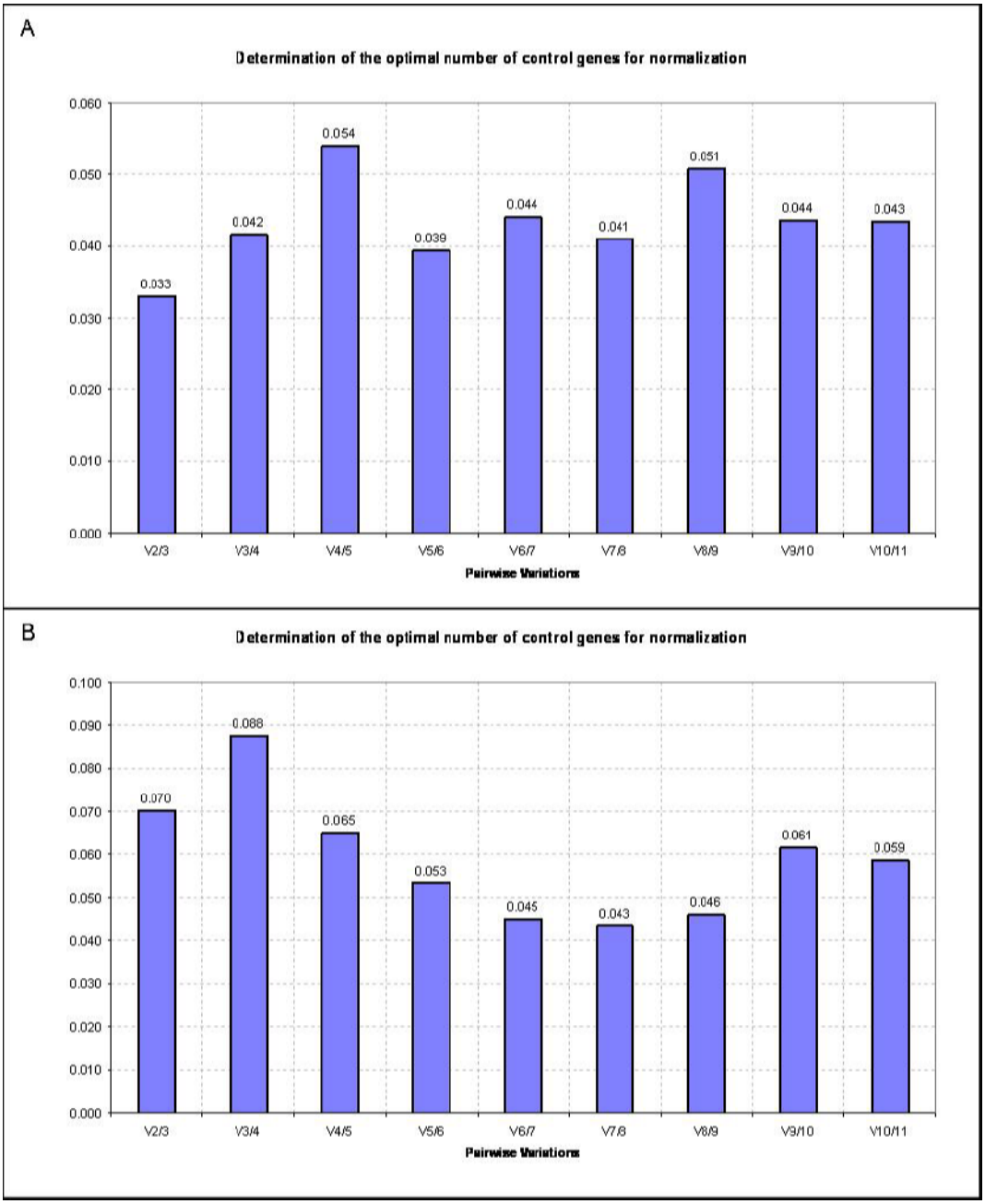

Figure 27: Pairwise variation for determination of optimal number of reference genes needed for normalisation of MCF7NeuT cells. A) pairwise variation values for MCF7/NeuT non-treated cells (-dox) and B) pairwise variation values for MCF7/NeuT cells treated (+dox, 7days). The variation value for 2 to 3 reference genes is below the 0.15 threshold therefore only 2 reference genes are needed for RT-qPCR normalisation. Values are an average from 3 independent experiments.

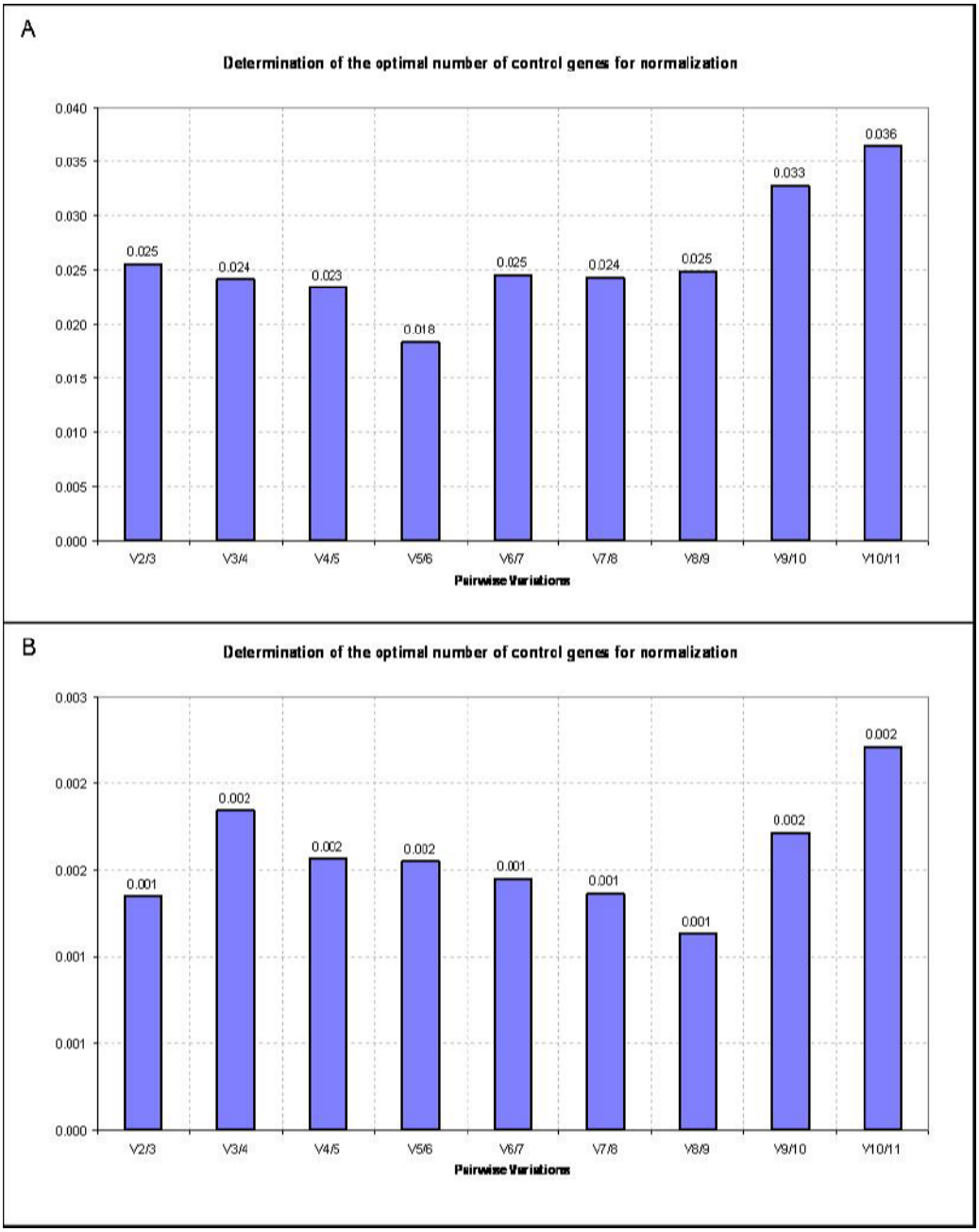

Figure 28: Pairwise variation for determination of optimal number of reference genes needed for normalisation of MCF7/EGFP cells. A) pairwise variation values for MCF7/EGFP non-treated cells (-dox) and B) pairwise variation values for MCF7/EGFP cells treated (+dox, 7days). The variation value for 2 to 3 reference genes is well below the 0.15 threshold value therefore, only 2 reference genes are needed for RT-qPCR normalisation. Values are an average from 3 independent experiments.

3.2.2.2 Gene Expression Analysis of Selected Senescence Biomarkers

Cyclin Dependent Kinase Inhibitor 1A (P21)

P21 was found to be significantly upregulated after 1 minute of dox incubation by approximately 2.0-fold (Figure 29). At 3 hours of dox incubation, P21 became highly upregulated and remained expressed with an average fold increase across the remaining time points of approximately 6.0. mRNA expression of P21 peaked at 6 hours (Figure 29) with an average fold increase of 12.0. This large increase in expression correlates with a decline in P53 expression at 6 hours which is to be expected since P53 upregulation initiates the upregulation of P21. Comparing MCF7/NeuT P21 expression to MCF7/EGFP P21 expression, P21 levels remain relatively low in the MCF7/EGFP cells and are expressed similarly in both non-treated and treated samples (Figure 30). These results indicate that without the overexpression of NeuT, P21 does not become upregulated.

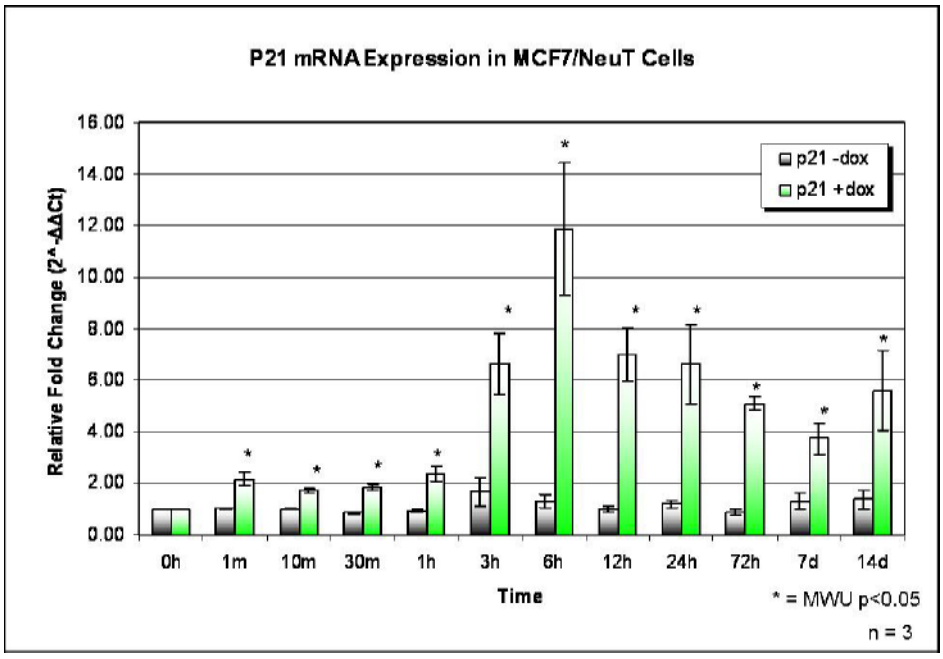

Figure 29: P21 mRNA expression in MCF7/NeuT cells treated with or without dox. P21 expression is highly upregulated in cells treated with dox. Data values represent the mean 2^-ΔΔCt values of three independent experiments. MWU – Mann-Whitney U test.

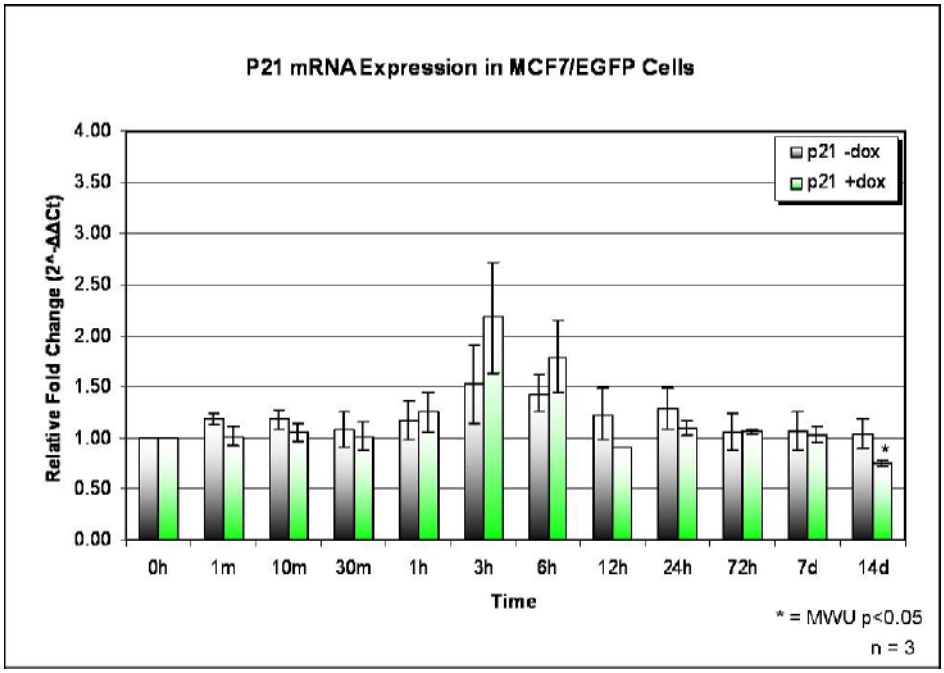

Figure 30: P21 mRNA expression in MCF7/EGFP cells treated with or without dox. P21 expression is expressed relatively at similar levels in cells treated with dox compared to those without. Data values represent the mean 2^-ΔΔCt values of three independent experiments. MWU – Mann-Whitney U test.

Tumour Protein 53 (P53)

mRNA expression levels of P53 were found to be significantly upregulated from 1 minute to 3 hours of dox incubation with an increase in expression between 2 – 2.5 fold (Figure 31). At 6 hours dox incubation, P53 levels began to decline toward normal levels reaching a significant 2 fold decrease in expression at 7 and 14 days dox incubation. This decline in P53 mRNA levels at 6 hours correlates with an increase in P21 expression (Figure 29). As part of a negative feedback mechanism, P53 mRNA levels decrease with increasing P21 levels. P53 levels in the MCF7/EGFP showed some significant upregulation 1 to 6 hours (Figure 32). However, when looking across the time course P53 mRNA levels in treated MCF7/EGFP samples remained relatively low, near non-treated levels. The slight increase in P53 expression may be a side effect from dox incubation or the cell samples could have been reaching confluency causing this fluctuation at a few of the time points due to the release of cell cycle arrest signals. This data demonstrates the use of the P53 pathway in overexpressing NeuT samples.

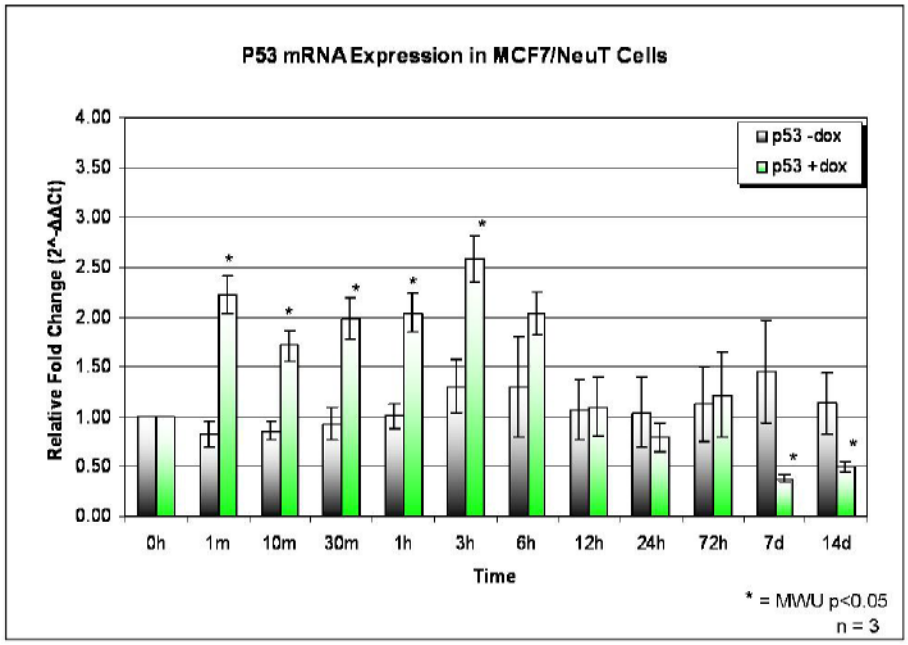

Figure 31: P53 mRNA expression in MCF7/NeuT cells treated with or without dox. P53 expression is upregulated in cells treated with dox at early time points and then declining in expression which correlates with an increase in P21 expression. Data values represent the mean 2^-ΔΔCt values of three independent experiments. MWU – Mann-Whitney U test.

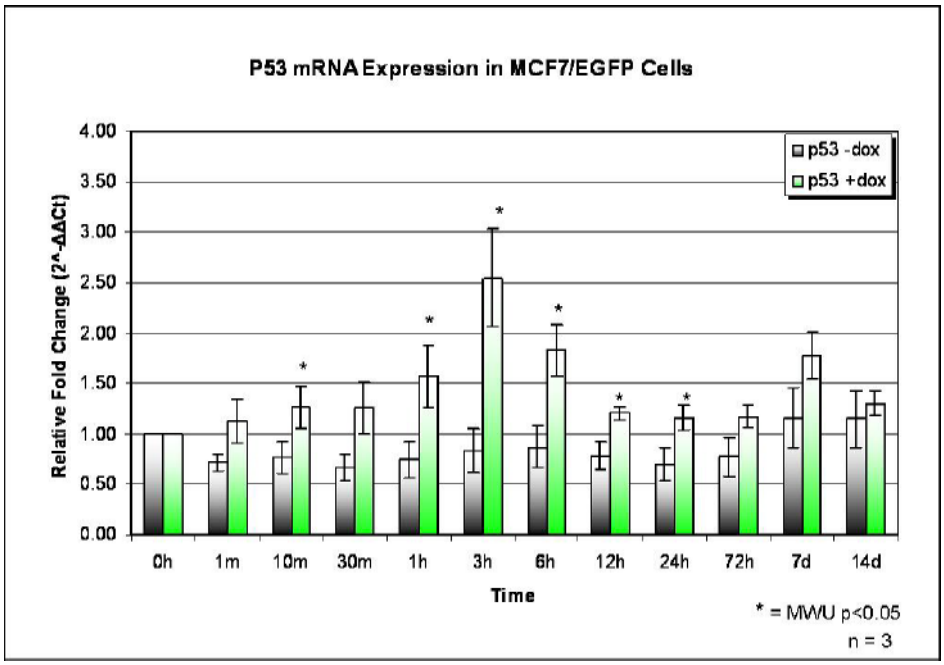

Figure 32: P53 mRNA expression in MCF7/EGFP cells treated with or without dox. P53 expression is expressed relatively at similar levels in cells treated with dox compared to those without. Although some significant increases, mRNA levels do not reach those of MCF7/NeuT cells treated with dox. This could be a side effect of dox incubation or the cell samples could have been reaching confluency and thereby releasing cell cycle arrest signals. Data values represent the mean 2^-ΔΔCt values of three independent experiments. MWU – Mann-Whitney U test.

Phosphatase and Tensin Homolog (PTEN)

In MCF7/NeuT cells, PTEN mRNA expression was significantly upregulated after 1 minute by approximately 1.75-fold peaking at 3 hours of incubation with an approximately 2.25-fold increase (Figure 33). Expression steadily declines after 24 hours of incubation to near non-treated levels throughout the rest of the time course. MCF7/EGFP cells show no changes in PTEN expression between non-treated and treated samples (Figure 34). These results indicate that PTEN expression can be regulated by the overexpression of NeuT in the initial stages of induction.

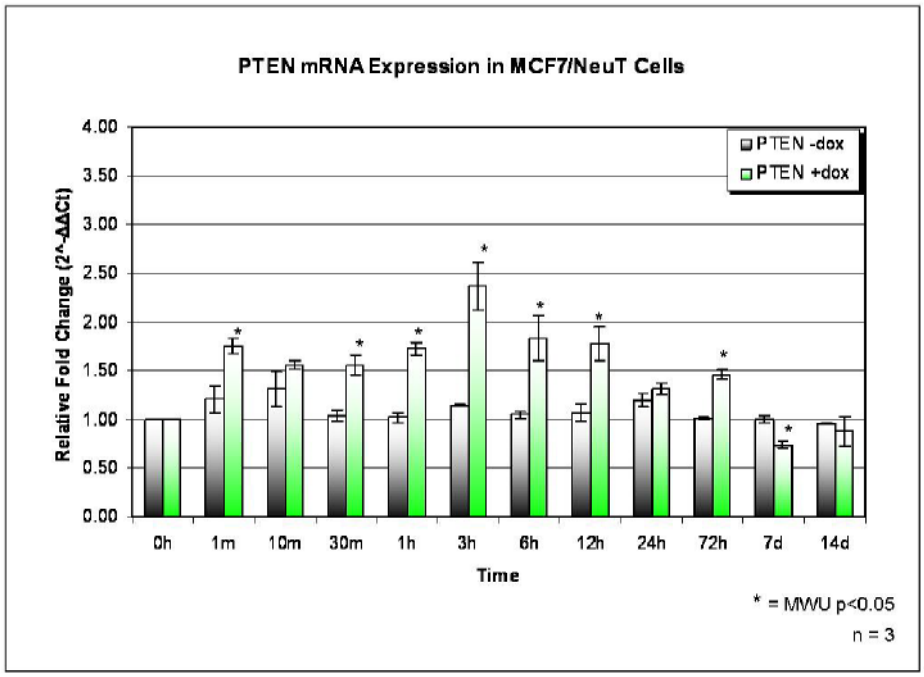

Figure 33: PTEN mRNA expression in MCF7/NeuT cells treated with or without dox. PTEN expression is upregulated in cells treated with dox at early time points and then declining to near levels of non-treated at later time points. Data values represent the mean 2^-ΔΔCt values of three independent experiments. MWU – Mann-Whitney U test.

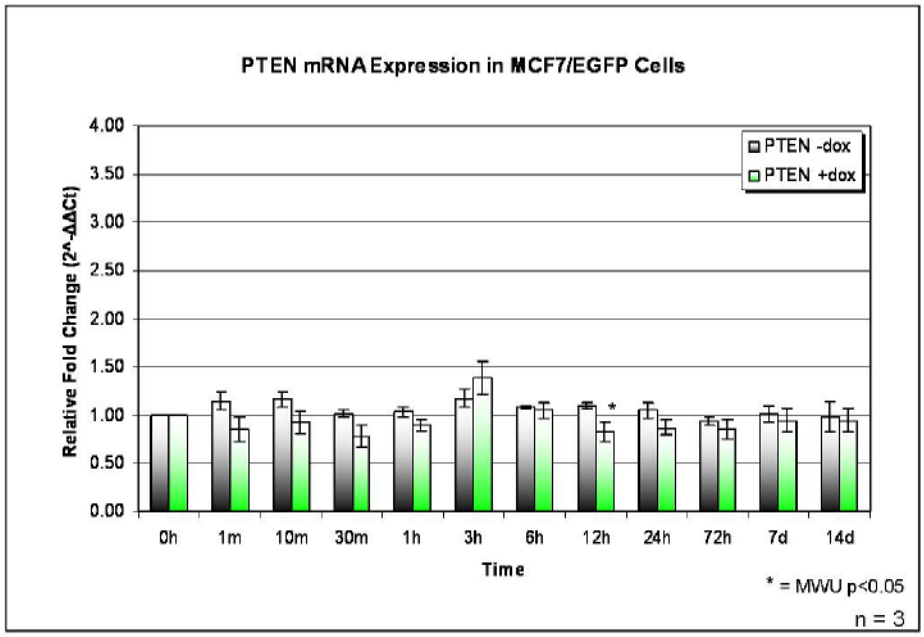

Figure 34: PTEN mRNA expression in MCF7/EGFP cells treated with or without dox. PTEN expression is expressed relatively at similar levels in cells treated with dox compared to those without. PTEN is not upregulated in MCF7/EGFP samples. Data values represent the mean 2^-ΔΔCt values of three independent experiments. MWU – Mann-Whitney U test.

Retinoblastoma (RB1)

RB1 was significantly upregulated after 10 minutes of dox incubation by approximately 2.75-fold in MCF7/NeuT cells (Figure 35). RB1 remains upregulated throughout the time course with levels averaging to about 2.25-fold and then decreasing to 1.25-fold at 7 and 14 days. Comparing MCF7/NeuT cells to MCF7/EGFP, MCF7/EGFP cells treated with dox showed significant upregulation of RB1 after 1 minute and remained slightly upregulated throughout the time course averaging around 1.5-fold (Figure 36). The levels of the treated MCF7/EGFP cells show some elevated expression. However, these mRNA levels are below that of the MCF7/NeuT cells treated with dox. Again like that of P53 this slight increase in dox treated samples could be a side effect of dox incubation or dependent on cellular stresses caused by confluency releasing then cell cycle arrest signals. These results depict RB1 upregulation in MCF7/NeuT cells overexpressing NeuT.

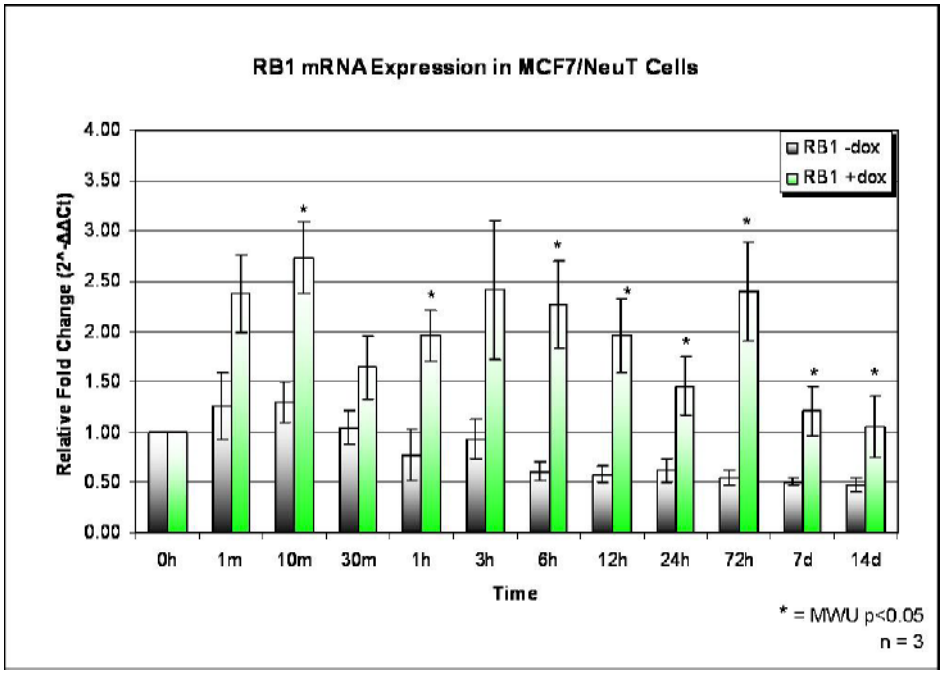

Figure 35: RB1 mRNA expression in MCF7/NeuT cells treated with or without dox. RB1 expression is upregulated in cells treated with dox early on and remains upregulated throughout the time course. Data values represent the mean 2^-ΔΔCt values of three independent experiments. MWU – Mann-Whitney U test.

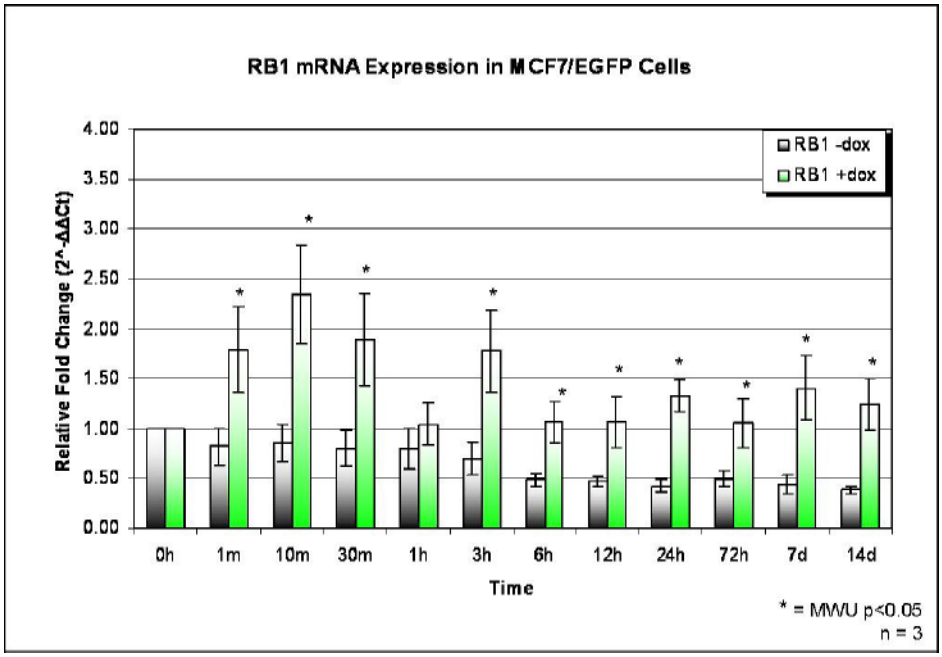

Figure 36: RB1 mRNA expression in MCF7/EGFP cells treated with or without dox. RB1 expression is upregulated in cells treated with dox compared to those without. RB1 mRNA levels are lower in treated MCF7/EGFP samples compared to treated MCF7/NeuT samples. However the slight increase in dox treated samples could be a side effect from dox or dependent on cellular stresses caused by confluency thereby releasing cell cycle arrest signals. Data values represent the mean 2^-ΔΔCt values of three independent experiments. MWU – Mann-Whitney U test.

Mitogen-Activated Protein Kinase 14 (P38)

P38 showed no upregulation in both MCF7/NeuT and MCF7/EGFP cells treated or non-treated with dox (Figure 37 and 38, respectively). This indicates that upon overexpression of NeuT, P38 mRNA expression does not change.

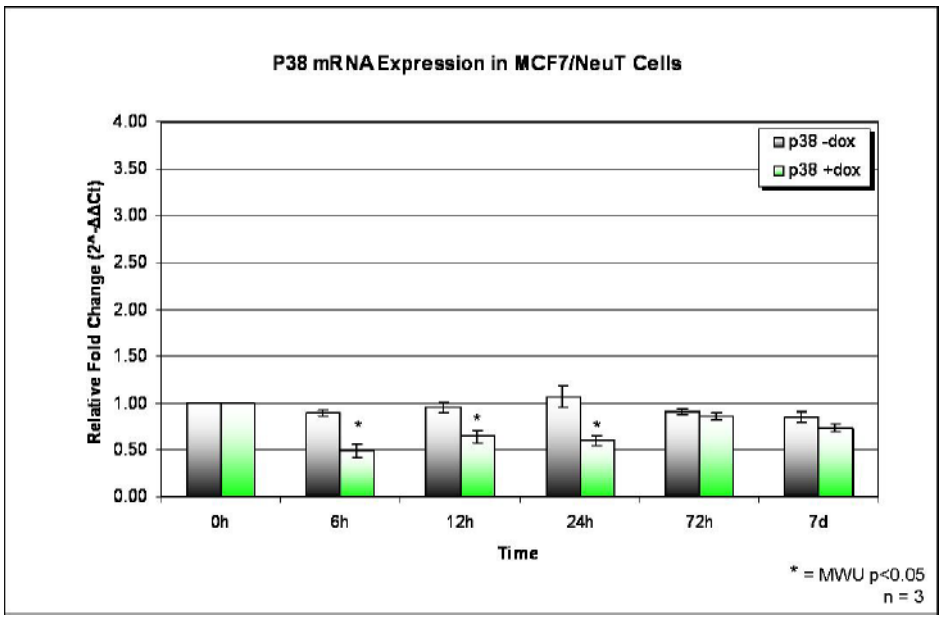

Figure 37: P38 mRNA expression in MCF7/NeuT Cells treated with or without dox. P38 expression is downregulated in cells treated with dox compared to those without. Data values represent the mean 2^-ΔΔCt values of three independent experiments. MWU – Mann-Whitney U test.

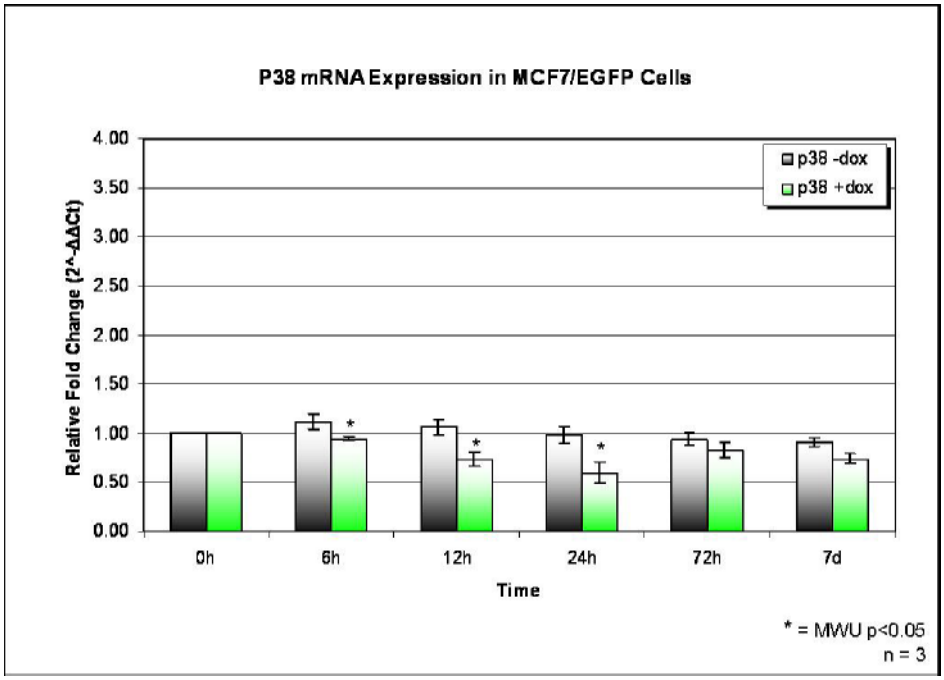

Figure 38: P38 mRNA expression in MCF7/EGFP cells treated with or without dox. P38 expression is downregulated in cells treated with dox compared to those without. Data values represent the mean 2^-ΔΔCt values of three independent experiments. MWU – Mann-Whitney U test.

3.2.2.3 Gene Expression Analysis of Selected Cyclin Biomarkers

Cyclin D1 (CCND1)

CCND1 was found to be significantly upregulated after 1 minute of treatment in MCF7/NeuT cells by approximately 1.75-fold (Figure 39). At 3 hours this increased to 3-fold and peaked at 24 hours by a 3.5-fold increase in CCND1 expression. CCND1 continues to remain elevated until about 3 days where it then declines at 7 days to non-treated mRNA levels. The MCF7/EGFP cells showed a significant downregulation in treated samples (Figure 40). However, these levels were found to be only slightly downregulated and remained relatively close to non-treated expression levels. These results indicate that upon overexpression of NeuT, CCND1 becomes upregulated in MCF7/NeuT cells.

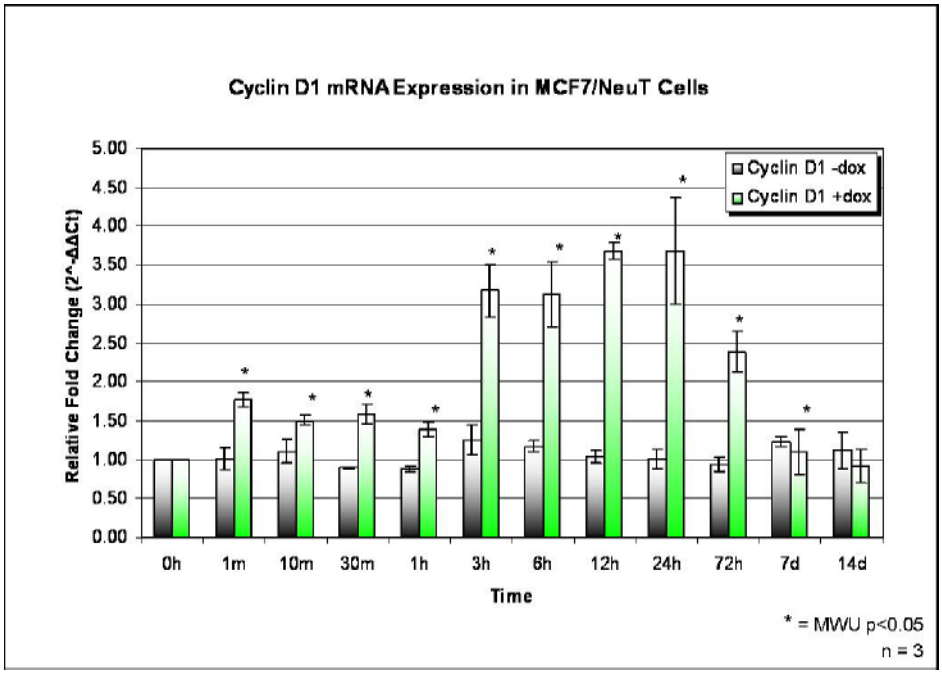

Figure 39: Cyclin D1 mRNA expression in MCF7/NeuT cells treated with or without dox. CCND1 expression is upregulated in cells treated with dox early on and remains upregulated throughout the time course. Data values represent the mean 2^-ΔΔCt values of three independent experiments. MWU – Mann-Whitney U test.

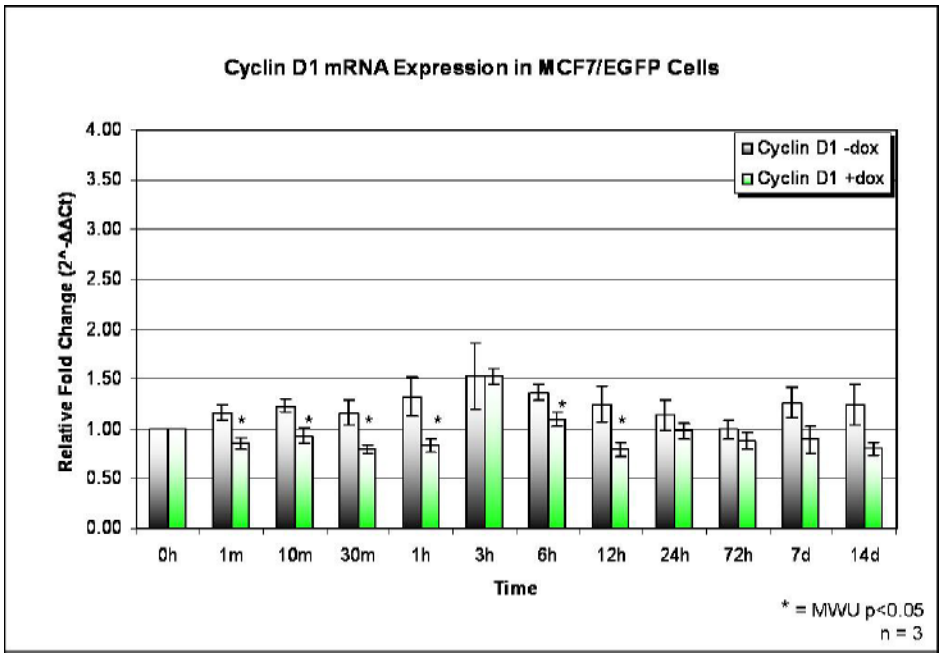

Figure 40: Cyclin D1 mRNA expression in MCF7/EGFP cells treated with or without dox. CCND1 expression slightly downregulated in cells treated with dox compared to those without. CCND1 mRNA levels are lower in MCF7/EGFP samples compared to treated MCF7/NeuT samples. Data values represent the mean 2^-ΔΔCt values of three independent experiments. MWU – Mann-Whitney U test.

Cyclin E1 (CCNE1)

Cyclin E1 mRNA expression was found to be significantly upregulated beyond non-treated levels after 3 hours of dox incubation and remained upregulated throughout the rest of the time course (Figure 41). At 6 hours, CCNE1 reached its highest expression with a 3.5-fold increase. These expression levels correlate with CCND1 where both become highly upregulated after 3 hours of dox incubation (Figures 39 and 41). Compared to MCF7/EGFP cells, CCNE1 is significantly downregulated at some time points (Figure 42). However, this could be due to variation in the cell cycle across cells and samples. These results conclude that upon NeuT upregulation a strong induction of CCNE1 is produced.

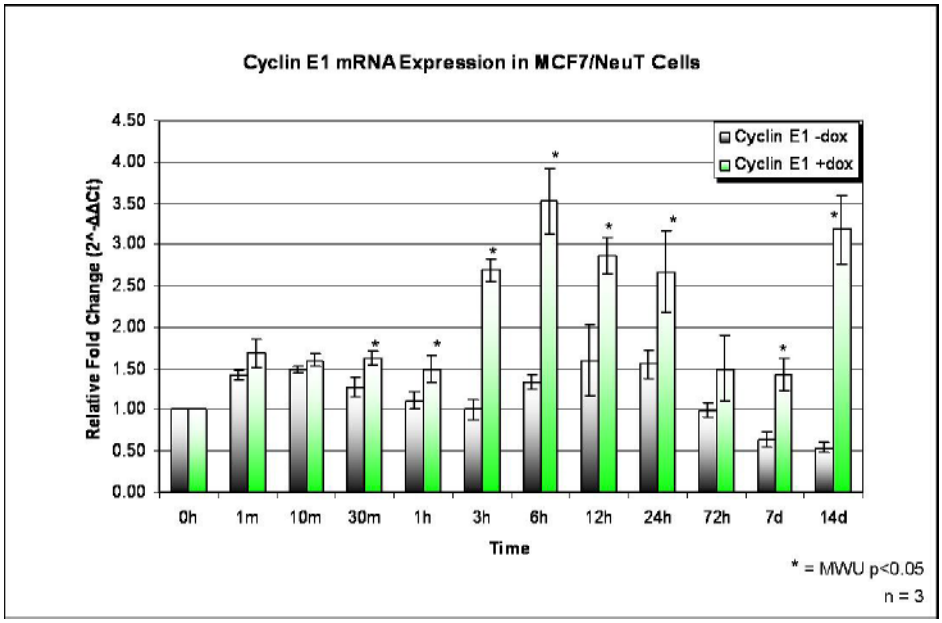

Figure 41: Cyclin E1 mRNA expression in MCF7/NeuT cells treated with or without dox. CCNE1 expression is upregulated in cells treated with dox. Data values represent the mean 2^-ΔΔCt values of three independent experiments. MWU – Mann-Whitney U test.

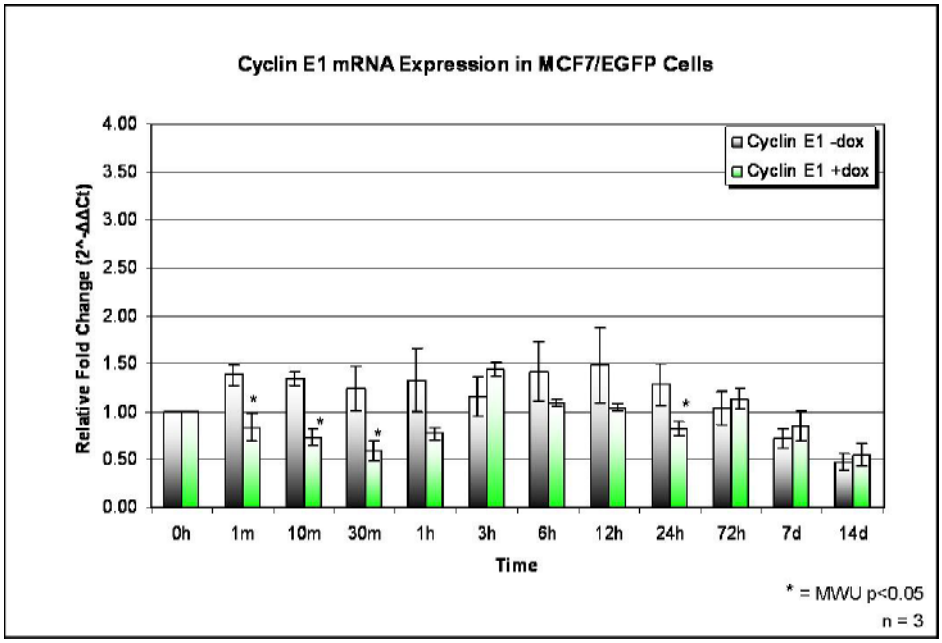

Figure 42: Cyclin E1 mRNA expression in MCF7/EGFP cells treated with or without dox. CCNE1 expression slightly downregulated in cells treated with dox compared to those without. CCNE1 mRNA levels are lower in MCF7/EGFP samples compared to treated MCF7/NeuT samples. Data values represent the mean 2^-ΔΔCt values of three independent experiments. MWU – Mann-Whitney U test.

Cyclin B2 (CCNB2)

Cyclin B2 mRNA expression levels were found to be relatively low compared to that of CCND1 (Figure 39) and CCNE1 (Figure 41). However, there was a significant increase in expression by more than 1.5-fold after 30 minutes of dox incubation in the MCF7/NeuT cells (Figure 43). Nevertheless, this level when comparing to other initial time points does not go above non-treated levels. Interestingly, a significant decrease in CCNB2 expression was detected after 6 hours of dox incubation. This decline then continues throughout the rest of the time course which correlates with the upregulation of P21 at 6 hours (Figure 29). MCF7/EGFP in comparison to MCF7/NeuT CCNB2 mRNA expression levels remained relatively unexpressed between non-treated and treated samples (Figure 44). These results indicate a strong decrease in CCNB2 upon NeuT overexpression.

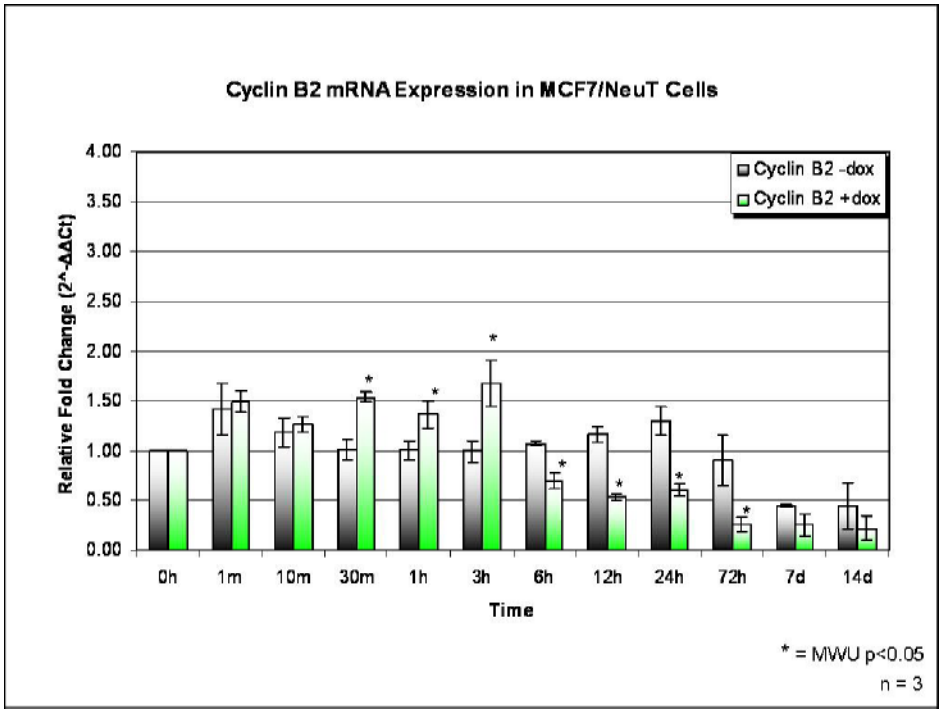

Figure 43: Cyclin B2 mRNA expression in MCF7/NeuT cells treated with or without dox. CCNB2 expression is significantly downregulated in cells after 6 hours of treatment. Data values represent the mean 2^-ΔΔCt values of three independent experiments. MWU – Mann-Whitney U test.

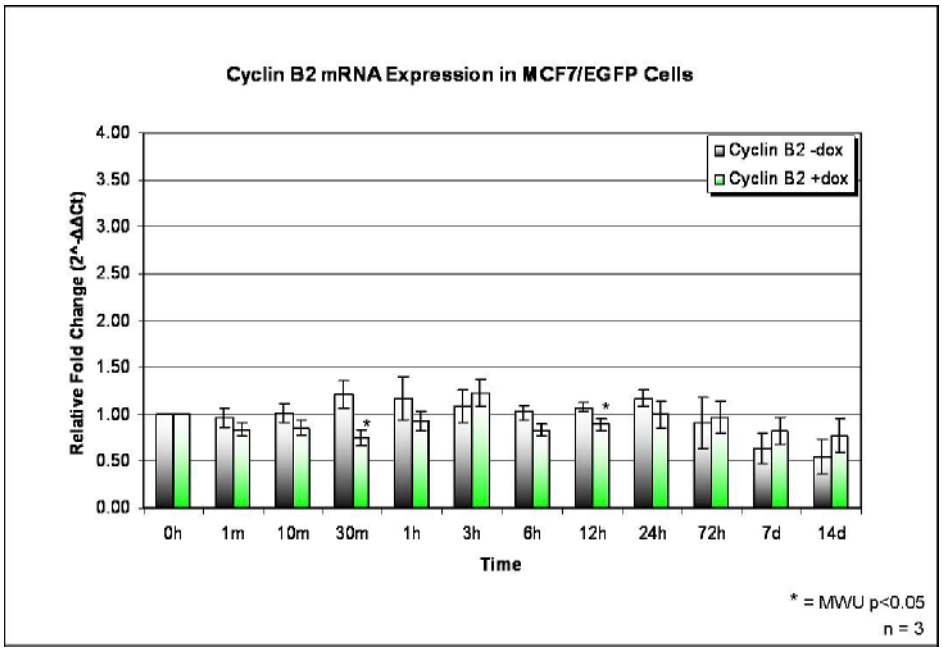

Figure 44: Cyclin B2 mRNA expression in MCF7/EGFP cells treated with or without dox. No change in CCNB2 expression levels in both non-treated and treated samples across the time course. Data values represent the mean 2^-ΔΔCt values of three independent experiments. MWU – Mann-Whitney U test.

3.2.2.4 Pituitary Tumour Transforming Gene 1 (PTTG1) Gene Expression Analysis in MCF7/NeuT and MCF7/EGFP Cells

PTTG1 was measured in non-treated and treated MCF7/NeuT and MCF7/EGFP cells. Overall there was little expression of PTTG1 in treated MCF7/NeuT cells with a 4-fold decrease in expression after 12 hours of dox incubation (Figure 45). Interestingly, this decline occurs soon after P21 becomes highly upregulated (Figure 29). MCF7/EGFP cells treated with dox showed significant increases in expression after 12 hours by approximately 2-fold indicating dox may have had a slight effect on PTTG1 mRNA expression (Figure 46). If this is a possibility than the levels of PTTG1 in NeuT overexpressing MCF7/NeuT samples would be much lower. Another possibility for the rise in PTTG1 expression in MCF7/EGFP cells treated with dox could be related to confluency at time of collection since PTTG1 is involved in cell prolieration. Nevertheless, PTTG1 downregulation was found to be significant in the MCF7/NeuT dox treated samples indicating that upon NeuT overexpression PTTG1 becomes downregulated.

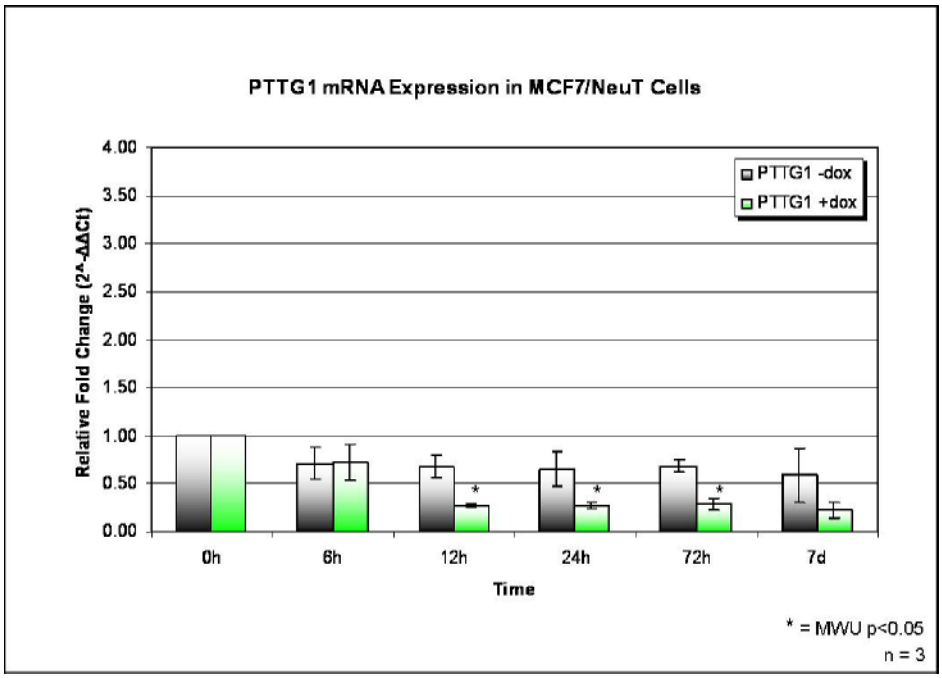

Figure 45: PTTG1 mRNA expression in MCF7/NeuT cells treated with or without dox. PTTG1 expression is significantly downregulated in cells after 12 hours of treatment. Data values represent the mean 2^-ΔΔCt values of three independent experiments. MWU – Mann-Whitney U test.

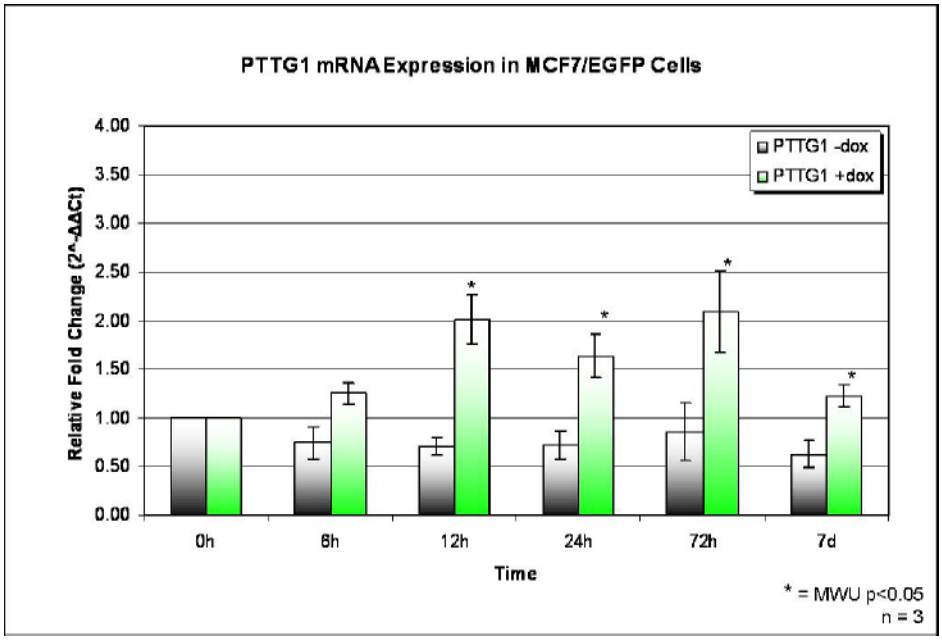

Figure 46: PTTG1 mRNA expression in MCF7/EGFP cells treated with or without dox. PTTG1 expression levels become significantly upregulated after 12 hours of treatment. This could be a side effect of dox incubation or due to cellular stresses caused by confluency. Data values represent the mean 2^-ΔΔCt values of three independent experiments. MWU – Mann-Whitney U test.

3.2.3 siRNA Inhibition of Cyclin Dependent Kinase Inhibitor 1A (P21) Abrogates Senescence

3.2.3.1 Optimisation and Validation of P21 Knockdown Oligoribonucleotides

Prior to the use of P21 siRNA oligoribonucleotides for investigation into senescence, siRNA oligoribonucleotides were optimised and validated using RT-qPCR. MCF7/NeuT cells were subjected to siRNA and prepared as stated in the Materials and Methods section 2.2.8. For optimisation, three unique P21 siRNA oligoribonucleotide sequences were measured at concentrations of 10nM and 30nM in two independent experiments. Knockdown of beta-actin (ACTB) was used as a positive control to ensure transfection agent efficiency. A non-sense oligoribonucleotide was also used to account for any off-target knockdown effects. Figures 47 and 48 depict the relative fold changes in gene expression used to measure the knockdown efficiency of the three P21 siRNA oligoribonucleotides at two different concentrations, 10nM and 30nM respectively. Along with P21 and ACTB mRNA expression measurements, the reference genes determined in section 3.2.2.1 TBP and UBC were also measured to ensure that the

knockdown was restricted to P21 and ACTB only. P21, ACTB, TBP and UBC were also measured in transfection agent only samples to ensure that the transfection agent did not affect the genes of interest. Looking at the two figures, a final concentration of 30nM was determined to be the best concentration for an effective knockdown of P21 with an efficiency of more than 80% (0.20/1.0 $2^{-\Delta\Delta Ct}$). For all P21 knockdown experiments 30nM oligoribonucleotide concentrations were used. To ensure P21 knockdown efficiency was consistent, efficiency was measured at each respective time point throughout the time course study (See appendix 4).

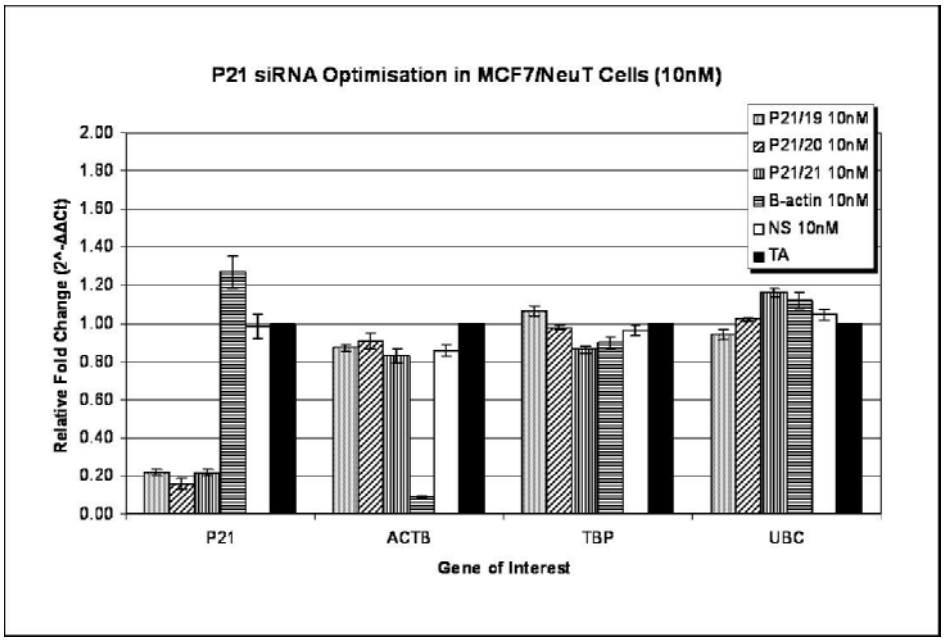

Figure 47: P21 siRNA optimisation in MCF7/NeuT cells (10nM). Relative fold change values for P21 (P21/19, P21/20, P21/21), beta-actin (β-actin), and nonsense (NS) siRNA oligoribonucleotides and transfection agent only (TA) samples. Gene expression was measured for P21, β-actin (ACTB) and the reference genes TBP and UBC. P21 knockdown efficiency in all three oligoribonucleotide sequences was >70% and ACTB knockdown efficiency for positive control was >80%.

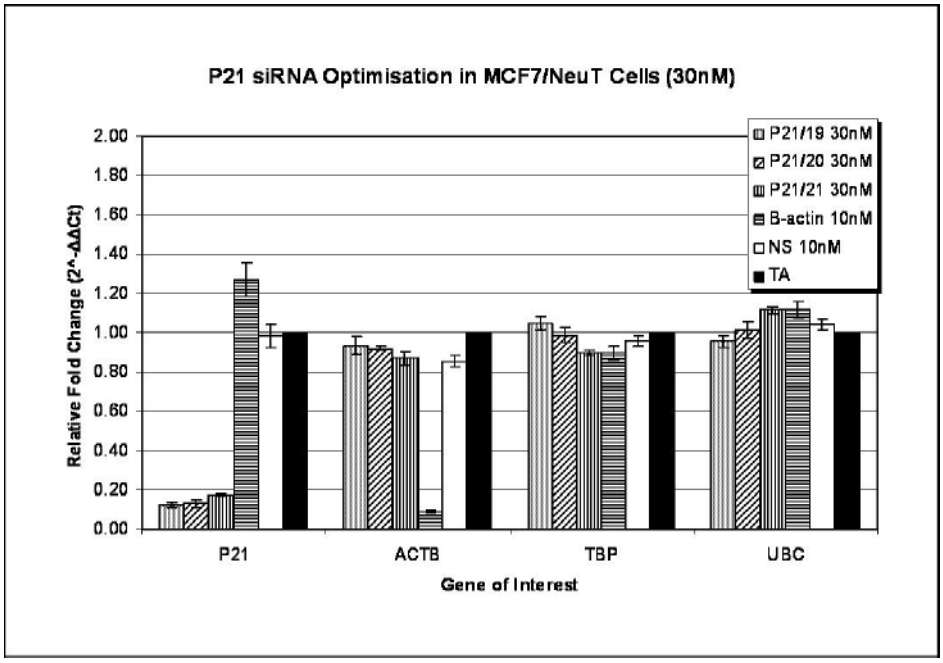

Figure 48: P21 siRNA optimisation in MCF7/NeuT cells (30nM). Relative fold change values for P21 (P21/19, P21/20, P21/21), beta-actin (β-actin), and nonsense (NS) siRNA oligoribonucleotides and transfection agent only (TA) samples. . Gene expression was measured for P21, β-actin (ACTB) and the reference genes TBP and UBC. P21 in all three oligoribonucleotide sequences and ACTB knockdown efficiency was measured to be >80%.

3.2.3.2 Gene Expression Analysis of Senescence Biomarkers in P21 Knockdown MCF7/NeuT Cells

After investigating the gene expression patterns of senescent and cyclin biomarkers in overexpressing NeuT MCF7 cells (Sections 3.2.2.2 – 3.2.2.4), P21 knockdown MCF7/NeuT cells were then measured for senescent and cyclin biomarker expression and compared to non-transfected MCF7/NeuT cells. The following graphs depict the gene expression patterns of selected senescent and cyclin biomarkers in P21 knockdown MCF7/NeuT cells treated with or without dox at the respected time points. A Mann-Whitney U test was performed on all samples to test for significant differences between those treated with or without dox. Then, to test for significant differences between treated transfected and non-transfected samples a Kruskall-Wallis test was performed followed by a post-hoc test the Bonferroni correction. See section 3.2.3.5, tables 4-7 for p-values of statistical significance tests.

ErbB2 (NeuT)

NeuT mRNA expression was measured in knockdown samples to ensure the upregulation of NeuT by dox was not hindered by the knockdown of P21. Figure 49 depicts the overexpression of NeuT which is significantly upregulated in all samples at all time points following 0 days. These results indicated that with the knockdown of P21, NeuT was able to continue to be overexpressed in the presence of dox.

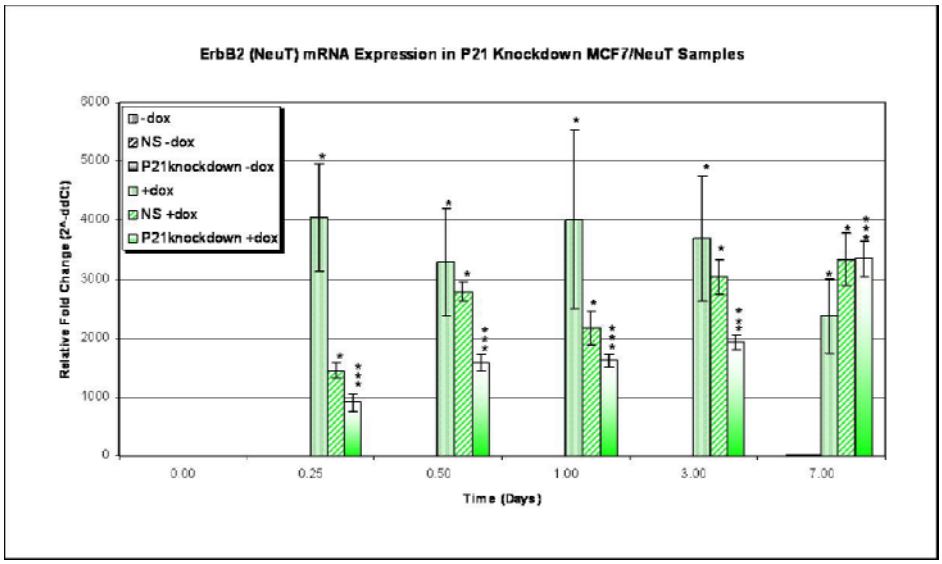

Figure 49: ErbB2 (NeuT) mRNA expression in P21 knockdown MCF7/NeuT cells. ErbB2 expression is significantly upregulated after 0.25 days of dox treatment. P21 inhibition has no effect on NeuT over expression. NB: Non-treated sample expression is not shown due to the high induction in NeuT expression upon dox incubation. 2^-ΔΔCt values represent an average of three independent experiments. -/+ dox - samples with no transfection; NS -/+ dox – non-sense oligoribonucleotide samples; P21 knockdown -/+ dox – represent the three P21 siRNA oligoribonucleotides transfected samples. A Mann-Whitney U test was performed for significant differences where $p \leq 0.05$.

Cyclin Dependent Kinase Inhibitor 1A (P21)

P21 was found to be significantly downregulated in P21 knockdown samples treated with or without dox after (Figure 50). This downregulation remained stable through to 3 days of treatment. Looking between the treated samples, the non-transfected and non-sense transfected treated samples continue to express high levels of P21 between 4 and 12-fold throughout the time course which is well above the P21 knockdown sample levels. These results indicate that the P21 knockdown was successful at decreasing P21 mRNA expression levels.

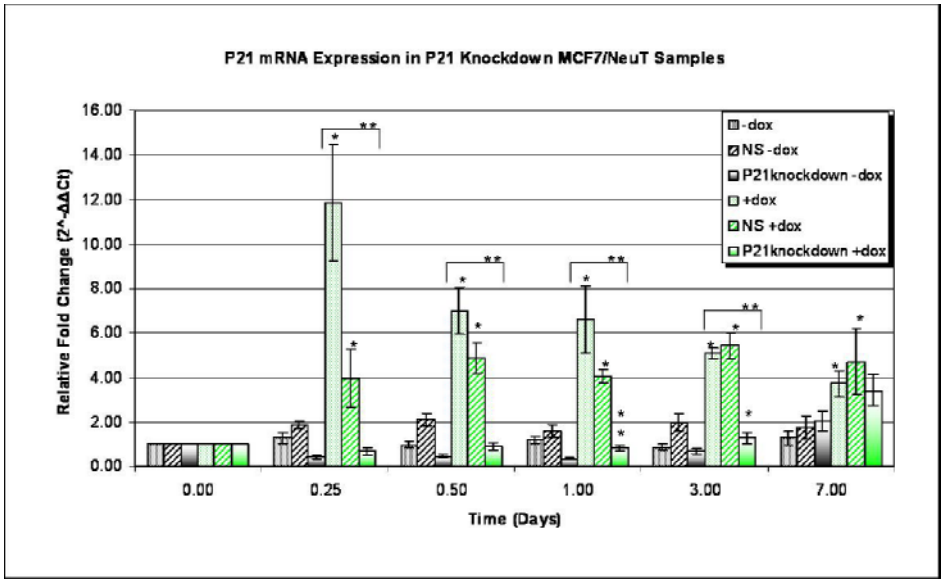

Figure 50: P21 mRNA expression in P21 knockdown MCF7/NeuT cells. P21 expression was significantly downregulated in P21 knockdown samples compared to non-transfected and non-sense transfected samples. 2^-ΔΔCt values represent an average of three independent experiments. -/+ dox - samples with no transfection; NS -/+ dox – non-sense oligoribonucleotide samples; P21 knockdown -/+ dox – represent the three P21 siRNA oligoribonucleotides transfected samples. A Mann-Whitney U test was performed for significant differences between treated and non-treated where $p \leq 0.05$. A Kruskall-Wallis test was performed to determine significant differences between the three treatments. Brackets above treated samples represent those significant for Kruskall-Wallis differences where $p \leq 0.05$.

Tumour Protein 53 (P53)

P53 mRNA levels were shown to be similarly expressed in all of the treated samples across all time points (Figure 51). A few of the time points showed significant downregulation of P53 in P21 knockdown treated samples. This could be due to the knockdown and dox incubation causing slight cellular stresses. However, when comparing all treated samples there were relatively little significant differences between them. Therefore, one can conclude that with P21 knockdown there was no change in P53 expression between non-transfected and transfected samples upon NeuT overexpression.

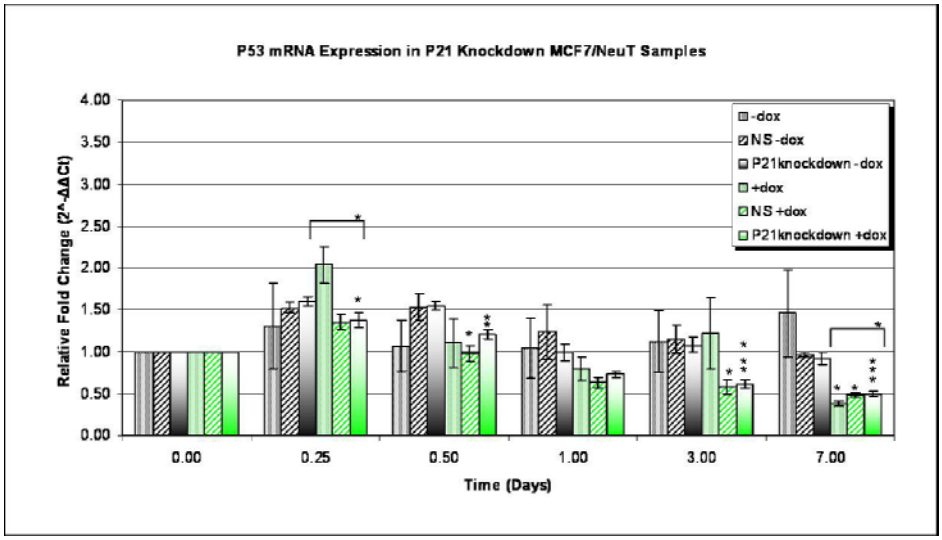

Figure 51: P53 mRNA expression in P21 knockdown MCF7/NeuT cells. P53 expression was significantly downregulated at 0.25 and 0.50 days of dox treatment in P21 knockdown samples. However, these changes were not so significant when compared non-transfected and non-sense transfected. 2^-ΔΔCt values represent an average of three independent experiments. -/+ dox - samples with no transfection; NS -/+ dox – non-sense oligoribonucleotide samples; P21 knockdown -/+ dox – represent the three P21 siRNA oligoribonucleotides transfected samples. A Mann-Whitney U test was performed for significant differences between treated and non-treated where $p \leq 0.05$. A Kruskall-Wallis test was performed to determine significant differences between the three treatments. Brackets above treated samples represent those significant for Kruskall-Wallis differences where $p \leq 0.05$.

Mitogen-Activated Protein Kinase 14 (P38)

P38 mRNA expression was shown to be significantly downregulated in both non-transfected and P21 knockdown treated samples at 0.25 and 0.50 days dox incubation by approximately 2- and 1.25-fold (Figure 52). However, these levels then reached near non-treated mRNA levels after 3 days incubation. These results confirmed that P38 mRNA expression has little influence on NeuT overexpressing samples regardless of treatment or transfection.

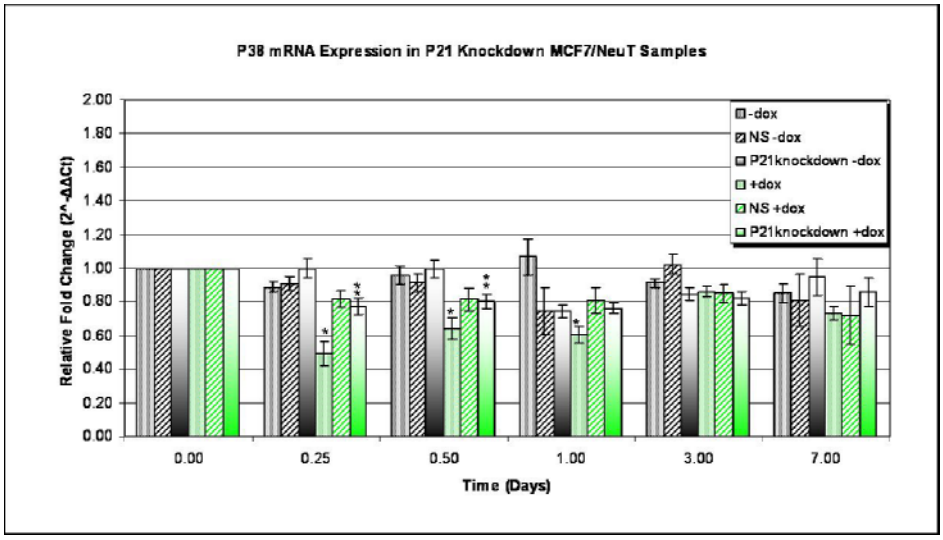

Figure 52: P38 mRNA expression in P21 knockdown MCF7/NeuT cells. P38 expression is significantly downregulated at 0.25 and 0.50 days of dox treatment in non-transfected and P21 knockdown samples. P38 has no effect upon NeuT overexpression. 2^-ΔΔCt values represent an average of three independent experiments. -/+ dox - samples with no transfection; NS -/+ dox – non-sense oligoribonucleotide samples; P21 knockdown -/+ dox – represent the three P21 siRNA oligoribonucleotides transfected samples. A Mann-Whitney U test was performed for significant differences where $p \leq 0.05$.

Pituitary Tumour Transforming Gene 1 (PTTG1)

PTTG1 mRNA expression was shown to be significantly downregulated in treated non-transfected and non-sense samples from 0.50 to 3 days (Figure 53). P21 knockdown treated samples were also shown to be downregulated at 0.50 and 3 days. Interestingly, P21 knockdown treated samples although downregulated compared to non-treated P21 knockdown samples, showed to have higher levels of PTTG1 expression, specifically at 0.50 and 1 day of incubation where there was a significant difference between treated P21 knockdown to treated non-sense and non-transfected samples. All of the non-treated samples whether transfected or not showed similar patterns of PTTG1 expression throughout the time course. These results indicated that PTTG1 expression may be influenced by P21 upregulation upon NeuT overexpression.

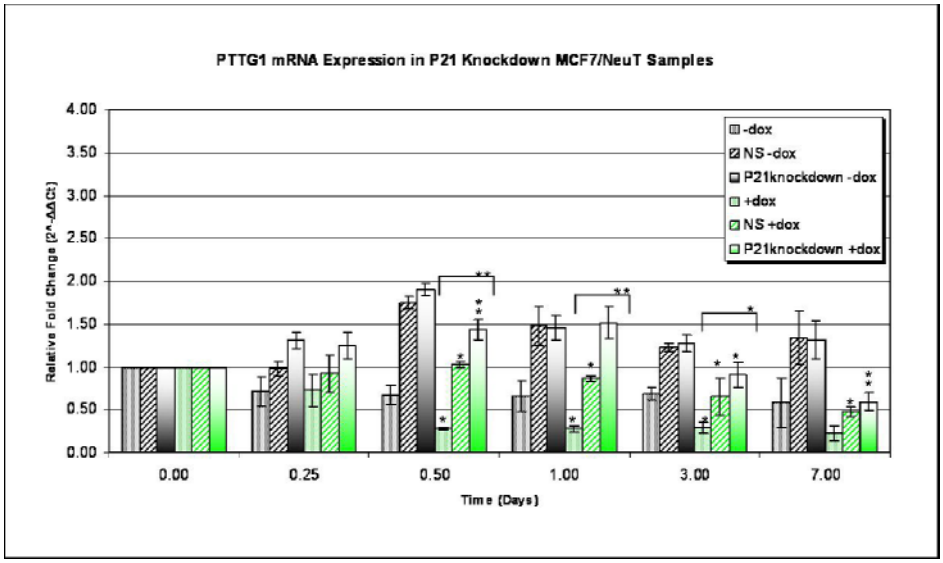

Figure 53: PTTG1 mRNA expression in P21 knockdown MCF7/NeuT cells. PTTG1 expression was significantly downregulated at 0.50 to 3 days of dox treatment in non-transfected and non-sense treated samples. PTTG1 expression was found to be higher in P21 knockdown treated samples. PTTG1 may be influenced by P21 upregulation. 2^-ΔΔCt values represent an average of three independent experiments. -/+ dox - samples with no transfection; NS -/+ dox – non-sense oligoribonucleotide samples; P21 knockdown -/+ dox – represent the three P21 siRNA oligoribonucleotides transfected samples. A Mann-Whitney U test was performed for significant differences between treated and non-treated where $p \leq 0.05$. A Kruskall-Wallis test was performed to determine significant differences between the three treatments. Brackets above treated samples represent those significant for Kruskall-Wallis differences where $p \leq 0.05$.

3.2.3.3 Gene Expression Analysis of Cyclins D1, E1 and B2 in P21 Knockdown MCF7/NeuT Cells

Cyclin D1 (CCND1)

CCND1 mRNA expression was found to be significantly upregulated after 1 day of dox treatment in all treated samples and then decreases to near non-treated levels after 3 days (Figure 54). Interestingly, when looking between the treated samples, although not significant, P21 knockdown CCND1 levels are lower in expression compared to non-transfected and non-sense transfected at 0.50, 1.00 and 3 days of treatment. These results indicated that with P21 inhibition in overexpressing NeuT cells CCND1 mRNA levels remain elevated although at lower expression levels.

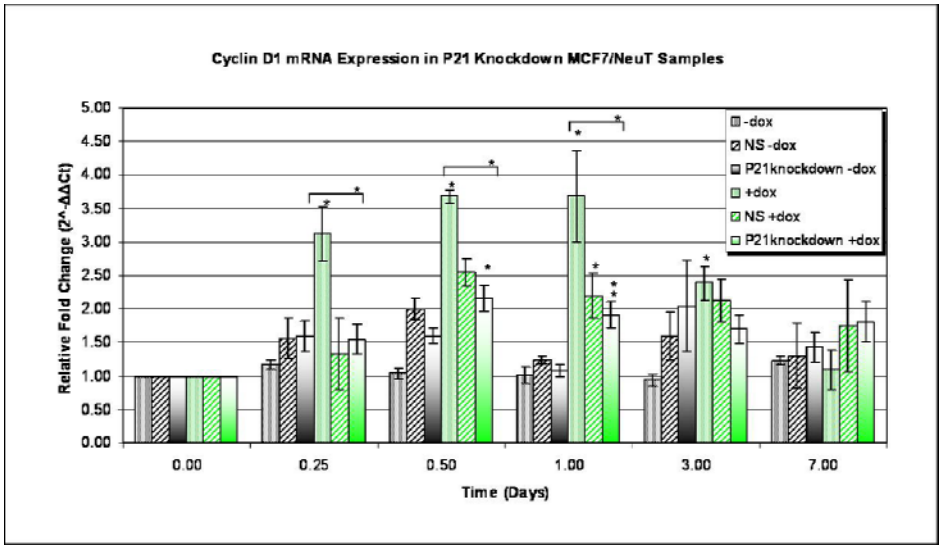

Figure 54: CCND1 mRNA expression in P21 knockdown MCF7/NeuT cells. CCND1 expression was significantly upregulated after 1 day dox treatment in all samples. CCND1 expression was found to be lower in P21 knockdown treated samples. 2^-ΔΔCt values represent an average of three independent experiments. -/+ dox - samples with no transfection; NS -/+ dox – non-sense oligoribonucleotide samples; P21 knockdown -/+ dox – represent the three P21 siRNA oligoribonucleotides transfected samples. A Mann-Whitney U test was performed for significant differences between treated and non-treated where $p \leq 0.05$. A Kruskall-Wallis test was performed to determine significant differences between the three treatments. Brackets above treated samples represent those significant for Kruskall-Wallis differences where $p \leq 0.05$.

Cyclin E1 (CCNE1)

CCNE1 mRNA levels were shown to be expressed at similar levels in non-sense transfected and P21 knockdown samples between non-treated and treated (Figure 55). Non-transfected samples showed to have significant upregulation between treated and non-treated. However, when looking between the treated samples there is relatively no difference in CCNE1 expression across the time course. These results depict that inhibition of P21 expression may have little effect on CCNE1 expression in overexpressing NeuT cells.

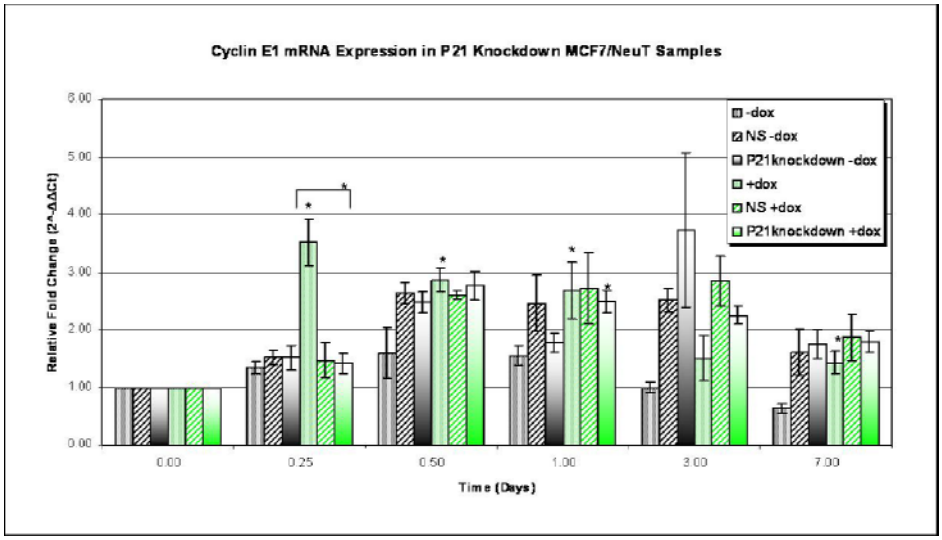

Figure 55: CCNE1 mRNA expression in P21 knockdown MCF7/NeuT cells. CCNE1 expression was significantly upregulated in non-transfected samples. CCNE1 expression was found to have little change in expression upon P21 knockdown in treated samples. 2^-ΔΔCt values represent an average of three independent experiments. -/+ dox - samples with no transfection; NS -/+ dox – non-sense oligoribonucleotide samples; P21 knockdown -/+ dox – represent the three P21 siRNA oligoribonucleotides transfected samples. A Mann-Whitney U test was performed for significant differences between treated and non-treated where $p \leq 0.05$. A Kruskall-Wallis test was performed to determine significant differences between the three treatments. Brackets above treated samples represent those significant for Kruskall-Wallis differences where $p \leq 0.05$.

Cyclin B2 (CCNB2)

CCNB2 mRNA expression in P21 knockdown samples was shown to be expressed at similar levels in both non-treated and treated samples (Figure 56). Comparing expression between the different treated samples revealed CCNB2 was found to be significantly downregulated in both non-transfected and non-sense transfected samples specifically between 0.50, 1 and 3 days. These results indicate that P21 may influence CCNB2 expression during NeuT upregulation.

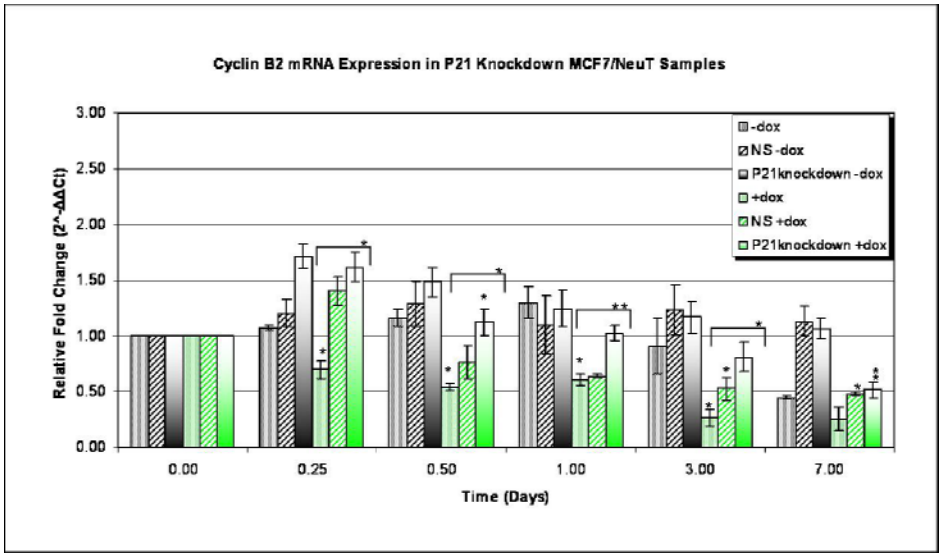

Figure 56: CCNB2 mRNA expression in P21 knockdown MCF7/NeuT Cells. CCNB2 expression was found to be similarly expressed in P21 knockdown non-treated and treated samples. CCNB2 expression was found to be significantly higher in expression in P21 knockdown treated samples compared to non-transfected and non-sense transfected treated samples. P21 expression influences CCNB2 expression. 2^-ΔΔCt values represent an average of three independent experiments. -/+ dox - samples with no transfection; NS -/+ dox – non-sense oligoribonucleotide samples; P21 knockdown -/+ dox – represent the three P21 siRNA oligoribonucleotides transfected samples. A Mann-Whitney U test was performed for significant differences between treated and non-treated where $p \leq 0.05$. A Kruskall-Wallis test was performed to determine significant differences between the three treatments. Brackets above treated samples represent those significant for Kruskall-Wallis differences where $p \leq 0.05$.

3.2.3.4 Phase-contrast Microscopy of P21 Knockdown MCF7/NeuT Cells

P21 knockdown MCF7/NeuT samples were subjected to phase-contrast microscopy prior to RNA collection. Images were taken to show the phenotypic changes through-out the timed incubation experiments of the transfected cells. Figures 57 and 58 depict the respective time points of samples treated with or without dox. Phenotypically the P21 knockdown shows prevention of senescence until approximately 7 days. Up until 7 days of dox treatment and transfection, the MCF7/NeuT cells show normal proliferating morphology having no presence of vacuoles or a large and flattened morphology. These results show that with inhibition of P21 expression in overexpressing NeuT cells, cells do not show phenotypic senescent characteristics.

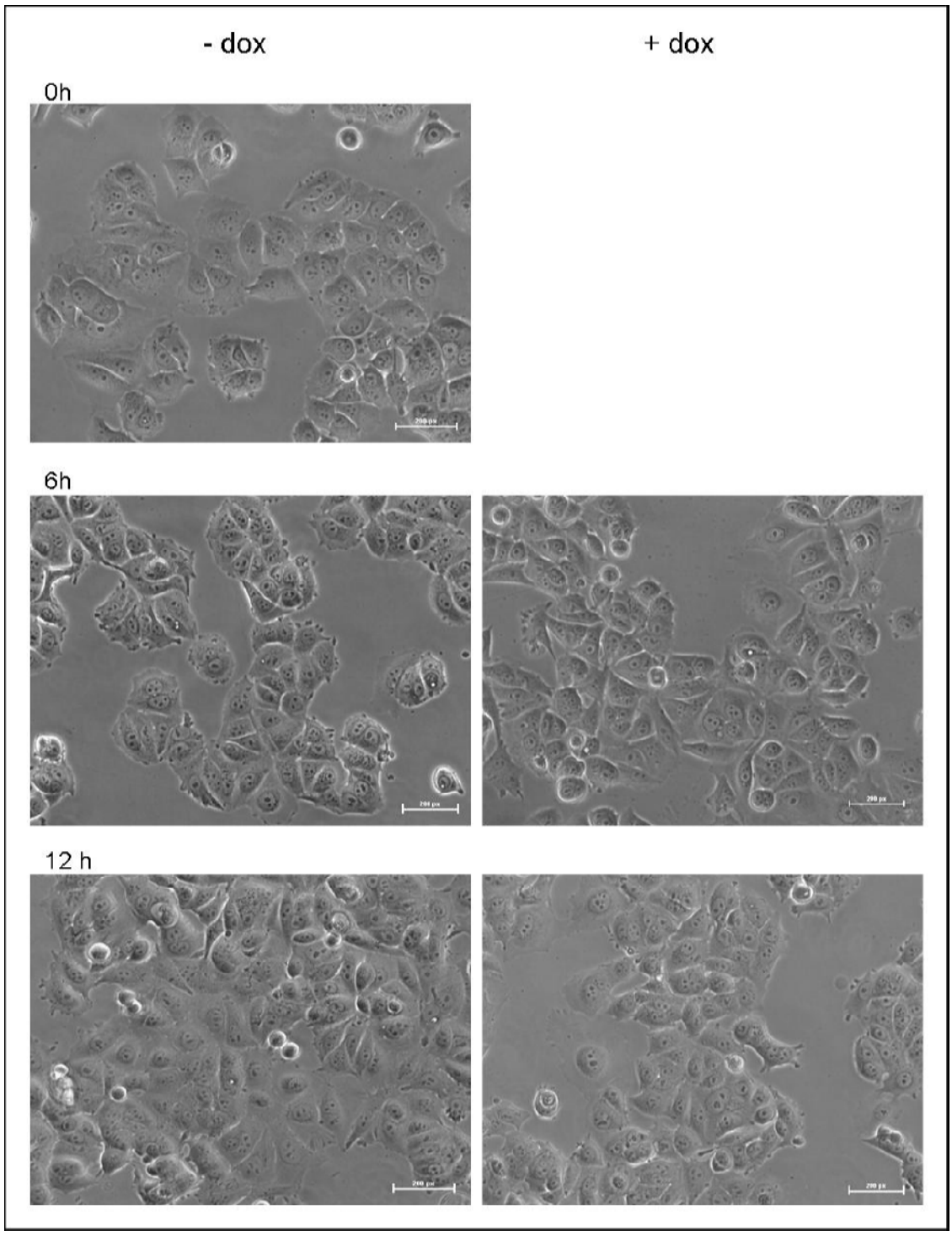

Figure 57: Phase-contrast microscopy on P21 knockdown MCF7/NeuT cells (0h – 12h). Images were taken with a 20x objective for each time point and represent the 3 different oligoribonucleotides used. Phenotypically at 6 and 12 hours incubation, MCF7/NeuT cells do not depict senescent characteristics when treated with dox.

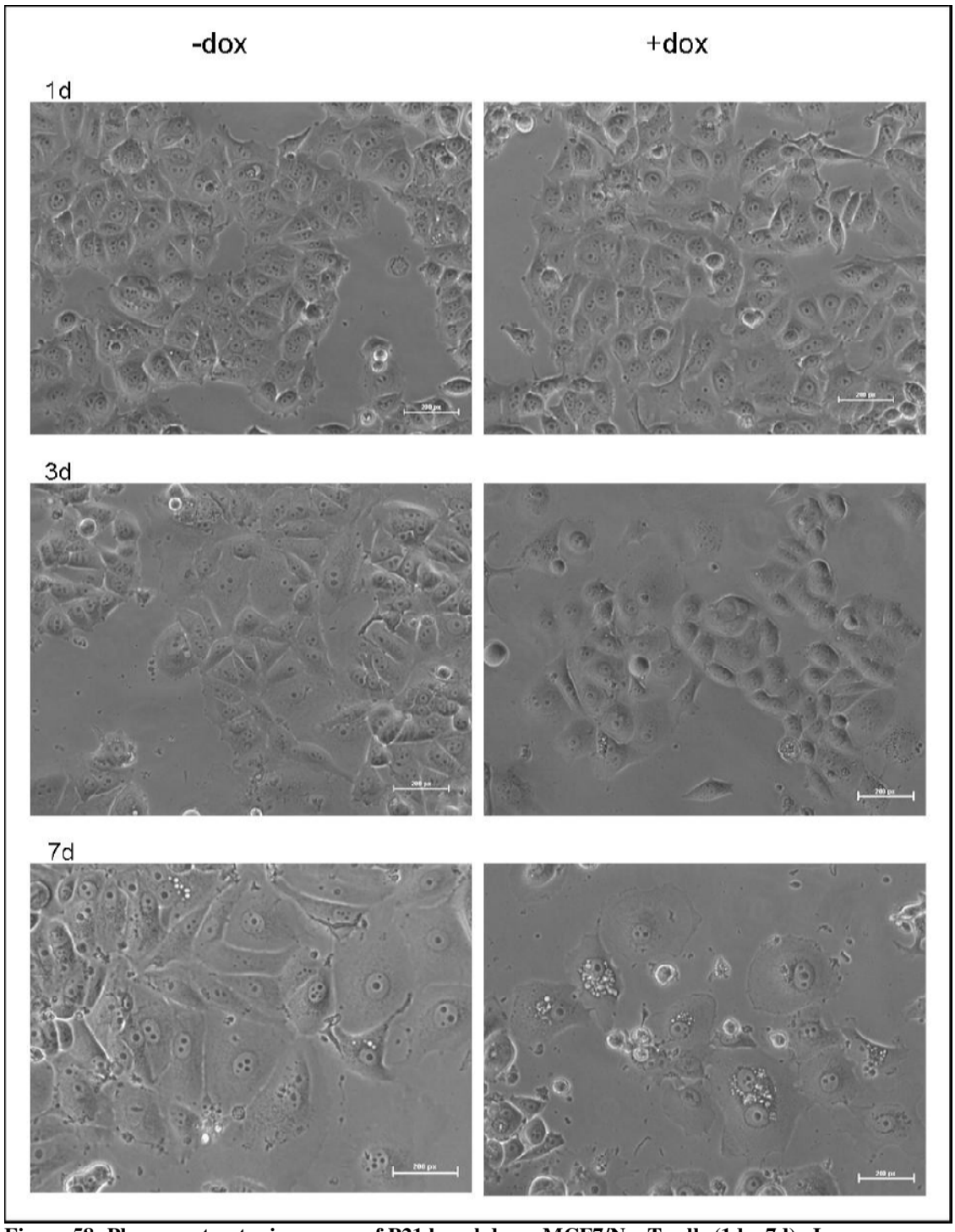

Figure 58: Phase-contrast microscopy of P21 knockdown MCF7/NeuT cells (1d – 7d). Images were taken with a 20x objective for each time point and represent the 3 different oligoribonucleotides used. Phenotypically at 1d and 3d incubation, MCF7/NeuT cells do not depict senescent characteristics when treated with dox. At 7d dox incubation cells begin to show signs of senescence indicating the P21 knockdown is no longer efficient.

3.2.3.5 Statistical Data Analysis of P21 Knockdown MCF7/NeuT Cells

To determine significant differences between non-treated and treated samples a Mann-Whitney U test was performed where significant p-values were equal to or less than 0.05 (Table 4). To measure the significant differences between the different treated samples a Kruskall-Wallis test was performed on all treated samples (Table 5). Those found to have significant differences among the three treated groups of a specific gene at a specific time point were then subjected to post-hoc tests. Mann-Whitney U was performed among the three treated groups (Table 6) which were determined to be significant by Kruskall-Wallis and was then followed by a Bonferroni correction (Table 7) where p-values equal to or less than 0.05 were considered significant. Values highlighted in bold showed significant differences. Looking at the Bonferroni correction table (Table 7) most significance was found between treated P21 knockdown and non-transfected cells especially in PTTG1 and CCNB2 gene expression ($p = 0.039$). There was no significance found between treated non-transfected and non-sense transfected samples. Some significance was found between treated non-sense transfected and P21 knockdown transfected samples in PTTG1 and CCNB2 gene expression ($p = 0.039$). The statistical results indicate that P21 knockdown did have a slight effect in NeuT overexpressing samples.

Table 4: Mann-Whitney U (p-values) statistical comparison of the relative quantity of gene expression of senescence and cyclin biomarkers in non-treated and treated P21 knockdown samples.

Non-Transfected Samples Non-Treated vs. Treated with Dox						
Time	0h	6h	12h	24h	3d	7d
Gene						
ErbB2(NeuT)		**0.050**	**0.050**	**0.050**	**0.050**	**0.050**
P21		**0.050**	**0.050**	**0.050**	**0.050**	**0.050**
PTTG1		0.827	**0.050**	**0.050**	**0.050**	0.275
P53		0.275	0.827	0.513	0.827	**0.046**
P38		**0.050**	**0.050**	**0.050**	0.275	0.121
CCNB2		**0.046**	**0.050**	**0.050**	**0.050**	0.184
CCND1		**0.050**	**0.050**	**0.050**	**0.050**	0.513
CCNE1		**0.050**	**0.050**	**0.050**	0.184	**0.050**
P21 Transfected Samples Non-Treated vs. Treated with Dox						
ErbB2(NeuT)		**0.000**	**0.000**	**0.000**	**0.000**	**0.000**
P21		0.427	0.093	**0.007**	**0.031**	0.085
PTTG1		0.354	**0.007**	0.659	**0.058**	**0.017**
P53		**0.030**	**0.002**	0.092	**0.001**	**0.000**
P38		**0.010**	**0.012**	0.825	0.535	0.508
CCNB2		0.508	**0.047**	0.270	0.064	**0.002**
CCND1		0.930	**0.024**	**0.002**	0.508	0.401
CCNE1		0.757	0.427	**0.027**	0.825	0.965
Non-Sense Transfected Samples Non-Treated vs. Treated with Dox						
ErbB2(NeuT)		**0.050**	**0.050**	**0.050**	**0.050**	**0.050**
P21		**0.050**	**0.050**	**0.050**	**0.050**	**0.050**
PTTG1		0.513	**0.050**	**0.050**	**0.050**	**0.050**
P53		0.127	**0.050**	0.127	**0.050**	**0.050**
P38		0.268	0.827	0.513	0.127	0.513
CCNB2		0.268	0.275	0.513	**0.050**	**0.050**
CCND1		0.827	0.127	**0.050**	0.275	0.513
CCNE1		0.513	1.000	0.827	0.513	0.513

Table 5: Kruskall-Wallis (p-value) statistical comparison of the relative quantity of gene expression of senescence and cyclin biomarkers in treated P21 knockdown samples.

Non-Transfected vs. P21 Knockdown Transfected vs. Non-Sense Transfected Samples Treated with Dox						
Time	0h	6h	12h	24h	3d	7d
Gene						
ErbB2(NeuT)						
P21		**0.005**	**0.005**	**0.005**	**0.006**	0.567
PTTG1		0.110	**0.010**	**0.005**	**0.041**	0.126
P53		**0.048**	0.219	0.429	0.113	**0.033**
P38		0.067	0.152	0.078	0.775	0.669
CCNB2		**0.027**	**0.033**	**0.006**	**0.036**	0.194
CCND1		**0.030**	**0.024**	**0.044**	0.158	0.508
CCNE1		**0.034**	0.659	0.989	0.091	0.670

Table 6: Mann-Whitney U (p-values) statistical comparison of the relative quantity of gene expression of senescence and cyclin biomarkers among treated P21 knockdown samples. NS – Not Significant.

Treated Non-Transfected vs. Treated P21 Knockdown Transfected Samples						
Time	0h	6h	12h	24h	3d	7d
Gene						
ErbB2(NeuT)						
P21		**0.013**	**0.013**	**0.013**	**0.013**	NS
PTTG1		NS	**0.013**	**0.013**	**0.013**	NS
P53		**0.021**	NS	NS	NS	**0.012**
P38		NS	NS	NS	NS	NS
CCNB2		**0.013**	**0.013**	**0.013**	**0.013**	NS
CCND1		**0.013**	**0.013**	**0.021**	NS	NS
CCNE1		**0.012**	NS	NS	NS	NS
Treated Non-Sense Transfected vs. Treated P21 Knockdown Transfected Samples						
ErbB2(NeuT)						
P21		**0.013**	**0.013**	**0.013**	**0.013**	NS
PTTG1		NS	**0.052**	**0.013**	0.405	NS
P53		0.853	NS	NS	NS	0.781
P38		NS	NS	NS	NS	NS
CCNB2		0.405	0.166	**0.013**	0.309	NS
CCND1		0.518	0.373	0.518	NS	NS
CCNE1		0.926	NS	NS	NS	NS
Treated Non-Transfected vs. Treated Non-Sense Transfected Samples						
ErbB2(NeuT)						
P21		**0.050**	**0.050**	0.127	0.827	NS
PTTG1		NS	**0.050**	**0.050**	0.184	NS
P53		**0.050**	NS	NS	NS	**0.046**
P38		NS	NS	NS	NS	NS
CCNB2		**0.050**	0.513	1.000	0.184	NS
CCND1		**0.050**	**0.050**	**0.050**	NS	NS
CCNE1		**0.050**	NS	NS	NS	NS

Table 7: Bonferroni correction (p-value) post-hoc statistical comparison of the relative quantity of gene expression of senescence and cyclin biomarkers among treated P21 knockdown samples. NS – Not Significant.

Treated Non-Transfected vs. Treated P21 Knockdown Transfected Samples						
Time	0h	6h	12h	24h	3d	7d
Gene						
ErbB2(NeuT)						
P21		**0.039**	**0.039**	**0.039**	**0.039**	NS
PTTG1		NS	**0.039**	**0.039**	**0.039**	NS
P53		0.063	NS	NS	NS	**0.036**
P38		NS	NS	NS	NS	NS
CCNB2		**0.039**	**0.039**	**0.039**	**0.039**	NS
CCND1		**0.039**	**0.039**	0.063	NS	NS
CCNE1		**0.036**	NS	NS	NS	NS
Treated Non-Sense Transfected vs. Treated P21 Knockdown Transfected Samples						
ErbB2(NeuT)						
P21		**0.039**	**0.039**	**0.039**	**0.039**	NS
PTTG1		NS	0.156	**0.039**	NS	NS
P53		NS	NS	NS	NS	NS
P38		NS	NS	NS	NS	NS
CCNB2		NS	NS	**0.039**	NS	NS
CCND1		NS	NS	NS	NS	NS
CCNE1		NS	NS	NS	NS	NS
Treated Non-Transfected vs. Treated Non-Sense Transfected Samples						
ErbB2(NeuT)						
P21		0.150	0.150	NS	NS	NS
PTTG1		NS	0.150	0.150	NS	NS
P53		0.150	NS	NS	NS	0.138
P38		NS	NS	NS	NS	NS
CCNB2		0.150	NS	NS	NS	NS
CCND1		0.150	0.150	0.150	NS	NS
CCNE1		0.150	NS	NS	NS	NS

3.2.4 siRNA Inhibition of Pituitary Tumour Transforming Gene 1 (PTTG1) has No Effect on Oncogene-induced Senescence

3.2.4.1 Optimisation and Validation of PTTG1 Knockdown Oligoribonucleotides

Similar to P21 knockdown studies, prior to the use of PTTG1 siRNA oligoribonucleotides for investigation into senescence, three PTTG1 siRNA oligoribonucleotides were optimised and validated by using RT-qPCR. MCF7/NeuT cells were subjected to siRNA reverse transfection and prepared as stated in the Materials and Methods section 2.2.8. For optimisation, PTTG1 siRNA oligoribonucleotides were measured at concentrations of 10nM and 30nM in two independent experiments. Knockdown of beta-actin was used as a positive control to ensure transfection agent efficiency. A non-sense oligoribonucleotide was also used to account for any off-target knockdown effects. Figures 59 and 60 depict the relative fold changes in gene expression used to measure the knockdown efficiency of the three PTTG1 siRNA oligoribonucleotides at two different concentrations, 10nM and 30nM respectively. Along with PTTG1 and beta-actin (ACTB) mRNA expression measurements, the reference genes determined in section 3.2.2.1 TBP and UBC were also analysed to ensure that the knockdown was restricted to PTTG1 and beta-actin only. PTTG1, ACTB, TBP and UBC were measured in transfection agent only samples to ensure that the transfection agent did not affect the genes of interest. Looking at the two figures, a final concentration of 10nM was determined to be the best concentration for an effective knockdown of PTTG1 with an efficiency of more than 80% (0.20/1.0 $2^{-\Delta\Delta Ct}$). For all PTTG1 knockdown experiments 10nM oligoribonucleotide concentrations were used. To ensure PTTG1 knockdown efficiency was consistent, efficiency was measured at each respective time point through-out the time course study (See appendix 5).

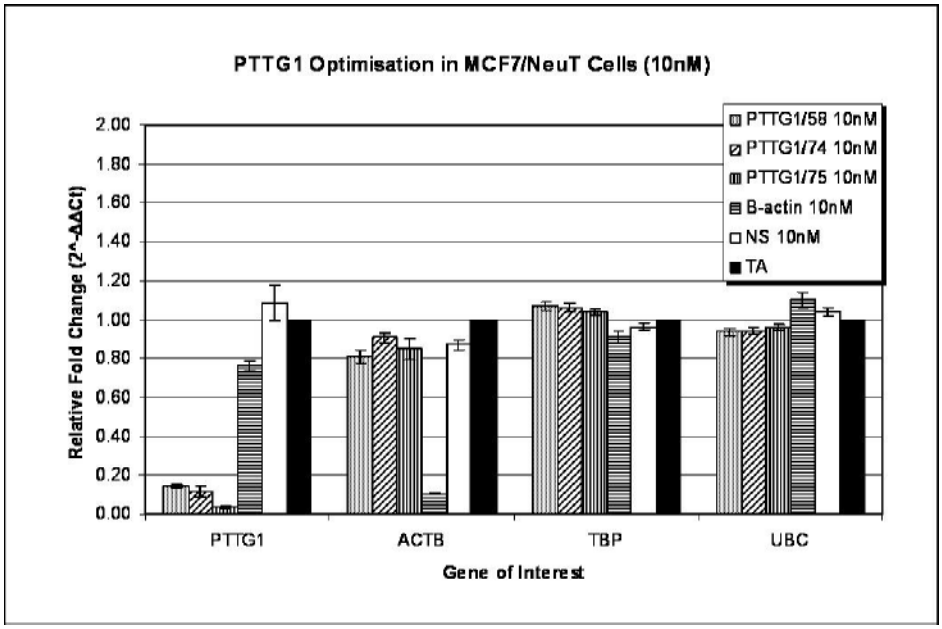

Figure 59: PTTG1 siRNA optimisation in MCF7/NeuT cells (10nM). Relative fold change values for PTTG1 (PTTG1/58, PTTG1/74, PTTG1/75), beta-actin (β-actin) and nonsense (NS) siRNA oligoribonucleotides at 10nM final concentrations and transfection agent only (TA) samples. Gene expression was measured for PTTG1, β-actin (ACTB) and the reference genes TBP and UBC. PTTG1 and ACTB for positive control knockdown efficiency was found to be >80%.

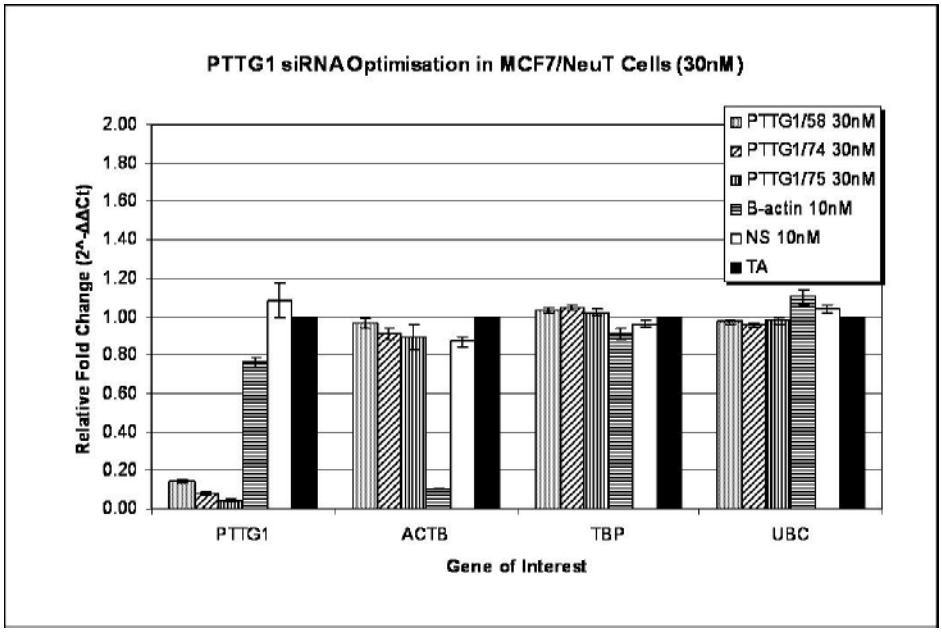

Figure 60: PTTG1 siRNA optimisation in MCF7/NeuT cells (30nM). Relative fold change values for PTTG1 (PTTG1/58, PTTG1/74, PTTG1/75), beta-actin (β-actin) and nonsense (NS) siRNA oligoribonucleotides at 30nM final concentrations and transfection agent only (TA) samples. Gene expression was measured for PTTG1, β-actin (ACTB) and the reference genes TBP and UBC. PTTG1 and ACTB for positive control knockdown efficiency was found to be >80%.

3.2.4.2 Gene Expression Analysis of Senescence Biomarkers in PTTG1 Knockdown MCF7/NeuT Cells

After investigating the gene expression patterns of senescent and cyclin biomarkers in overexpressing NeuT MCF7/NeuT cells (Sections 3.2.2.2 – 3.2.2.4), PTTG1 knockdown MCF7/NeuT cells were then measured for senescent and cyclin biomarker expression and compared to non-transfected MCF7/NeuT cells. The following graphs depict the gene expression patterns of selected senescent and cyclin biomarkers in PTTG1 knockdown MCF7/NeuT cells treated with or without dox at the respected time points. Mann-Whitney U test was performed on all samples to test for significant differences between those treated with or without dox. To test for significant differences between treated samples a Kruskall-Wallis test was performed followed by a post-hoc Bonferroni correction. See tables 8-11 in section 3.2.4.5 for p-values of statistical significance tests.

ErbB2 (NeuT)

NeuT mRNA expression was measured in knockdown samples to ensure the upregulation of NeuT by dox was not hindered by the knockdown of PTTG1. Figure 61 depicts the overexpression of NeuT which is significantly upregulated in all samples at all time points following 0 days. These results indicated that with the knockdown of PTTG1, NeuT remained overexpressed in the presence of dox.

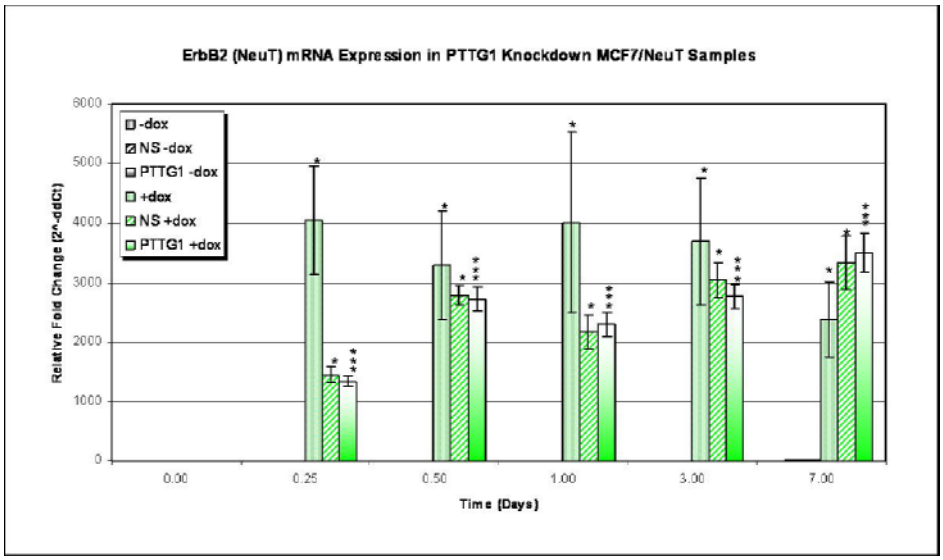

Figure 61: ErbB2 (NeuT) mRNA expression in PTTG1 knockdown MCF7/NeuT cells. ErbB2 expression is significantly upregulated after 0.25 days of dox treatment. PTTG1 inhibition has no effect on NeuT over expression. NB: Non-treated sample expression is not shown due to the high induction in NeuT expression upon dox incubation. 2^-ΔΔCt values represent an average of three independent experiments. -/+ dox - samples with no transfection; NS -/+ dox – non-sense oligoribonucleotide samples; PTTG1 knockdown -/+ dox – represent the three PTTG1 siRNA oligoribonucleotides transfected samples. A Mann-Whitney U test was performed for significant differences where $p \leq 0.05$.

Cyclin Dependent Kinase Inhibitor 1A (P21)

P21 mRNA expression was found to be significantly upregulated in all treated samples and similarly expressed between samples (Figure 62). These results indicate that the inhibition of PTTG1 expression has no effect on P21 upregulation upon NeuT overexpression.

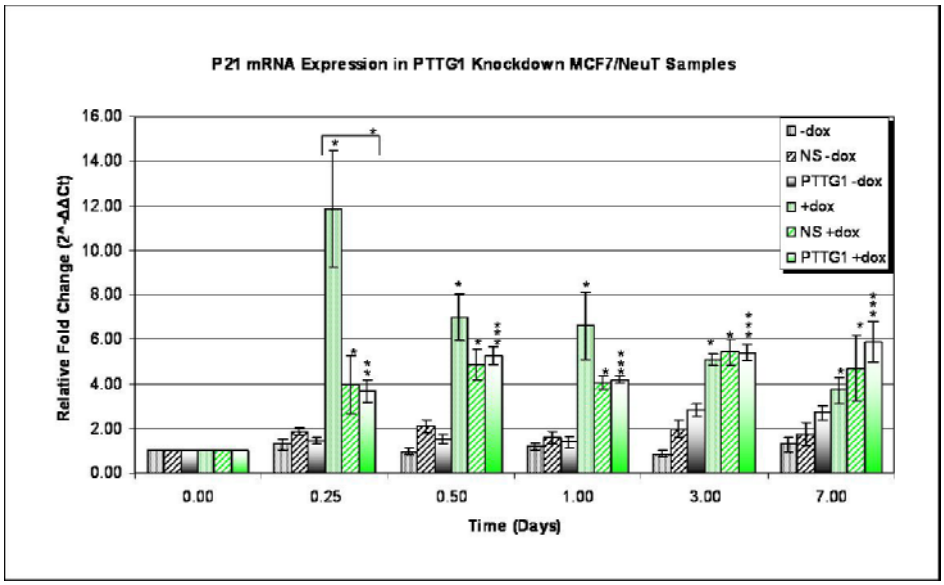

Figure 62: P21 mRNA expression in PTTG1 knockdown MCF7/NeuT cells. P21 expression was significantly upregulated in all treated samples. PTTG1 has no effect on P21 expression. 2^-ΔΔCt values represent an average of three independent experiments. -/+ dox - samples with no transfection; NS -/+ dox – non-sense oligoribonucleotide samples; PTTG1 knockdown -/+ dox – represent the three PTTG1 siRNA oligoribonucleotides transfected samples. A Mann-Whitney U test was performed for significant differences between treated and non-treated where p≤0.05. A Kruskall-Wallis test was performed to determine significant differences between the three treatments. Brackets above treated samples represent those significant for Kruskall-Wallis differences where p≤0.05.

Pituitary Tumour Transforming Gene 1 (PTTG1)

As expected, PTTG1 mRNA expression was found to be significantly downregulated in treated non-transfected and non-sense transfected samples (Figure 63). PTTG1 knockdown samples for both treated and non-treated samples showed significant downregulation when compared to the other non-treated and treated samples. These results indicated that the PTTG1 knockdown was maintained throughout the time course during NeuT upregulation.

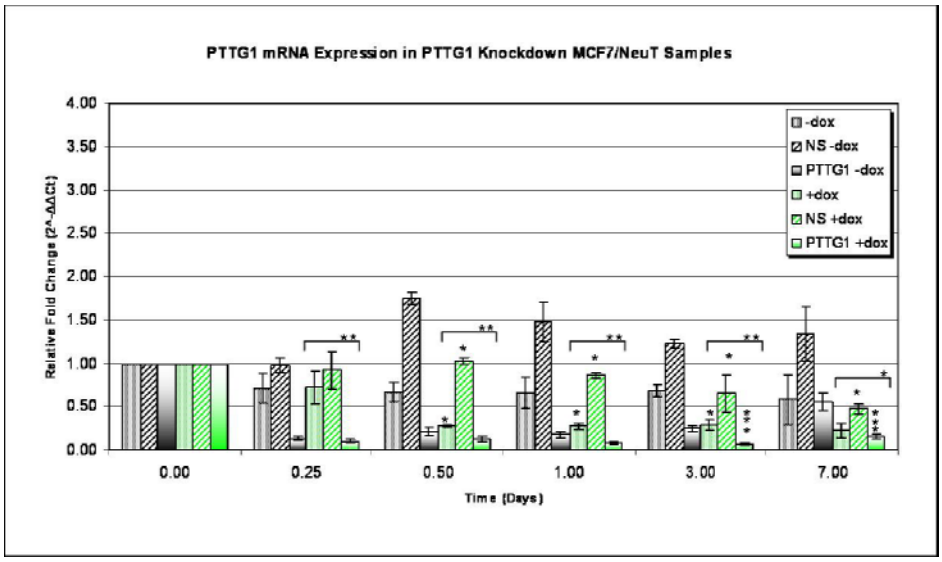

Figure 63: PTTG1 mRNA expression in PTTG1 knockdown MCF7/NeuT cells. PTTG1 expression was significantly downregulated in all treated samples. 2^-ΔΔCt values represent an average of three independent experiments. -/+ dox - samples with no transfection; NS -/+ dox – non-sense oligoribonucleotide samples; PTTG1 knockdown -/+ dox – represent the three PTTG1 siRNA oligoribonucleotides transfected samples. A Mann-Whitney U test was performed for significant differences between treated and non-treated where $p \leq 0.05$. A Kruskall-Wallis test was performed to determine significant differences between the three treatments. Brackets above treated samples represent those significant for Kruskall-Wallis differences where $p \leq 0.05$.

Tumour Protein 53 (P53)

P53 mRNA expression was found to be downregulated in PTTG1 knockdown treated samples compared to PTTG1 knockdown non-treated samples (Figure 64). Significant differences in P53 expression was also found between treated and non-treated non-sense transfected samples. Looking between the treated samples there was little significant differences between both transfected samples and non-transfected samples. These results indicate PTTG1 inhibition has little effect on P53 expression upon NeuT overexpression.

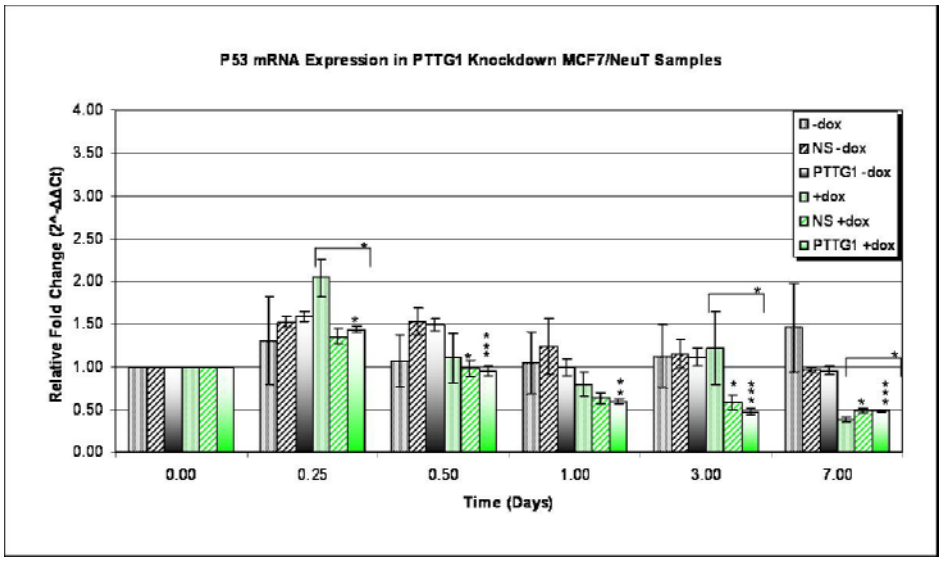

Figure 64: P53 mRNA expression in PTTG1 knockdown MCF7/NeuT cells. P53 expression was slightly downregulated in treated PTTG1 knockdown samples. 2^-ΔΔCt values represent an average of three independent experiments. -/+ dox - samples with no transfection; NS -/+ dox – non-sense oligoribonucleotide samples; PTTG1 knockdown -/+ dox – represent the three PTTG1 siRNA oligoribonucleotides transfected samples. A Mann-Whitney U test was performed for significant differences between treated and non-treated where $p \leq 0.05$. A Kruskall-Wallis test was performed to determine significant differences between the three treatments. Brackets above treated samples represent those significant for Kruskall-Wallis differences where $p \leq 0.05$.

Mitogen-Activated Protein Kinase 14 (P38)

P38 mRNA expression was shown to be significantly downregulated in both non-transfected and PTTG1 knockdown treated samples at 0.25 and 0.50 days dox incubation by approximately 2- and 1.25-fold (Figure 65). However, these levels then reached near non-treated mRNA levels after 1 day of incubation. These results confirmed that P38 mRNA expression has little influence on NeuT overexpressing samples regardless of treatment or transfection.

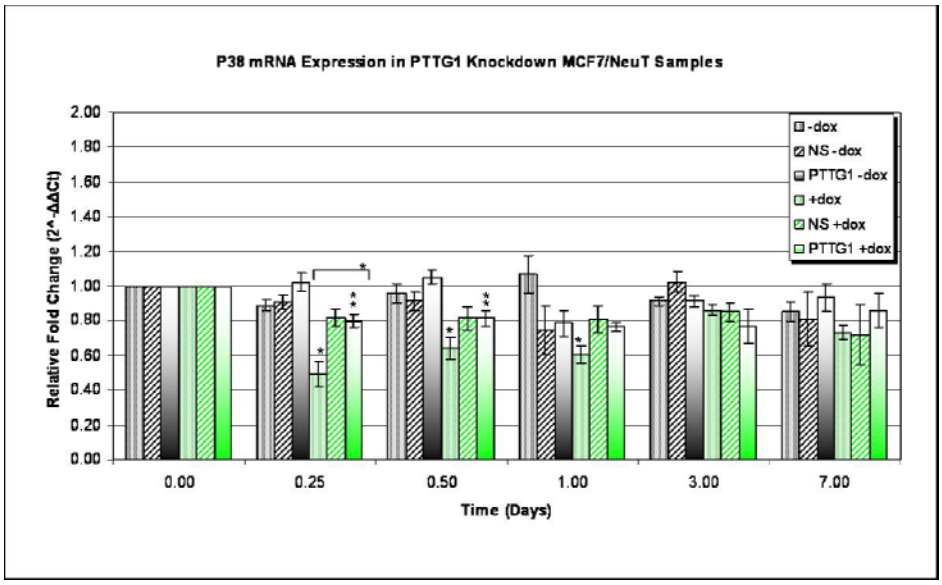

Figure 65: P38 mRNA expression in PTTG1 knockdown MCF7/NeuT cells. P38 expression is significantly downregulated at 0.25 and 0.50 days of dox treatment. PTTG1 knockdown has no effect on P38 in the presence of NeuT overexpression. 2^-ΔΔCt values represent an average of three independent experiments. -/+ dox - samples with no transfection; NS -/+ dox – non-sense oligoribonucleotide samples; PTTG1 knockdown -/+ dox – represent the three PTTG1 siRNA oligoribonucleotides transfected samples. A Mann-Whitney U test was performed for significant differences where $p \leq 0.05$. A Kruskall-Wallis test was performed to determine significant differences between the three treatments. Brackets above treated samples represent those significant for Kruskall-Wallis differences where $p \leq 0.05$.

3.2.4.3 Gene Expression Analysis of Cyclin B2 (CCNB2) in PTTG1 Knockdown MCF7/NeuT Cells

CCNB2 was found to be significantly downregulated in treated samples after 0.50 days of dox treatment (Figure 66). Interestingly, PTTG1 knockdown had no effect on CCNB2 downregulation as it was similarly expressed to the other treated samples. These results indicate that the inhibition of PTTG1 has no effect on CCNB2 regulation upon NeuT upregulation.

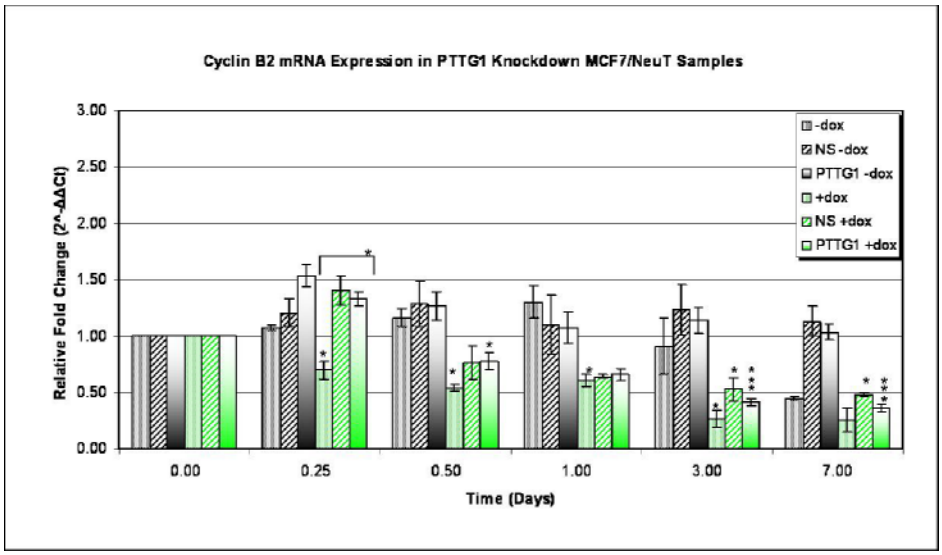

Figure 66: CCNB2 mRNA expression in PTTG1 knockdown MCF7/NeuT cells. CCNB2 expression was found to be downregulated in treated samples. PTTG1 expression has little effect on CCNB2 expression. 2^-ΔΔCt values represent an average of three independent experiments. -/+ dox - samples with no transfection; NS -/+ dox – non-sense oligoribonucleotide samples; PTTG1 knockdown -/+ dox – represent the three PTTG1 siRNA oligoribonucleotides transfected samples. A Mann-Whitney U test was performed for significant differences between treated and non-treated where $p \leq 0.05$. A Kruskall-Wallis test was performed to determine significant differences between the three treatments. Brackets above treated samples represent those significant for Kruskall-Wallis differences where $p \leq 0.05$.

3.2.4.4 Phase-contrast Microscopy of PTTG1 Knockdown MCF7/NeuT Cells

PTTG1knockdown MCF7/NeuT samples were subjected to phase-contrast microscopy prior to RNA collection. Images were taken to show the phenotypic changes through-out the timed incubation experiments of the transfected cells. Figures 67 and 68 depict the respective time points of samples treated with or without dox. Phenotypically, PTTG1 knockdown does not prevent senescence. After 1 day of dox incubation, PTTG1 knockdown samples begin to show characteristics of senescence vacuole formation and a large and flattened morphology. These results demonstrate that with inhibition of PTTG1 expression in overexpressing NeuT cells senescence morphological characteristics are still depicted.

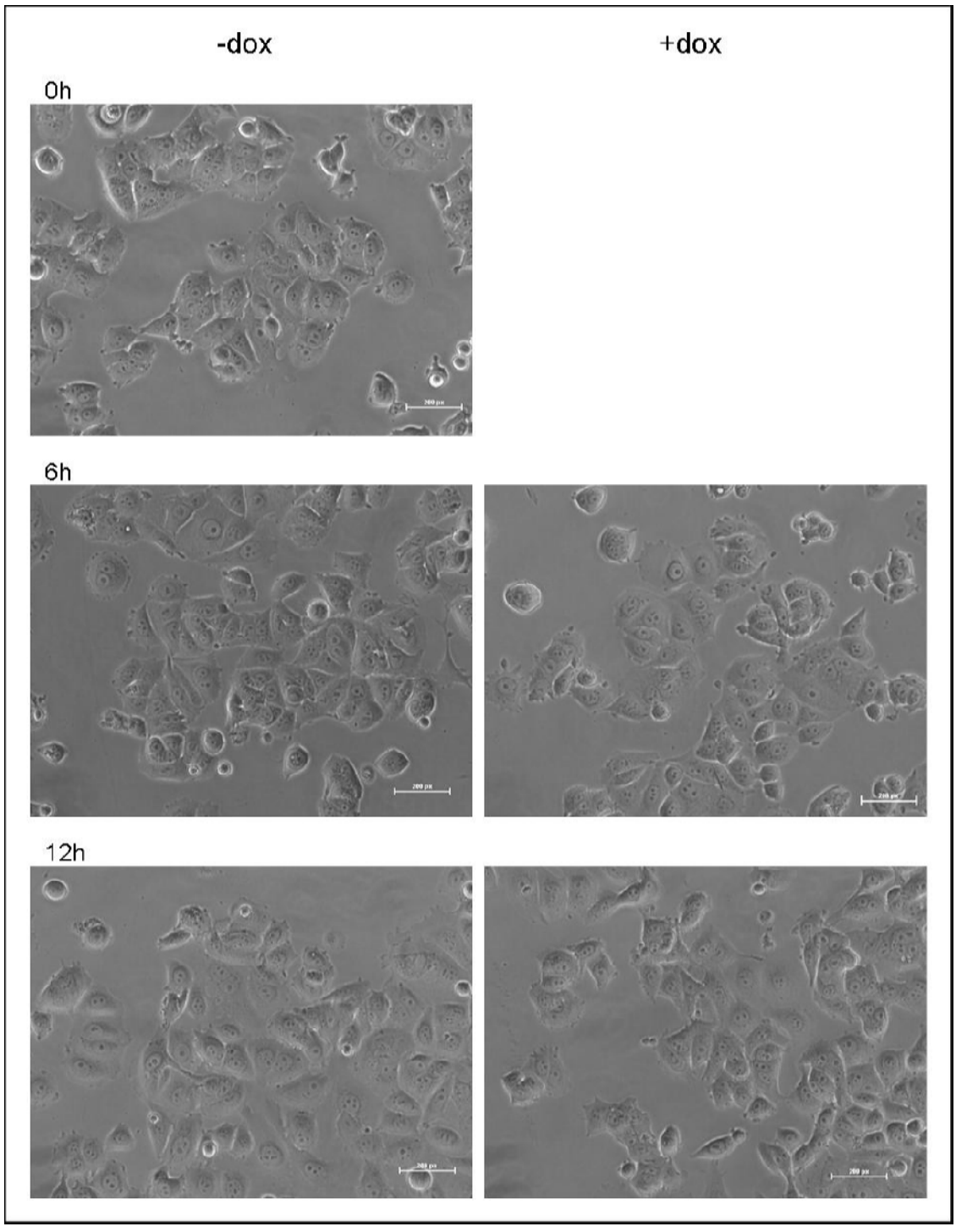

Figure 67: Phase-contrast microscopy on PTTG1 knockdown MCF7/NeuT cells (0h – 12h). Images were taken with a 20x objective for each time point and represent the 3 different oligoribonucleotides used. Phenotypically between 0h and 12h cells do not depict senescent characteristics.

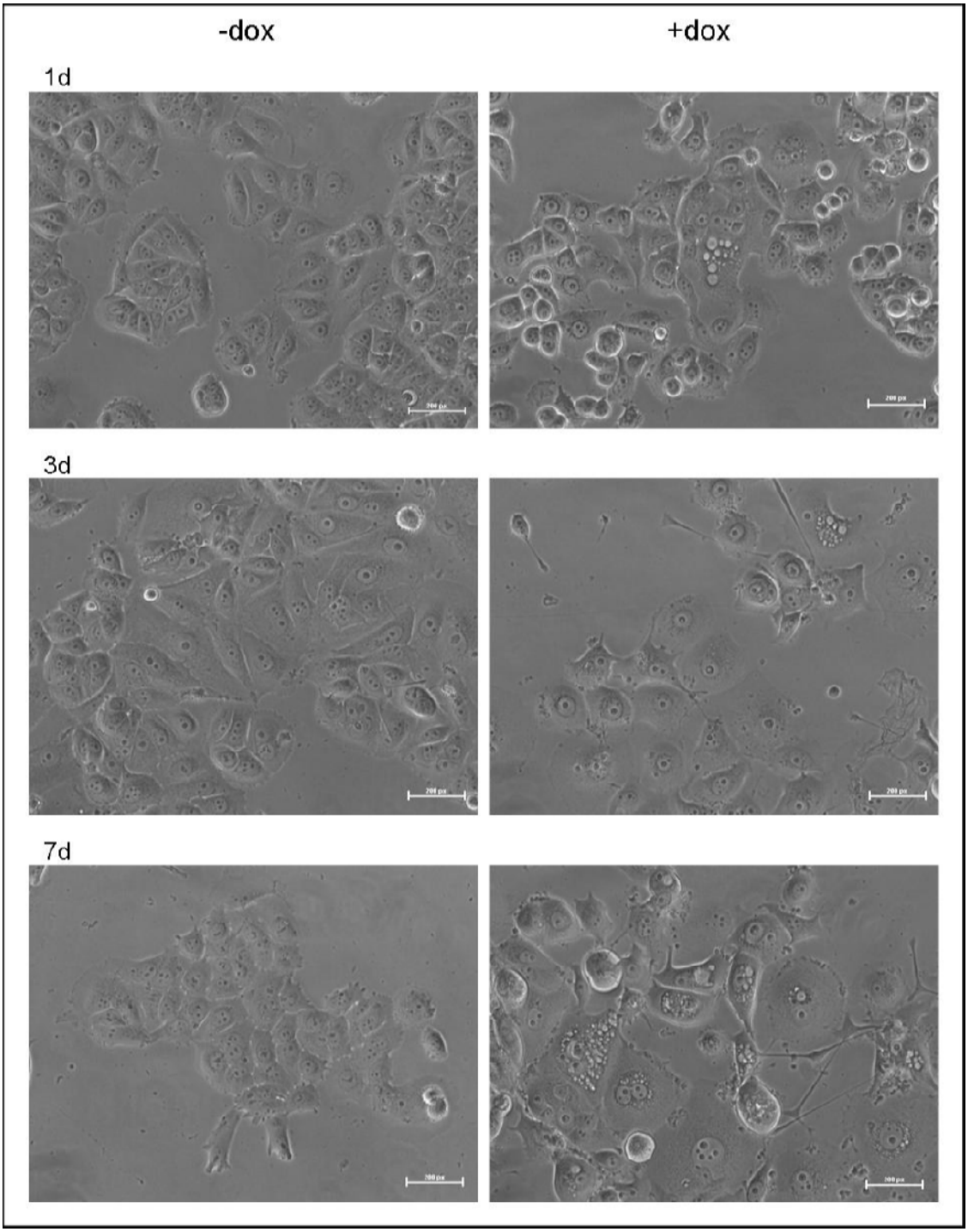

Figure 68: Phase-contrast microscopy of PTTG1 knockdown MCF7/NeuT (1d – 7d). Images were taken with a 20x objective for each time point and represent the 3 different oligoribonucleotides used. Phenotypically, after 1d of dox incubation MCF7/NeuT cells begin to show characteristics of senescence. PTTG1 has no effect on senescence.

3.2.4.5 Statistical Data Analysis of PTTG1 Knockdown MCF7/NeuT Cells

To determine significant differences between non-treated and treated samples a Mann-Whitney U test was performed where significant p-values were equal to or less than 0.05 (Table 8). To measure the significant differences between the different treated samples a Kruskall-Wallis test was performed on all samples (Table 9). Those found to have significant differences among the three treated groups of a specific gene at a specific time point were then subjected to post-hoc tests. Mann-Whitney U was performed among the three treated groups (Table 10) followed by a Bonferroni correction (Table 11) where p-values were equal to or less than 0.05 are considered significant. Values highlighted in bold showed significant differences. Looking at the Bonferroni correction table (Table 11) no significant difference was found between treated samples. The statistical results indicate that PTTG1 knockdown had no effect on NeuT overexpressing samples in senescent and cyclin biomarker gene expression.

Table 8: Mann-Whitney U (p-values) statistical comparison of the relative quantity of gene expression of senescence and cyclin biomarkers in non-treated and treated PTTG1 knockdown samples.

Non-Transfected Samples Non-Treated vs. Treated with Dox						
Time	0h	6h	12h	24h	3d	7d
Gene						
ErbB2(NeuT)		**0.050**	**0.050**	**0.050**	**0.050**	**0.050**
P21		**0.050**	**0.050**	**0.050**	**0.050**	**0.050**
PTTG1		0.827	**0.050**	**0.050**	**0.050**	0.275
P53		0.275	0.827	0.513	0.827	**0.046**
P38		**0.050**	**0.050**	**0.050**	0.275	0.121
CCNB2		**0.046**	**0.050**	**0.050**	**0.050**	0.184
PTTG1 Transfected Samples Non-Treated vs. Treated with Dox						
ErbB2(NeuT)		**0.000**	**0.000**	**0.000**	**0.000**	**0.000**
P21		**0.006**	**0.001**	**0.000**	**0.000**	**0.000**
PTTG1		0.268	0.200	0.074	**0.000**	**0.000**
P53		**0.034**	**0.000**	**0.012**	**0.000**	**0.000**
P38		**0.004**	**0.003**	0.825	0.093	0.402
CCNB2		0.122	**0.030**	0.093	**0.000**	**0.000**
Non-Sense Transfected Samples Non-Treated vs. Treated with Dox						
ErbB2(NeuT)		**0.050**	**0.050**	**0.050**	**0.050**	**0.050**
P21		**0.050**	**0.050**	**0.050**	**0.050**	**0.050**
PTTG1		0.513	**0.050**	**0.050**	**0.050**	**0.050**
P53		0.127	**0.050**	0.127	**0.050**	**0.050**
P38		0.268	0.827	0.513	0.127	0.513
CCNB2		0.268	0.275	0.513	**0.050**	**0.050**

Table 9: Kruskall-Wallis (p-value) statistical comparison of the relative quantity of gene expression of senescence and cyclin biomarkers in treated PTTG1 knockdown samples.

Non-Transfected vs. PTTG1 Knockdown Transfected vs. Non-Sense Transfected Samples Treated with Dox						
Time	0h	6h	12h	24h	3d	7d
Gene						
ErbB2(NeuT)						
P21		**0.033**	0.184	0.208	0.949	0.308
PTTG1		**0.006**	**0.009**	**0.004**	**0.005**	**0.027**
P53		**0.029**	0.937	0.513	**0.020**	**0.048**
P38		**0.032**	0.148	0.087	0.867	0.587
CCNB2		**0.030**	0.508	0.956	0.159	0.081

Table 10: Mann-Whitney U (p-values) statistical comparison of the relative quantity of gene expression of senescence and cyclin biomarkers among treated PTTG1 knockdown samples. NS – Not Significant

Non-Transfected vs. PTTG1 Knockdown Transfected Treated Samples						
Time	0h	6h	12h	24h	3d	7d
Gene						
ErbB2(NeuT)						
P21		**0.013**	NS	NS	NS	NS
PTTG1		**0.012**	**0.042**	**0.012**	**0.012**	0.404
P53		**0.012**	NS	NS	**0.012**	**0.020**
P38		**0.013**	NS	NS	NS	NS
CCNB2		**0.013**	NS	NS	NS	NS
Non-Sense Transfected vs. PTTG1 Knockdown Transfected Treated Samples						
ErbB2(NeuT)						
P21		0.792	NS	NS	NS	NS
PTTG1		**0.012**	**0.013**	**0.012**	**0.012**	**0.012**
P53		0.515	NS	NS	0.194	1.000
P38		0.664	NS	NS	NS	NS
CCNB2		0.518	NS	NS	NS	NS
Non-Transfected vs. Non-Sense Transfected Treated Samples						
ErbB2(NeuT)						
P21		**0.050**	NS	NS	NS	NS
PTTG1		0.513	**0.050**	**0.050**	0.184	**0.050**
P53		**0.050**	NS	NS	**0.050**	**0.046**
P38		**0.050**	NS	NS	NS	NS
CCNB2		**0.050**	NS	NS	NS	NS

Table 11: Bonferroni correction (p-value) post-hoc statistical comparison of the relative quantity of gene expression of senescence and cyclin biomarkers among treated PTTG1 knockdown samples. NS – Not Significant.

Non-Transfected vs. PTTG1 Knockdown Transfected Treated Samples						
Time	0h	6h	12h	24h	3d	7d
Gene						
ErbB2(NeuT)						
P21		**0.039**	NS	NS	NS	NS
PTTG1		**0.036**	0.126	**0.036**	**0.036**	NS
P53		**0.036**	NS	NS	**0.036**	0.060
P38		**0.039**	NS	NS	NS	NS
CCNB2		**0.039**	NS	NS	NS	NS
Non-Sense Transfected vs. PTTG1 Knockdown Transfected Treated Samples						
ErbB2(NeuT)						
P21		NS	NS	NS	NS	NS
PTTG1		**0.036**	**0.039**	**0.036**	**0.036**	**0.036**
P53		NS	NS	NS	NS	NS
P38		NS	NS	NS	NS	NS
CCNB2		NS	NS	NS	NS	NS
Non-Transfected vs. Non-Sense Transfected Treated Samples						
ErbB2(NeuT)						
P21		0.150	NS	NS	NS	NS
PTTG1		NS	0.150	0.150	NS	0.150
P53		0.150	NS	NS	0.150	0.138
P38		0.150	NS	NS	NS	NS
CCNB2		0.150	NS	NS	NS	NS

3.2.5 NeuT Overexpression Influences Cytochrome *c* Expression

3.2.5.1 Detection of Cytochrome c in MCF7/NeuT Cells Overexpressing NeuT by Raman micro-Spectroscopy

Single MCF7/NeuT cells were imaged by Raman micro-Spectroscopy (RMS) to observe changes in the chemical and molecular structures of cells as they enter senescence by the overexpression of NeuT. MCF7/NeuT cells were prepared and analysed as described in the Materials and Methods section (2.2.13). RMS images revealed an increase in cytochrome c expression in overexpressing NeuT cells after 7 days of dox treatment. Figure 69 depicts images of the measurements gathered.

Images were divided into three different groups. The first group is the chemical images taken from the raster scattering by the laser as it excites the sample, collecting one spectrum per pixel (pixel size approx. 550nm). The second group represents images derived from the vertical component analysis which is created when spectral data taken from the chemical image undergoes hierarchical cluster analysis. The hyper-spectral matrices are clustered into areas of similar chemical and molecular composition which is represented by assigned false colouring. Finally, the third group of images are the visible images which is the image seen under the microscope prior to imaging.

Therefore, Image A represents the control sample where there was no transfection or treatment with dox. The vertical component analysis image revealed two types of clusters representing lipids (Green Cluster, Endmember 6) and proteins (Blue Cluster, Endmember 11) (Figure 69, A). This was determined by looking at the spectral data in figure 70 (Inlet 1) where endmember 6 was specific for lipid content due to the doublet for CH_2-stretching from 3000-2800 cm^{-1}. Endmember 11 in figure 70 (Inlet 1) was predominantly protein due to the single peak found at 2936 cm^{-1}. The second inlet in figure 71 representing wavenumbers in the range of 2000-800 cm^{-1} consists of mostly lipids with some protein content.

Image B represents the 7-day dox treated sample where cells were incubated with dox for 7 days with no transfection. Interestingly, vertical component analysis revealed a third cluster, shown in red (Figure 69, B). Upon closer inspection, spectral data revealed changes in cytochrome *c* expression (Figure 71). Figure 71, represents the spectral data from the MCF7/NeuT samples overexpressing NeuT after 7 days of dox incubation. When looking at inlet 1, a pattern of CH_2-stretching at 2898 cm^{-1} and 2882 cm^{-1} indicated membrane phospholipids and CH_2-stretching at 2855 cm^{-1} and 2847 cm^{-1} represented protein content. Comparing this to inlet 2, CH_2-stretching at 1460 cm^{-1} and 1436 cm^{-1} elucidated a deformation of methlyene groups in lipid and protein contents respectively. These variances were attributed to changes in cytochrome *c* binding in the intra- and extracellular membranes during senescence which was confirmed in the literature[74].

RMS successfully detected changes in cytochrome *c* expression in senescent cells. Therefore, MCF7/NeuT cells were then transfected with cytochrome *c* siRNA at 30nM (See appendix 6 for efficiency graphs), incubated with dox for 7 days and then imaged by RMS to re-confirm cytochrome *c* expression was isolated to senescing non-transfected cells only. Image C represents the spectra of MCF7/NeuT cells transfected with cytochrome *c* siRNA. The vertical component analysis data revealed only two clusters similar to that of the control cells (Figure 69, C). When looking closer at the spectral data (Figure 72) of 1600-800 cm^{-1} in treated cytochrome *c* transfected samples there was no detection of cytochrome *c* showing similar spectral patterns to that of the control samples. In conclusion, the Raman results revealed changes in cytochrome *c* expression upon upregulation of NeuT.

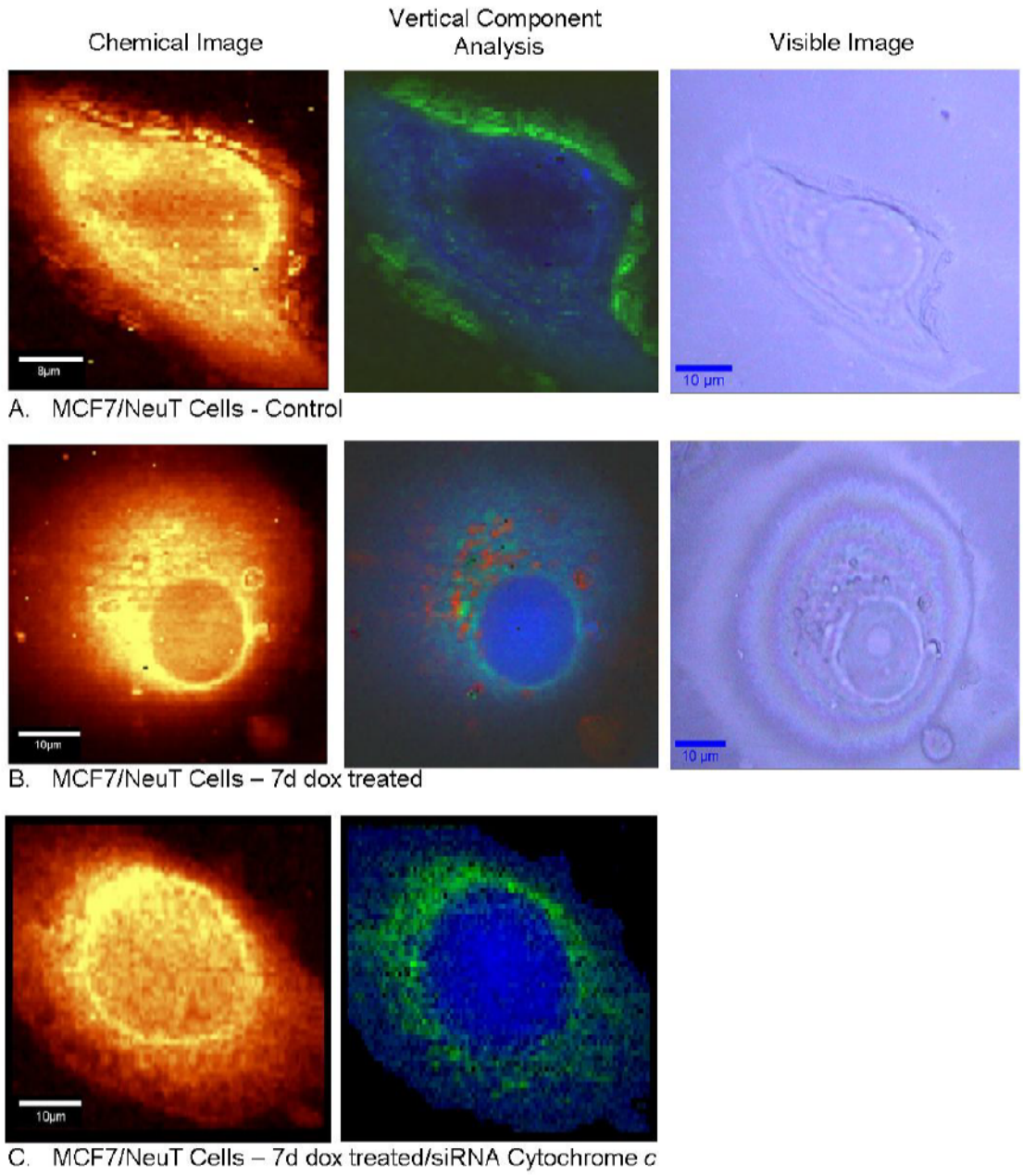

Figure 69: Raman micro-Spectroscopy analysis on single MCF7/NeuT cells. Changes in cytochrome *c* levels were detected in senescent MCF7/NeuT cells (Image B, shown in red under vertical component analysis). A) MCF7/NeuT cells without treatment or transfection used as control; B) MCF7/NeuT cells treated with dox for 7 days; C) MCF7/NeuT cells transfected with cytochrome *c* siRNA and treated with dox for 7 days. Individual cell images are a representation of five cells measured for each condition tested. Each pixel shown (approx. 100,000 per image) contains one spectral acquisition.

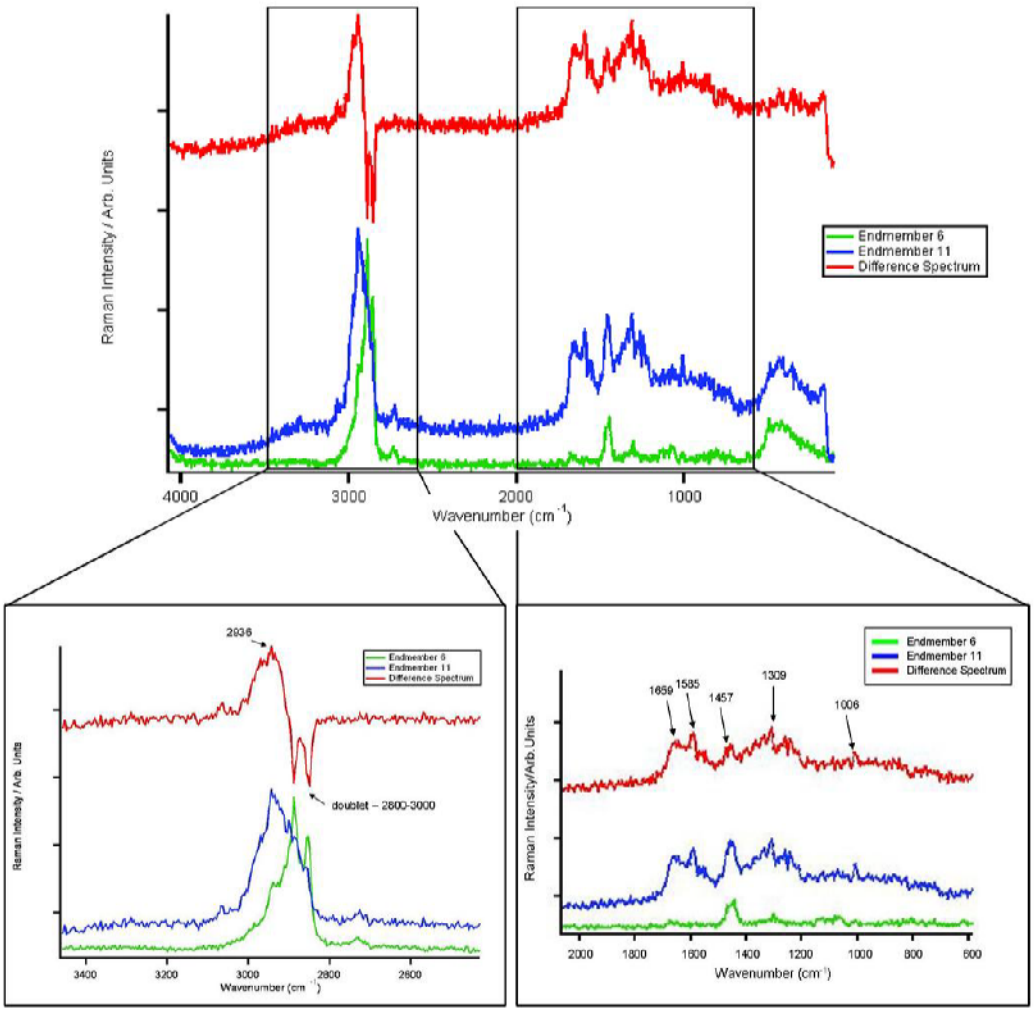

Figure 70: Average spectrum for each cluster (Endmembers 6 and 11) in MCF7/NeuT control samples. Spectral comparison revealed lipid and protein content in control cells. Top image represents an average of all spectra and inlets 1 (Left) and 2 (Right) represent the high- and low wavenumbers of these averages respectively. Endnumbers represent clusters of spectra which were extrapolated based on their spectral differences and were assigned arbitrary colours. Each spectrum is composed from and average of five independent cells.

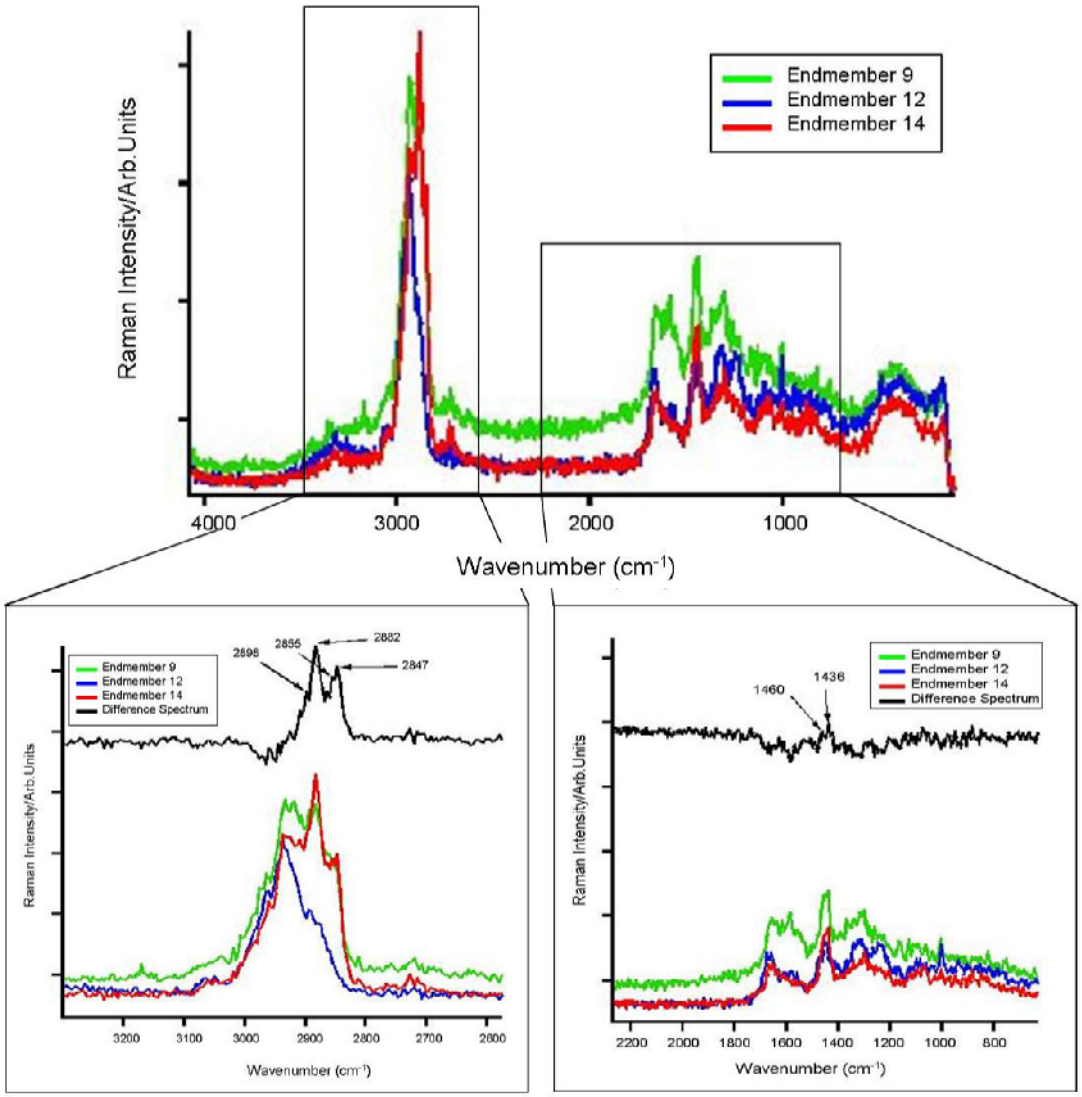

Figure 71: Average spectrum for each cluster (Endmembers 9, 12 and 14) in MCF7/NeuT 7-day dox treated samples. Spectral comparison revealed changes in cytochrome *c* content in 7 day dox treated cells. Top image represents an average of all spectra and inlets 1 (Left) and 2 (Right) represent the high- and low wavenumbers of these averages respectively. Endnumbers represent clusters of spectra which were extrapolated based on their spectral differences and were assigned arbitrary colours. Each spectrum is composed from an average of five independent cells.

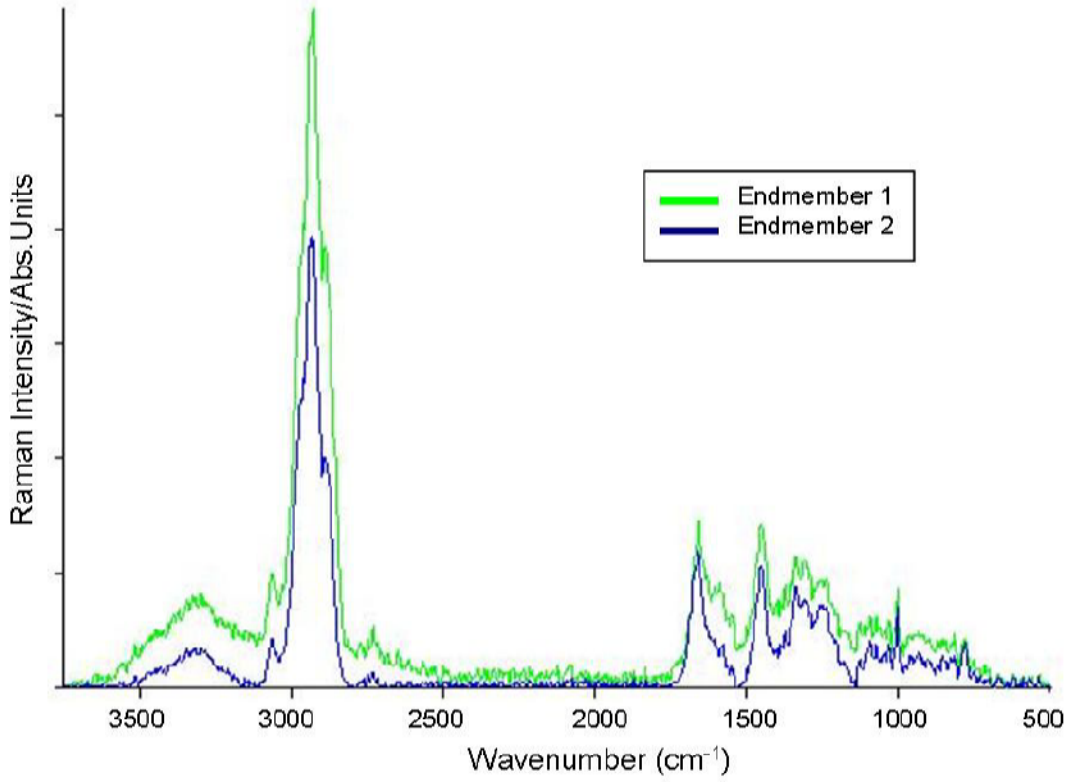

Figure 72: Average spectrum for each cluster (Endmembers 1 and 2) in MCF7/NeuT 7-day dox treated cytochrome *c* siRNA transfected samples. Spectral comparison revealed lipid and protein content similar to control cells. Endnumbers represent clusters of spectra which were extrapolated based on their spectral differences and were assigned arbitrary colours. Each spectrum is composed from an average of five independent cells.

3.2.5.2 Cytochrome c Detected in MCF7/NeuT Cells Overexpressing NeuT by Immunofluorescence

Cytochrome *c* expression was detected by immunofluorescence in MCF7/NeuT cells treated with or without dox. MCF7/NeuT cells were subjected to immunofluorescence as described in the Materials and Methods section 2.2.11. Figures 73 and 74 represent MCF7/NeuT non-treated and treated with dox samples respectively. Comparing the two sets of images, cytochrome *c* expression is greater in the 7 day dox treated sample than the non-treated sample (Figures 73 and 74 - merged with MitoTracker DeepRed shown in yellow). This could be due to the presence of fewer mitochondria in the non-treated sample compared to the treated sample. These results suggest that upon NeuT upregulation there is an increase in cytochrome *c* expression within the mitochondria.

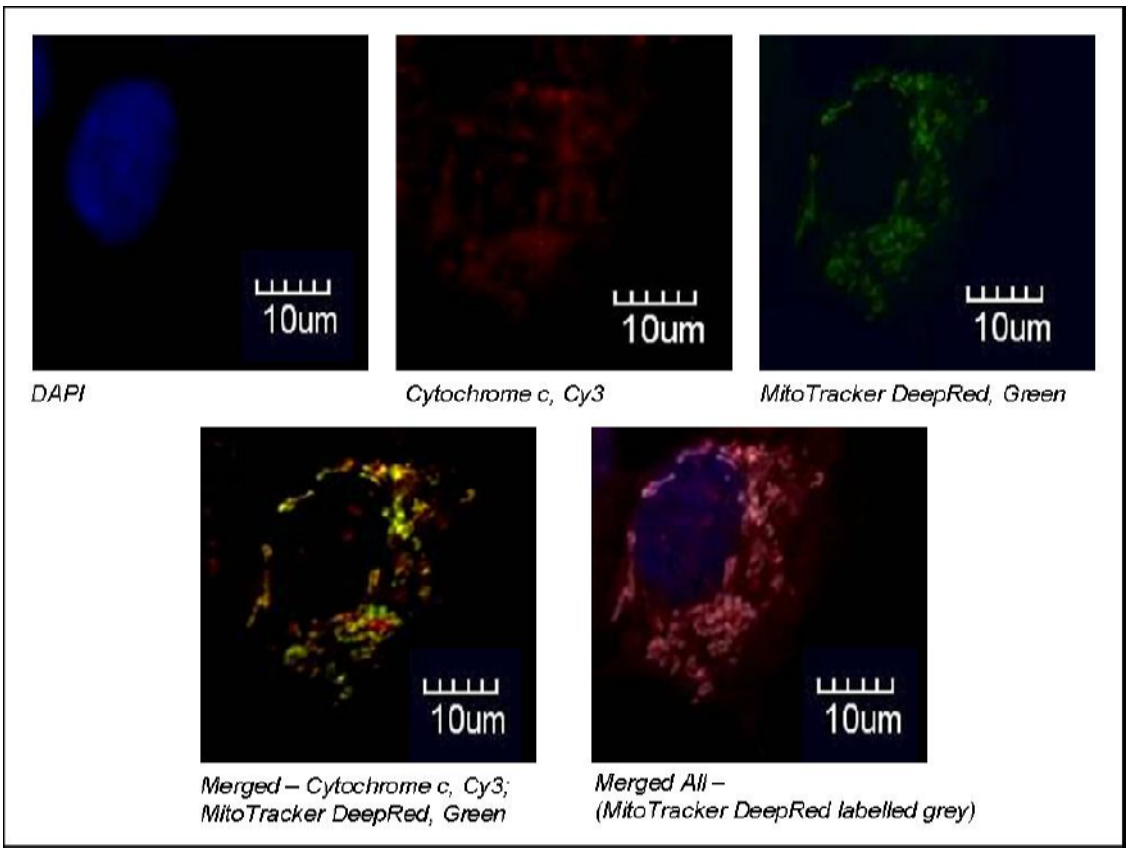

Figure 73: Non-treated MCF7/NeuT cells immunostained for cytochrome c expression. Low levels of cytochrome *c* expression was detected (merged with MitoTracker DeepRed, yellow). No EGFP was detected in the cells. NB: MitoTracker DeepRed was measured using Cy3 and then imaged in green to detect changes in cytochrome *c* expression. Image represents multiple cells stained.

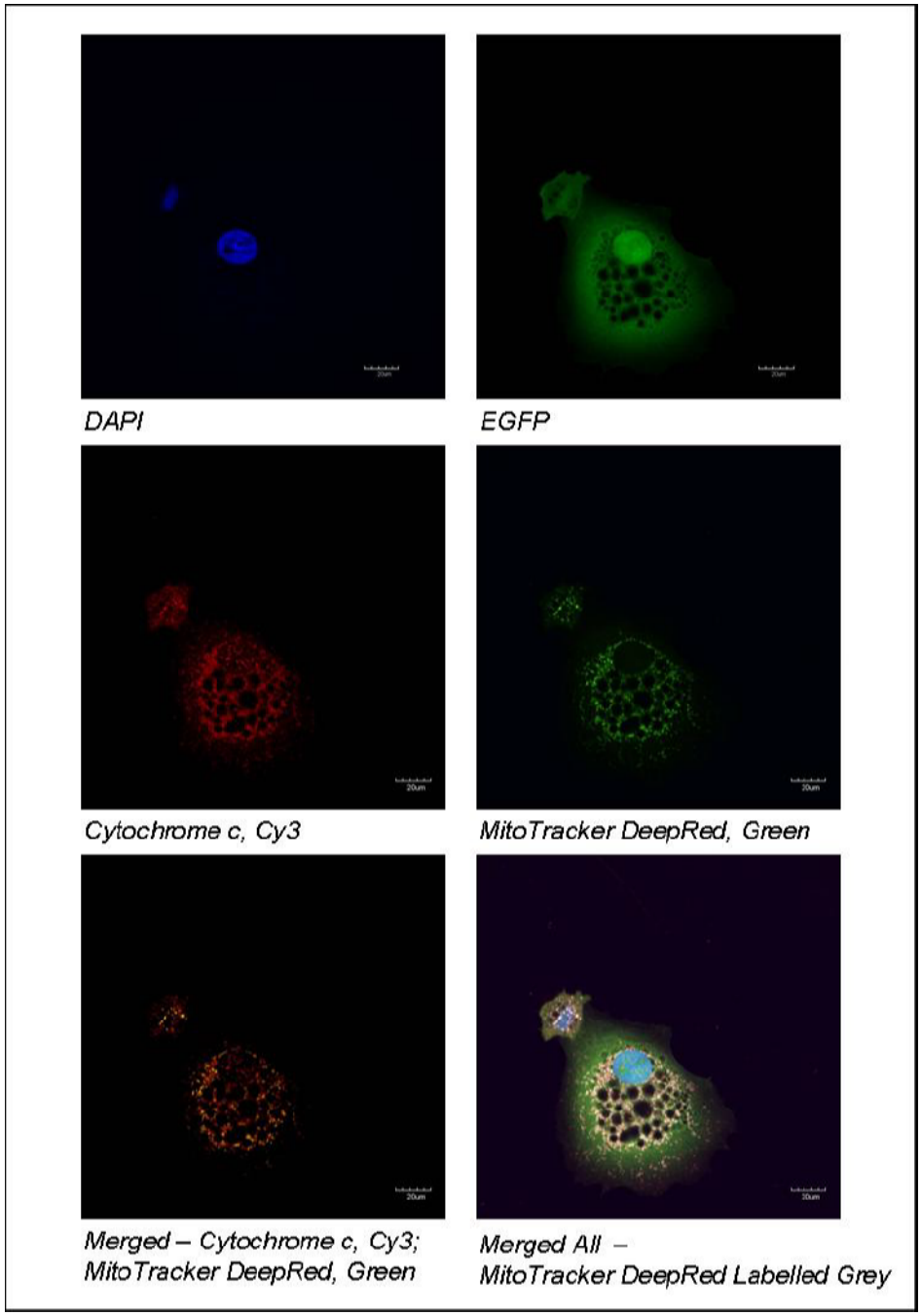

Figure 74: Treated (7 days dox) MCF7/NeuT cells immunostained for cytochrome c expression. Higher levels of cytochrome *c* expression was detected in overexpressing NeuT cells in the mitochondria (merged with MitoTracker DeepRed, yellow). NB: MitoTracker DeepRed was measured using Cy3 and then imaged in green to detect changes in cytochrome *c* expression. Image represents multiple cells stained.

3.2.5.3 Cytochrome c Protein Analysis Revealed an Increase in Expression in Overexpressing NeuT MCF7/NeuT Cells

Cytochrome *c* protein expression was measured by Western blot in MCF7/NeuT and MCF7/EGFP cells treated with and without (0h) dox. Results revealed an increase in cytochrome *c* expression after 3 days of dox incubation and having the highest protein concentration at 7 days of dox incubation in MCF7/NeuT cells (Figure 75). Low levels of cytochrome *c* expression were detected in MCF7/EGFP cells which was similar in expression to the MCF7/NeuT 0h sample. Protein analysis revealed an increase in cytochrome c expression upon upregulation of NeuT.

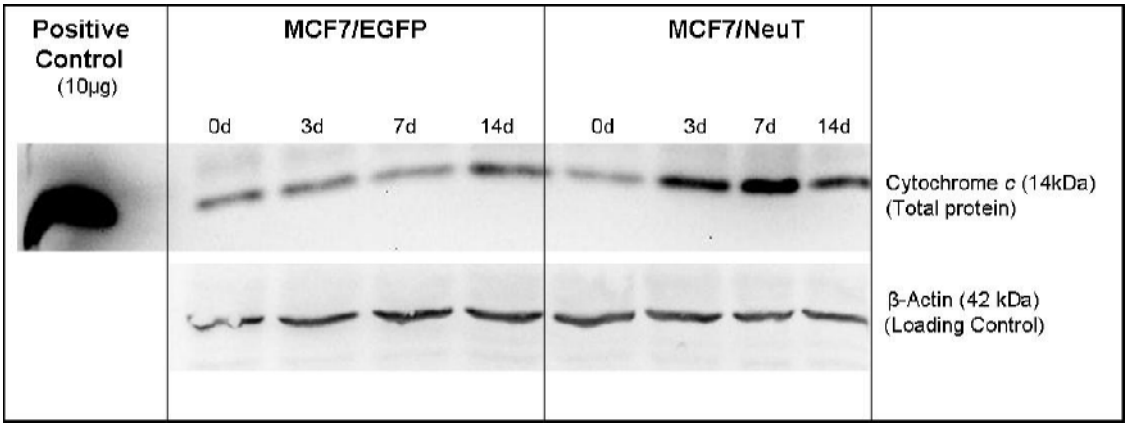

Figure 75: Western blot of cyctochrome c protein expression in MCF7/NeuT and MCF7/EGFP cells treated with or without dox.

3.2.5.4 Cytochrome c mRNA Expression in MCF7/NeuT and MCF7/EGFP Cells

Cytochrome *c* mRNA levels were found to be significantly increased in treated NeuT cells after 1 minute of dox incubation by approximately 2.75-fold (Figure 76). Cytochrome *c* levels then dropped below non-treated levels to then increase again after 12 hours of dox incubation, although not significant. Compared to MCF7/EGFP cells there is relatively little changes in cytochrome *c* expression in both non-treated and treated across the time course (Figure 77). In some cases there is a significant decrease by about 2-fold (30 minutes and 6 hours). These results indicate a slight increase in cytochrome *c* mRNA expression upon NeuT induction; however not significant after 1 minute of NeuT induction.

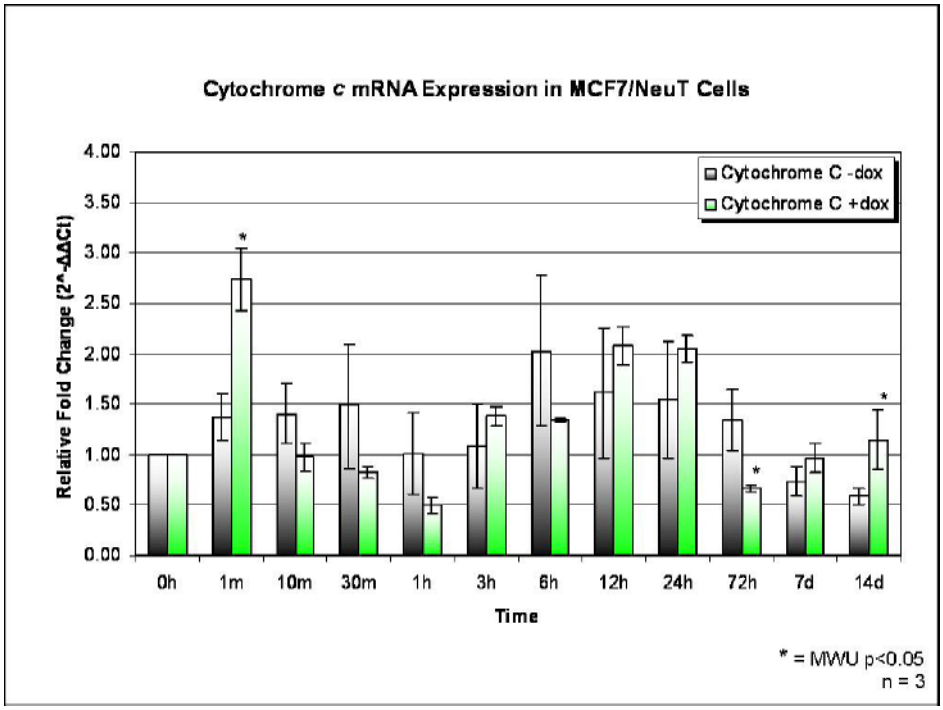

Figure 76: Cytochrome *c* mRNA expression in MCF7/NeuT cells treated with or without dox. Cytochrome *c* expression levels is significantly upregulated at 1 minute of treatment. Data values represent the mean 2^-ΔΔCt values of three independent experiments. MWU – Mann-Whitney U test.

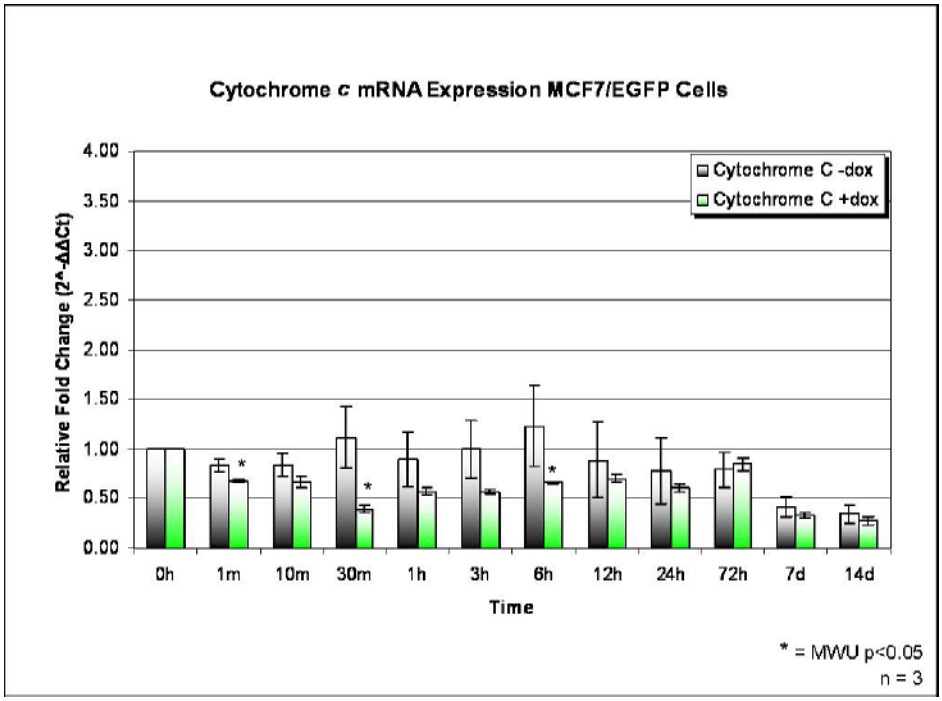

Figure 77: Cytochrome *c* mRNA expression in MCF7/EGFP cells treated with or without dox. Cytochrome *c* expression levels remain unexpressed or downregulated in both non-treated and treated samples throughout the time course. Data values represent the mean 2^-ΔΔCt values of 3 independent experiments.MWU–Mann-Whitney U test.

CHAPTER FOUR:
DISCUSSION

4.0 Discussion

4.1 Characterisation of Senescent Pathways Upon ErbB2/HER2 (NeuT) Upregulation

The epidermal growth factor family of receptors when activated trigger multiple networks of signalling pathways which lead to responses ranging from cell division to senescence and death, and from motility to adhesion[4]. Specifically, the receptor ErbB2 was found that upon overexpression induces senescence in the breast carcinoma cell line MCF7 via oncogenic *Ras* induction[25]. Activation of ErbB2 followed by *Ras* upregulation leads to multiple signalling cascades that eventually cause senescence. In this cell model, three known senescent signalling pathways were investigated to characterise and gain a better insight into oncogene-induced senescence via ErbB2/NeuT upregulation. Described by Bringold and Serrano, these three known pathways are the PTEN/$P27^{Kip1}$, $P16^{INK4a}$/Rb, and $P14^{ARF}$/P53/$P21^{Cip1}$ senescence-inducing pathways[44]. A number of biomarkers were investigated that are either apart of or affected by one these senescence-inducing pathways. Based on the data presented in this thesis, we propose that the MCF7/NeuT cells utilise all three of these known pathways to establish senescence upon NeuT overexpression. Increases in P21 expression was found to decrease levels of cyclin B2 which is essential in cell cycle progression. The pituitary tumour transforming gene 1 (PTTG1) which plays a role in tumour formation and cell growth was found to be expressed at higher levels in P21 siRNA transfected NeuT overexpressing samples compared to NeuT upregulated non-transfected and non-sense transfected samples (Figure 53). Interestingly, P38 which is involved in cell cycle regulation and known to trigger P53 production[75] showed no increase in expression and in some cases downregulation (Figures 37 and 38). This could indicate that other pathways may have been used to achieve senescence via oncogenic *Ras* and not through the classical P38 pathway[75] according to the low levels in RNA expression that was found.

4.1.1 PTEN/P27^{Kip1} Senescence Pathway in NeuT Upregulation

Gene expression studies indicated an upregulation in PTEN expression upon NeuT overexpression (Figure 33) compared to non-treated MCF7/NeuT and MCF7/EGFP cells treated and non-treated (Figures 33 and 34). This upregulation in PTEN occurs in the initial hours of NeuT overexpression and then decreases as the cells reach full senescence around day 7. PTEN expression is believed to aid in P53 regulation by restricting the ubiquitinase protein hdm2 (mdm2 is the mouse form) in the cytoplasm through blocking PI3K/Akt signalling thereby preventing its translocation into the nucleus and degradation of P53[76]. We see this activity by comparing the upregulation at individual time points between PTEN and P53 in NeuT upregulated samples (Figures 33 and 31). PTEN upregulation peaks at 3hrs and then begins to decrease in expression as the cells enter full senescence at 7 days. This pattern was also noticed in P53 expression, peaking at 3hrs followed by a decrease in expression to below non-treated levels at day 7 (Figure 31).

4.1.2 P16^{INK4a}/Rb Senescence Pathway in NeuT Upregulation

Rb gene expression was found to be upregulated in MCF7/NeuT dox treated cells. However, Rb was also found to be upregulated in MCF7/EGFP dox treated cells. This may be explained by dox having had a slight effect on Rb regulation or it could depend on the confluency of the cell culture flask prior to collection. However, when looking closely at the levels of Rb expression in MCF7/NeuT and MCF7/EGFP cells (Figures 35 and 36) the level of expression in MCF7/EGFP treated cells is relatively lower than that of MCF7/NeuT. Inactivation of Rb occurs with every cell cycle by the action of a group of cyclin dependent kinases which regulate the ability of Rb to restrain the cell cycle[57]. The upregulation of Rb is triggered by a series of upstream signalling events. Overexpression of P16 ^{INK4a} which is activated upon *Ras* upregulation[46] leads to a block in the cyclin dependent kinases 4/6 which are responsible for cyclin D activation. This allows for Rb to remain in its unphosphorylated/active state and bound to the cell cycle promoting transcription factor E2F restraining cell cycle progression. We see this continuous Rb expression throughout the time points including when cells reach full

senescence at 7 days (Figure 35) indicating that through overexpression of NeuT MCF7/NeuT cells utilise Rb expression.

4.1.3 $P14^{ARF}$/P53/$P21^{Cip1}$ Senescence Pathway in NeuT Upregulation

Gene expression studies of P53 and P21 expression upon NeuT upregulation depicted results that confirm tight regulation between P53 and P21 transcription. A downstream target of P53 is P21 which inhibits the binding of cyclin dependent kinase 2 to cyclin E[44]. Interestingly, P53 is upregulated in the beginning of the time course study from 1 minute to about 3 hours, at 6 hours when P21 becomes highly upregulated, P53 expression begins to decline. This phenomenon could represent a negative feedback loop on P53 expression where once P21 becomes highly expressed and begins to inhibit the cyclin dependent kinases involved in activating cyclins D and E, P53 is no longer needed for cell cycle arrest. It is citied that the upregulation of $P14^{ARF}$ where $P14^{ARF}$ is expressed upon *Ras* induction, in turn binds to the ubiquitinase protein hdm2 (mdm2 is mouse form) and allows for upregulation of P53 which then has a negative effect on $P14^{ARF}$ by preventing it's expression[77] eventually leading to a decline in P53 and P21. We were able to demonstrate this observation through analysing the mRNA expression of P53 and P21 after 7 days of dox incubation where both transcripts were expressed at lower levels compared to earlier time points (Figures 29 and 31). These findings suggest that upon NeuT overexpression MCF7/NeuT cells utilise the $P14^{ARF}$/P53/$P21^{Cip1}$ pathway to initiate senescence.

4.1.4 Cyclin Regulation Upon Senescent Pathway Induction

Cyclins are found to be overexpressed in many cancers in particular cyclin D1 is deregulated in breast tumours[78]. Gene expression studies of treated MCF7/NeuT cells revealed an upregulation in cyclin D1 (Figure 39) and E1 (Figure 41) and a downregulation in cyclin B2 (Figure 43). Cyclin D1 became highly over expressed at 3 hours, however; after 72 hours it began to decrease as senescence progressed. Interestingly, cyclin E1 increased at the same time points as cyclin D1 and then began to decrease at 72 hours however; it increased again at 14 days. This maintenance of cyclin

E1 during senescence could be due to *Ras* activation caused by NeuT overexpression[79]. Cyclin B2 was shown to decline in expression after 6 hours of dox treatment (Figure 43). Interestingly, this decline in cyclin B2 occurs as P21 becomes highly upregulated. Cyclin B2 is downstream of the $P14^{ARF}$/P53/$P21^{Cip1}$ pathway and is inhibited by targets of P53 upregulation. We conclude from this data that cyclin D1, E1 and B2 may be regulated by senescence induced pathways and oncogenic *Ras* expression in MCF7/NeuT cells overexpressing NeuT.

4.2 Silencing P21 Expression Leads to Signalling Changes Upon NeuT Upregulation

Researchers have speculated the role of P21 in senescence in its ability to establish senescence[75, 76]. However, in this study using siRNA technology we were able to successfully inhibit P21 expression (Figure 50) and senescence in NeuT overexpressing MCF7/NeuT cells. P53 mRNA expression was measured in P21 siRNA transfected samples and interestingly P53 expression was found to be similar across all of the treated samples. This could be explained by the findings in P53 expression of non-transfected samples. At the initial time points measured P53 expression was elevated and then declined to normal levels during the time points that were only measured with the siRNA transfection samples. Therefore the differences between non-transfected and transfected were not found to be significant. As expected, P38 showed no changes in mRNA expression in P21 siRNA transfected samples compared to non-transfected and non-sense transfected samples (Figure 52). According to the low levels in mRNA expression that was found it could indicate that other pathways might have been used to achieve senescence via oncogenic *Ras* and not through the classical P38 pathway[77]. Interestingly, the pituitary tumour transforming gene 1 (PTTG1) showed expression levels to that of non-treated at 0.50 and 1 day dox incubation in P21 siRNA transfected samples (Figure 53). These levels were significantly different from that of treated P21 non-transfected samples. This could point towards a possible regulation of PTTG1 expression upon P21 overexpression. Chesnokova et al. in 2008 observed a similar effect in $Rb^{+/-}PTTG1^{-/-}P21^{-/-}$ mice where background PTTG1 expression was restored upon P21 deletion and cell proliferation persisted[66]. We see in the PTTG1 siRNA transfected

samples, P21 expression is expressed at similar levels to that of non-transfected and non-sense transfected samples depicting that PTTG1 may not have an effect on P21 but that P21 may have an effect on PTTG1 expression upon upregulation of NeuT.

As mentioned earlier cyclins are deregulated in many types of cancers. Here, after P21 knockdown, we detected slight changes in cyclin B2 expression which is important for transition from the G2 phase to mitosis. Cyclin B2 expression was found to be significantly higher at 0.50, 1 and 3 days dox incubation in P21 siRNA transfected samples (Figure 56) (Table 7). We notice this increase in Cyclin B2 expression to be higher in P21 siRNA transfection samples until 3 days of dox incubation. Due to the inefficiency of the siRNAs, P21 was no longer able to remain silenced and at day 7 a decline in Cyclin B2 expression was seen at the level of the non-transfected and non-sense transfected samples. This is confirmed when observing the phase contrast microscopy images (Figures 57 and 58) where until 7 days of dox incubation cells retained normal non-senescencent morphology. We can conclude that upon P21 inhibition MCF7/NeuT cells are able to escape senescence when overexpressing NeuT according to the upregulation in cyclin B2 mRNA and phase contrast morphology images.

Cyclins D1 and E1 were found to be expressed at similar levels in all treated samples in a majority of the time points (Figures 54 and 55). It is known that P21 blocks the binding of cyclin dependent kinases involved in activating cyclins D1 and E1. Therefore upon P21 inhibition we should have seen a decline in cyclins D and E expression to that of non-treated samples at all time points due to the activation and degradation by cyclin dependent kinases. In P21 siRNA transfected samples we see the level in cyclin D and E expression to be at that of non-treated samples however; compared to non-sense siRNA transfected samples cyclin D and E levels are also at the same level of expression as P21 siRNA transfected samples. This could be explained by the possibility of other off-target effects caused from the non-sense transfection. Another possibility could be the confluency of the culture dishes making the non-treated samples have higher basal expression levels of cyclin D and E therefore, the difference between non-treated and

treated is then insignificant. Interestingly, cyclin D1 was found to be expressed at lower levels in treated P21 siRNA transfected samples at 0.50, 1 and 3 days compared to treated non-transfected and non-sense transfected samples. Although not significant, treated P21 siRNA transfected samples cells were able to continue to proliferate therefore one would assume then that Rb was able to be phosphorylated in order to progress through the cell cycle. This would then cause a decline in cyclin D1 as cells enter the S-phase. In conclusion looking across these findings it can be suggested that P21 has an important role in maintaining senescence in NeuT overexpressing MCF7/NeuT cells through changes in senescent biomarkers as well as changes in cyclins important for cell cycle progression.

4.3 PTTG1 Portrays No Effect on ErbB2/HER2 (NeuT) Oncogene-induced Senescence

Our findings suggest that inhibition of PTTG1 has no effect on senescence progression. Levels of P21 were shown to be upregulated in treated PTTG1 siRNA transfected samples similar to that of treated non-transfected and non-sense transfected samples (Figure 62). P53 mRNA expression in treated PTTG1 siRNA transfected samples was also shown to be expressed at similar levels to the non-transfected and non-sense transfected samples, indicating that PTTG1 has no effect on P53 expression. As expected P38 expression depicted little changes between treated and non-treated samples again indicating that according to mRNA expression another pathway may be being used to initiate senescence. Interestingly, when looking at cyclin B2 levels in treated PTTG1 siRNA transfected samples they were expressed at relatively similar levels to that of treated non-transfected and non-sense transfected samples (Figure 66). One could then speculate that P21 may be at the crossroad for tumour cells to either enter senescence or to continue proliferating given the significant differences in cyclin B2 expression in both types of transfected samples. Looking at the phenotypic morphology of PTTG1 siRNA transfected samples it was observed that after 24 hours of dox treatment cells began to show senescent morphology characteristics such as the appearance of vacuoles and a flattened shape (Figure 68) similar to that of non-transfected treated MCF7/NeuT cells (Figure 23). These findings suggest that PTTG1 does not have a function for preventing

senescence however; due to its increase in expression during dox incubation in P21 siRNA transfected samples it may play a role in MCF7 cell proliferation.

4.4 ErbB2/HER2 (NeuT) Oncogene-induced Senescence Increases Cytochrome c Expression

It is well documented that several P53 regulated genes are known to enhance cytochrome *c* expression to increase cell cycle arrest potential[78]. We were able to confirm this phenomenon in overexpressing NeuT MCF7/NeuT cells. Using the novel technique, Raman micro-Spectroscopy we detected chemical changes of cytochrome *c* expression (Figure 69) at the molecular level in NeuT induced MCF7/NeuT cells. Upon this finding we were also able confirm cytochrome *c* expression by immunofluorescence where MCF7/NeuT cells treated with dox for 7 days showed higher levels of cytochrome *c* expression (Figure 74) compared to non-treated cells (Figure 73). Protein expression by Western blot (Figure 75) and mRNA expression by RT-qPCR (Figure 76) of cytochrome *c* also confirmed elevated levels of cytochrome *c* expression in NeuT overexpressing cells. Increased cytochrome *c* expression could be explained by changes in cellular metabolism activity during senescence. Recent studies found that products of certain oncogenes, in particular, *Ras*, can upregulate the gene expression of various cellular metabolic reactions[79, 80]. Another possibility is that P53, a downstream product of *Ras*, is known to regulate mitochondrial respiration[81] thereby effecting cytochrome *c* expression. Nevertheless, our findings suggest that there is a correlation between senescence and cytochrome *c* expression.

4.5 Conclusions

Taken together, our data shows that upon ErbB2/NeuT upregulation a series of orchestrated events must occur to drive oncogene-induced senescence. The cyclin dependent kinase inhibitor, P21 seems to portray an important role in cell cycle regulation upon NeuT activation. Although not investigated in this study, other cyclin dependent kinase inhibitors such as $P27^{Kip1}$ and $P16^{INK4a}$ may also be important for cell cycle regulation upon NeuT overexpression and oncogenic *Ras* activation. Moreover, the newly discovered oncogene PTTG1 should be further investigated since it was found to be higher expressed in P21 depleted cells overexpressing NeuT. Finally, Raman micro-Spectroscopy has proven to be a useful technique in detecting chemical and molecular changes in non-senescent and senescent cells showing its importance in cancer diagnostics and research. Our findings provide a strong biological characterisation and background for mRNA based expression of NeuT overexpressing MCF7/NeuT cells for an oncogene-induced senescence model and could be used for further study in discovering possible mechanisms for cancer cells to escape senescence.

1. Gschwind, A., O.M. Fischer, and A. Ullrich, *The discovery of receptor tyrosine kinases: targets for cancer therapy.* Nature Reviews, 2004. **4**(361-370).
2. Mitsudomi, T. and Y. Yatabe, *Epidermal growth factor receptor in relation to tumor development: EGFR gene and cancer.* FEBS J., 2009(November).
3. Burden, S. and Y. Yarden, *Neuregulins and their receptors: a versatile signalling module in organogenesis and oncogenesis.* Neuron, 1997. **18**(847-855).
4. Yarden, Y. and M.X. Sliwkowski, *Untangling the ErbB signalling network.* Nature Reviews Molecular Cell Biology, 2001. **2**(February 2001): p. 127-137.
5. Roskoski, R., *The ErbB/HER receptor protein-tyrosine kinases and cancer.* Biochemical and Biophysical Research Communications, 2004. **319**: p. 1-11.
6. Olayioye, M.A., et al., *The ErbB signalling network: receptor heterodimerization in development and cancer.* EMBO Journal, 2000. **19**(13): p. 3159-3167.
7. Graus-Porta, D., et al., *ErbB-2, the preferred heterodimerisation partner of all ErbB receptors, is a mediator of lateral signaling.* EMBO Journal, 1997. **16**(7): p. 1647-1655.
8. Burgess, A.W., et al., *An open-and-shut case? Recent insights into the activation of EGF/ErbB receptors.* Molecular Cell, 2003. **12**(3): p. 541-52.
9. Ogiso, H., et al., *Crystal structure of the complex of human epidermal growth factor and receptor extracellular domains.* Cell, 2002. **110**(6): p. 775-87.
10. Ferguson, K.M., et al., *EGF activates its receptor by removing interactions that autoinhibit ectodomain dimerization.* Molecular Cell, 2003. **11**(2): p. 507-17.
11. Schlessinger, J., *Cell signaling by receptor tyrosine kinases.* Cell, 2000. **103**(2): p. 211-25.
12. Lammerts van Bueren, J.J., et al., *The antibody zalutumumab inhibits epidermal growth factor receptor signaling by limiting intra- and intermolecular flexibility.* PNAS, 2008. **105**(16): p. 6109-6114.
13. Beerli, R.R., et al., *Neu differentiation factor activation of ErbB-3 and ErbB-4 is cell specfic and displays a differential requirement for ErbB-2.* Molecular and Cellular Biology, 1995. **15**: p. 6496-6505.
14. Hynes, N.E. and H.A. Lane, *Erbb receptors and cancer: the complexity of targeted inhibitors.* Nature Reviews Cancer, 2005. **5**: p. 341-354.
15. Chausovsky, A., et al., *Molecular requirements for the effect of neuregulin on cell spreading, motility and colony organization.* Oncogene, 2000. **19**(7): p. 878-888.
16. Alimandi, M., et al., *Cooperative signaling of ErbB3 and ErbB2 in neoplastic transformation and human mammary carcinomas.* Oncogene, 1995. **10**(9): p. 1813-1821.
17. Schechter, A.L., et al., *The neu gene: an erbB-homologous gene distinct from and unlinked to the gene encoding the EGF receptor.* Science, 1985. **229**(4717): p. 976-980.
18. Coussens, L., et al., *Tyrosine kinase receptor with extensive homology to EGF receptor shares chromosomal location with neu oncogene.* Science, 1985. **230**(4730): p. 1132-1139.
19. Akiyama, T., et al., *The product of the human c-erbB-2 gene: a 185-kilodalton glycoprotein with tyrosine kinase activity.* Science, 1986. **232**(4758): p. 1644-1646.

20. Slamon, D.J., et al., *Studies of the HER-2/neu proto-oncogene in human breast and ovarian cancer.* Science, 1989. **244**(4905): p. 707-712.
21. Pegram, M.D., et al., *The effect of HER-2/neu overexpression on chemotherapeutic drug sensitivity in human breast and ovarian cancer cells.* Oncogene, 1997. **15**(5): p. 537-547.
22. Lin, W., et al., *Aberrant development of motor axons and neuromuscular synapses in erbB2-deficient mice.* PNAS, 2000. **97**(3): p. 1299-1304.
23. Andrechek, E.R., et al., *ErbB2 is required for muscle spindle and myoblast cell survival.* Molecular and Cellular Biology, 2002. **22**(13): p. 4714-4722.
24. Crone, S.A., et al., *ErbB2 is essential in the prevention of dilated cardiomyopathy.* Nature Medicine, 2002. **8**(5): p. 459-465.
25. Trost, T.M., et al., *Premature senescence is a primary fail-safe mechanism of ErbB2-driven tumorigenesis in breast carcinoma cells.* Cancer Research, 2005. **65**(3): p. 840-849.
26. Bos, J.L., *Ras oncogenes in human cancer: A review.* Cancer Research, 1989. **49**: p. 4682-4689.
27. Lewis, T.S., P.S. Shapiro, and N.G. Ahn, *Signal transduction through MAP kinase cascades.* Advances in Cancer Research, 1998. **74**: p. 49-139.
28. Kolch, W., et al., *The organisation and function of the Ras-Raf-MEK-ERK pathway.* Expert Reviews in Molecular Medicine, 2002(April).
29. Cully, M., et al., *Beyond PTEN mutations: the PI3K pathway as an integrator of multiple inputs during tumorigenesis.* Nature Reviews Cancer, 2006. **6**: p. 184-192.
30. Treins, C., et al., *Rictor is a novel target of p70 S6 kinase-1.* Oncogene, 2009(Nov.).
31. Chien, C.S., et al., *Antimetastatic potential of fisetin involves inactivation of the PI3K/Akt and JNK signaling pathways with downregulation of MMP-2/9 expressions in prostate cancer PC-3 cells.* Molecular Cellular Biochemistry, 2009(Jul).
32. Jiang, B.H. and L.Z. Liu, *PI3K/PTEN signaling in angiogenesis and tumorigenesis.* Advances in Cancer Research, 2009. **102**: p. 19-65.
33. Ross, J.S. and J.A. Fletcher, *The HER-2/neu oncogene in breast cancer: prognosic factor, predictive factor, and target for therapy.* Stem Cells, 1998. **16**: p. 413-428.
34. Jannot, C.B., et al., *Intracellular expression of a single-chain antibody directed to the EGFR leads to growth inhibition of tumour cells.* Oncogene, 1996. **13**: p. 275-282.
35. Pietras, R.J., et al., *HER-2 tyrosine kinase pathway targets estrogen receptor and promotes hormone-independent growth in human breast cancer cells.* Oncogene, 1995. **10**(12): p. 2435-2446.
36. Giani, C., et al., *Increased expression of c-erbB-2 in hormone-dependent breast cancer cells inhibits cell growth and induces differentiation.* Oncogene, 1998. **17**(4): p. 425-432.
37. Sliwkowski, M.X., et al., *Nonclinical studies addressing the mechanism of action of trastuzumab (Herceptin).* Semin. Oncol., 1999. **26**(4): p. 60-70.

38. Saez, E., et al., *Inducible gene expression in mammalian cells and transgenic mice.* Current Opinion Biotechnology, 1997. **8**: p. 608-616.
39. Saez, E., *Identification of ligands and coligands for the ecdysone-regulated gene switch.* PNAS, 2000. **97**: p. 14512-14517.
40. Cronin, C.A., W. Gluba, and H. Scrable, *The lac-operator-repressor system is functional in the mouse.* Genes Development, 2001. **15**: p. 1506-1517.
41. Wang, X.J., et al., *Development of gene-switch transgenic mice that inducibly express transforming growth factor beta-1 the epidermis.* PNAS, 1999. **96**: p. 8483-8488.
42. Gossen, M. and H. Bujard, *Tight control of gene expression in mammalian cells by tetracycline-responsive promoters.* PNAS, 1992. **89**: p. 5547-5551.
43. Zhu, Z., et al., *Tetracycline-controlled transcriptional regulation systems: advances and application in transgenic animal modeling.* Cell and Developmental Biology, 2002. **13**: p. 121-128.
44. Bringold, F. and M. Serrano, *Tumor suppressors and oncogenes in cellular senescence.* Experimental Gerontology, 2000. **35**: p. 317-329.
45. Mulumbres, M. and A. Pellicer, *Ras pathways to cell cycle control and cell transformation.* Frontiers in Bioscience, 1998. **6**: p. 887-912.
46. Serrano, M., et al., *Oncogenic ras provokes premature cell senescence associated with accumulation of p53 and p16INK4a.* Cell, 1997. **88**: p. 593-602.
47. Serrano, M., *The tumour suppressor protein p16INK4a.* Experimental Cell Research, 1997. **237**: p. 7-13.
48. Lin, A.W., et al., *Premature senescence involving p53 and p16 is activated in response to constitutive MEK/MAPK mitogenic signaling.* Genes Development, 1998. **12**: p. 3008-3019.
49. Zhu, J., et al., *Senescence of human fibroblasts induced by oncogenic Raf.* Genes Development, 1998. **12**: p. 2997-3007.
50. Palmero, I., C. Pantoja, and M. Serrano, *p19ARF links the tumour supressor p53 to Ras.* Nature, 1998. **395**: p. 125-126.
51. Kamijo, T., et al., *Tumor suppression at the mouse INK4a locus mediated by the alternative reading frame product p19ARF.* Cell, 1997. **91**: p. 649-659.
52. Campisi, J., *Cellular senescence as a tumor-suppressor mechanism.* TRENDS in Biochemical Sciences, 2001. **11**: p. S27-S31.
53. Lundberg, A.S., et al., *Genes involved in senescence and immortalization.* Current Opinion Biotechnology, 2000. **12**: p. 705-709.
54. Cantley, L.C. and B.G. Neel, *New insights into tumor suppression: PTEN suppresses tumor formation by restraining the phosphoinositide 3-kinase/AKT pathway.* PNAS, 1999. **96**: p. 4240-4245.
55. Li, D.M. and H. Sun, *PTEN/MMAC1/TEP1 suppresses the tumorigenicity and induces G1 cell cycle arrest in human glioblastoma cells.* PNAS, 1998. **95**: p. 15406-15411.
56. Tresini, M., et al., *A phosphatidylinositol 3-kinase inhibitor induces a senescent-like growth arrest in human diploid fibroblasts.* Cancer Research, 1998. **58**: p. 1-4.
57. Yamasaki, L., *Rold of the Rb tumor suppressor in cancer.* Cancer Treatment Research, 2003. **115**: p. 209-239.

58. Ruas, M. and G. Peters, *The p16INK4a/CDKN2a tumor suppressor and its relatives.* Biochim Biophys Acta, 1998. **14**: p. 115-177.
59. Giaccia, A.J. and M.B. Kastan, *The complexity of p53 modulation: emerging patterns from divergent signals.* Genes Development, 1998. **12**: p. 2973-2983.
60. Chen, Z., et al., *Crucial role of p53-dependent cellular senescence in suppression of Pten-deficient tumorigenesis.* Nature, 2005. **436**(7051): p. 725-730.
61. Pei, L. and S. Melmed, *Isolation and characterization of a pituitary tumor-transforming gene (PTTG).* Molecular Endocrinology, 1997. **11**: p. 433-441.
62. Zou, H., et al., *Identification of a vertebrate sister-chromatid separation inhibitor involved in transformation and tumorigenesis.* Science, 1999. **285**: p. 418-422.
63. Tong, Y., et al., *Pituitary tumor transforming gene interacts with Sp1 to modulate G1/S cell phase transition.* Oncogene, 2007. **26**: p. 5596-5605.
64. Romero, F., et al., *Human securin, hPTTG, is associated with Ku heterodimer, the regulatory subunit of the DNA-dependent protein kinase.* Nucleic Acids Research, 2001. **29**: p. 1300-1307.
65. Wang, Z., et al., *Pituitary tumor transforming gene-null male mice exhibit impaired pancreatic beta cell proliferation and diabetes.* PNAS, 2003. **100**: p. 3428-3432.
66. Chesnokova, V., et al., *P21 (Cip1) restrains pituitary tumor growth.* PNAS, 2008. **105**(45): p. 17498-17503.
67. Lee, I.A., C. Seong, and I.S. Choe, *Cloning and expression of human cDNA encoding human homologue of pituitary tumor transforming gene.* Biochemistry and Molecular Biology International, 1999. **47**: p. 891-897.
68. Kakar, S.S. and L. Jennes, *Molecular cloning and characterization of the tumor transforming gene (TUTR1): a novel gene in human tumorigenesis.* Cytogenetics and Cell Genetics, 1999. **84**: p. 211-216.
69. Tong, Y. and T. Eigler, *Transcriptional targets for pituitary tumor-transforming gene-1.* Journal of Molecular Endocrinology 2009. **43**: p. 179-185.
70. Yu, R., et al., *Pituitary tumor transforming gene causes aneuploidy and p53-dependent and p53-independent apoptosis.* Journal of Biological Chemistry, 2000. **275**: p. 36502-36505.
71. Hamid, T. and S.S. Kakar, *PTTG/securin activates expression of p53 and modulates its function.* Molecular Cancer, 2004. **3**: p. 18.
72. Chesnokova, V., et al., *Senescence mediates pituitary hypoplasia and restrains pituitary tumor growth.* Cancer Research, 2007. **67**: p. 10564-10572.
73. Vandesompele, J., et al., *Accurate normalization of real-time quantitative RT-PCR data by geometric averaging of multiple internal control genes.* Genome Biology, 2002. **3**(7).
74. Berezhna, S., H. Wohlrab, and P.M. Champion, *Resonance raman investigations of cytochrome c conformational change upon interaction with the membranes of intact and Ca2+ exposed mitochondria.* Biochemistry, 2003. **42**(20): p. 6149-6158.
75. Brown, J.P., W. Wei, and J.M. Sedivy, *Bypass of senescence after disruption of p21 (Cip1/Waf1) gene in normal diploid human fibroblasts.* Science, 1997. **277**: p. 831-834.

76. Pantoja, C. and M. Serrano, *Murine fibroblasts lacking p21 undergo senescence and are resistant to transformation by oncogenic Ras.* Oncogene, 1999. **18**: p. 4974-4982.
77. Han, J. and P. Sun, *The pathways to tumor suppression via route p38.* TRENDS in Biochemical Sciences, 2007. **32**(8): p. 364-371.
78. Menendez, D., A. Inga, and M.A. Resnick, *The expanding universe of p53 targets.* Nature Reviews Cancer, 2009. **9**(10): p. 724-737.
79. Elstrom, R.L., et al., *Akt stimulates aerobic glycolysis in cancer cells.* Cancer Research, 2004. **64**: p. 3892–3899.
80. Osthus, R.C., et al., *Deregulation of glucose transporter 1 and glycolytic gene expression by c-Myc.* Journal of Biological Chemistry, 2000. **275**: p. 21797–21800.
81. Matoba, S., et al., *p53 regulates mitochondrial respiration.* Science, 2006. **312**: p. 1650–1653.

APPENDICES

Appendix 1: NanoDrop® Concentrations for Quantitative RNA Yield

Timed Doxycycline Incubation Samples

Table A1: Timed doxycycline incubation MCF7/NeuT control samples.

Sample Name	Concentration (ng/µL)	260:280 Ratio	260:230 Ratio
MCF7/NeuT Control			
Batch I			
Control NeuT 0h BI	1493.05	2.11	1.85
Control NeuT 1m BI	1242.65	2.12	1.48
Control NeuT 10m BI	1246.88	2.12	1.85
Control NeuT 30m BI	1408.21	2.11	1.53
Control NeuT 1h BI	1334.81	2.11	1.90
Control NeuT 3h BI	1366.50	2.12	1.45
Control NeuT 6h BI	1750.16	2.12	1.82
Control NeuT 12h BI	1242.63	2.09	1.99
Control NeuT 24h BI	1854.55	2.10	1.69
Control NeuT 72h BI	1310.29	2.11	1.77
Control NeuT 7d BI	1353.45	2.09	1.79
Control NeuT 14d BI	1218.29	2.10	1.99
Batch II			
Control NeuT 0h BII	1031.95	2.09	2.01
Control NeuT 1m BII	865.99	2.07	2.17
Control NeuT 10m BII	821.69	2.06	1.77
Control NeuT 30m BII	930.28	2.07	1.87
Control NeuT 1h BII	998.32	2.08	1.80
Control NeuT 3h BII	1304.04	2.07	2.17
Control NeuT 6h BII	1838.64	2.10	2.01
Control NeuT 12h BII	1107.01	2.08	2.03
Control NeuT 24h BII	1113.45	2.09	1.90
Control NeuT 72h BII	1818.04	2.09	1.6
Control NeuT 7d BII	2045.20	2.10	1.94
Control NeuT 14d BII	1183.98	2.09	2.19
Batch III			
Control NeuT 0h BIII	1576.91	2.10	2.19
Control NeuT 1m BIII	1538.13	2.11	1.93
Control NeuT 10m BIII	1815.16	2.10	2.07
Control NeuT 30m BIII	1369.70	2.09	1.06
Control NeuT 1h BIII	1739.51	2.08	2.01
Control NeuT 3h BIII	1637.85	2.10	1.88
Control NeuT 6h BIII	1968.49	2.10	1.88
Control NeuT 12h BIII	1822.12	2.09	2.06
Control NeuT 24h BIII	1385.10	2.09	2.14
Control NeuT 72h BIII	1200.73	2.11	1.78
Control NeuT 7d BIII	1249.39	2.09	2.17
Control NeuT 14d BIII	1479.93	2.08	1.37

Table A2: Timed doxycycline incubation MCF7/NeuT treated samples.

Sample Name	Concentration (ng/µL)	260:280 Ratio	260:230 Ratio
MCF7/NeuT Treated			
Batch I			
NeuT 0h BI	1517.83	2.13	2.08
NeuT 1m BI	1849.17	2.12	1.84
NeuT 10m BI	1672.28	2.12	2.06
NeuT 30m BI	1635.23	2.13	2.02
NeuT 1h BI	1677.55	2.12	1.65
NeuT 3h BI	963.35	2.10	2.00
NeuT 6h BI	1300.19	2.11	2.04
NeuT 12h BI	2376.62	2.10	1.88
NeuT 24h BI	3030.96	2.09	2.01
NeuT 72h BI	3017.80	2.06	1.96
NeuT 7d BI	1425.63	2.11	1.94
NeuT 14d BI	3045.0	2.06	1.67
Batch II			
NeuT 0h BII	1831.04	2.10	1.80
NeuT 1m BII	1767.44	2.11	1.96
NeuT 10m BII	1933.55	2.12	2.05
NeuT 30m BII	1827.10	2.11	1.81
NeuT 1h BII	1733.26	2.12	1.87
NeuT 3h BII	1940.07	2.11	1.88
NeuT 6h BII	1701.16	2.10	1.65
NeuT 12h BII	2168.87	2.11	1.78
NeuT 24h BII	2318.55	2.10	1.85
NeuT 72h BII	2355.44	2.10	2.05
NeuT 7d BII	2461.36	2.10	2.11
NeuT 14d BII	2182.78	2.11	2.03
Batch III			
NeuT 0h BIII	2020.34	2.10	2.09
NeuT 1m BIII	1650.90	2.11	2.00
NeuT 10m BIII	1185.01	2.10	1.93
NeuT 30m BIII	1509.78	2.11	1.17
NeuT 1h BIII	1278.65	2.10	1.78
NeuT 3h BIII	1758.16	2.11	2.08
NeuT 6h BIII	1910.86	2.10	2.16
NeuT 12h BIII	3047.26	2.06	1.85
NeuT 24h BIII	3300.22	2.02	2.02
NeuT 72h BIII	3480.07	1.98	1.80
NeuT 7d BIII	2054.25	2.12	2.09
NeuT 14d BIII	3094.55	2.08	1.94

Table A3: Timed doxycycline incubation MCF7/EGFP control samples.

Sample Name	Concentration (ng/µL)	260:280 Ratio	260:230 Ratio
MCF7/EGFP Control			
Batch I			
Control EGFP 0h BI	1628.17	2.10	1.96
Control EGFP 1m BI	1662.35	2.11	1.82
Control EGFP 10m BI	1467.82	2.10	1.50
Control EGFP 30m BI	1474.80	2.11	1.75
Control EGFP 1h BI	1842.78	2.09	1.88
Control EGFP 3h BI	1902.85	2.09	2.16
Control EGFP 6h BI	1766.04	2.11	1.87
Control EGFP 12h BI	1571.16	2.09	1.91
Control EGFP 24h BI	1063.37	2.10	1.03
Control EGFP 72h BI	1692.73	2.10	1.49
Control EGFP 7d BI	1906.44	2.09	1.93
Control EGFP 14d BI	1527.97	2.08	1.96
Batch II			
Control EGFP 0h BII	528.01	2.06	1.39
Control EGFP 1m BII	690.59	2.06	2.15
Control EGFP 10m BII	596.73	2.06	1.88
Control EGFP 30m BII	515.33	2.03	1.59
Control EGFP 1h BII	305.99	2.10	1.30
Control EGFP 3h BII	1411.93	2.07	2.07
Control EGFP 6h BII	1200.00	2.07	1.86
Control EGFP 12h BII	952.12	2.06	2.16
Control EGFP 24h BII	1001.61	2.06	2.10
Control EGFP 72h BII	1647.60	2.10	1.81
Control EGFP 7d BII	1396.63	2.09	1.95
Control EGFP 14d BII	1050.35	2.08	1.81
Batch III			
Control EGFP 0h BIII	1044.65	2.09	1.69
Control EGFP 1m BIII	1287.32	2.09	1.71
Control EGFP 10m BIII	957.51	2.08	1.92
Control EGFP 30m BIII	938.92	2.07	1.87
Control EGFP 1h BIII	1235.53	2.08	2.10
Control EGFP 3h BIII	1765.36	2.10	1.98
Control EGFP 6h BIII	1287.00	2.10	1.47
Control EGFP 12h BIII	1625.54	2.10	2.01
Control EGFP 24h BIII	1629.11	2.09	1.95
Control EGFP 72h BIII	1105.82	2.09	1.78
Control EGFP 7d BIII	1505.26	2.09	1.92
Control EGFP 14d BIII	1179.97	2.09	1.44

Table A4: Timed doxycycline incubation MCF7/EGFP treated samples.

Sample Name	Concentration (ng/µL)	260:280 Ratio	260:230 Ratio
MCF7/EGFP Treated			
Batch I			
EGFP 0h BI	1709.63	2.11	1.92
EGFP 1m BI	1807.54	2.11	1.80
EGFP 10m BI	2510.00	2.11	1.92
EGFP 30m BI	922.03	2.08	2.05
EGFP 1h BI	1510.11	2.11	2.08
EGFP 3h BI	1644.17	2.11	1.71
EGFP 6h BI	2098.07	2.10	2.05
EGFP 12h BI	932.65	2.08	1.55
EGFP 24h BI	970.16	2.06	2.06
EGFP 72h BI	2407.81	2.10	2.05
EGFP 7d BI	3480.15	2.00	1.99
EGFP 14d BI	910.16	2.10	1.76
Batch II			
EGFP 0h BII	1264.74	2.10	2.07
EGFP 1m BII	2462.54	2.10	2.08
EGFP 10m BII	1135.63	2.10	1.79
EGFP 30m BII	1147.64	2.11	1.91
EGFP 1h BII	1907.64	2.11	2.05
EGFP 3h BII	2560.02	2.10	1.94
EGFP 6h BII	2834.26	2.11	2.06
EGFP 12h BII	1564.07	2.09	2.13
EGFP 24h BII	2071.73	2.11	2.10
EGFP 72h BII	2461.28	2.08	2.06
EGFP 7d BII	1479.09	2.10	1.89
EGFP 14d BII	1149.71	2.11	1.71
Batch III			
EGFP 0h BIII	1270.01	2.10	2.01
EGFP 1m BIII	1428.22	2.11	1.93
EGFP 10m BIII	1532.84	2.11	2.11
EGFP 30m BIII	1816.91	2.11	2.02
EGFP 1h BIII	1385.83	2.11	1.93
EGFP 3h BIII	1667.78	2.11	1.81
EGFP 6h BIII	1545.94	2.10	2.06
EGFP 12h BIII	1770.62	2.11	2.05
EGFP 24h BIII	843.11	2.08	1.86
EGFP 72h BIII	2248.10	2.09	2.14
EGFP 7d BIII	2104.47	2.10	1.75
EGFP 14d BIII	997.09	2.13	1.98

siRNA Gene Knockdown Samples

***NB*: P21 – Cyclin Dependent Kinase Inhibitor 1A; G1 – Pituitary Tumour Transforming Gene 1; NC – Negative Control; LF – Transfection Agent; /## - specific oligoribonucleotide tested.**

Table A5: siRNA knockdown samples 0h -6h batch I.

Sample Name	Concentration (ng/µL)	260:280 Ratio	260:230 Ratio
Batch I			
-0h P21/19 BI	118.96	2.00	2.29
-0h P21/20BI	198.32	1.98	2.22
-0h P21/21 BI	204.11	2.01	2.26
-0h G1/58 BI	197.33	2.01	2.23
-0h G1/74 BI	195.16	2.02	2.04
-0h G1/75 BI	183.96	1.99	2.14
-0h NC BI	185.10	2.01	2.14
-0h LF BI	193.88	1.97	2.15
+0h P21/19 BI	191.58	2.00	2.22
+0h P21/20BI	200.39	2.01	1.90
+0h P21/21 BI	198.81	1.99	1.97
+0h G1/58 BI	193.47	2.00	2.03
+0h G1/74 BI	180.45	1.98	2.02
+0h G1/75 BI	162.65	2.03	1.39
+0h NC BI	175.60	2.00	2.14
+0h LF BI	189.28	1.99	1.93
-6h P21/19 BI	151.97	1.98	2.20
-6h P21/20BI	157.55	1.99	2.33
-6h P21/21 BI	169.96	1.99	2.10
-6h G1/58 BI	170.84	2.00	2.17
-6h G1/74 BI	149.75	1.98	2.24
-6h G1/75 BI	158.18	2.01	1.66
-6h NC BI	154.51	2.01	2.22
-6h LF BI	158.56	1.98	2.30
+6h P21/19 BI	171.75	2.02	2.12
+6h P21/20BI	166.11	2.02	1.95
+6h P21/21 BI	170.43	2.00	1.77
+6h G1/58 BI	160.22	2.00	2.26
+6h G1/74 BI	174.42	1.98	2.21
+6h G1/75 BI	159.29	2.00	2.26
+6h NC BI	163.02	2.03	1.15
+6h LF BI	162.13	2.02	1.40

Table A6: siRNA knockdown samples 12h - 24h batch I.

Sample Name	Concentration (ng/µL)	260:280 Ratio	260:230 Ratio
Batch I			
-12h P21/19 BI	225.09	2.02	1.38
-12h P21/20BI	212.38	2.02	1.03
-12h P21/21 BI	206.73	1.99	1.99
-12h G1/58 BI	229.45	2.00	1.81
-12h G1/74 BI	214.58	2.01	1.70
-12h G1/75 BI	195.20	1.99	2.04
-12h NC BI	234.68	1.99	2.07
-12h LF BI	251.70	2.01	2.03
+12h P21/19 BI	236.82	2.00	2.13
+12h P21/20BI	241.22	2.02	2.04
+12h P21/21 BI	216.31	1.99	2.06
+12h G1/58 BI	230.51	2.03	2.09
+12h G1/74 BI	217.19	2.02	1.90
+12h G1/75 BI	222.25	2.02	2.05
+12h NC BI	248.51	2.00	2.13
+12h LF BI	230.57	2.00	2.08
-24h P21/19 BI	242.28	2.02	2.11
-24h P21/20BI	226.81	2.02	1.83
-24h P21/21 BI	222.73	2.00	2.06
-24h G1/58 BI	236.39	1.98	1.94
-24h G1/74 BI	173.08	2.00	2.10
-24h G1/75 BI	219.61	2.00	2.07
-24h NC BI	219.21	2.00	1.79
-24h LF BI	221.55	2.00	1.79
+24h P21/19 BI	271.19	2.02	1.92
+24h P21/20BI	246.49	2.02	2.01
+24h P21/21 BI	231.62	1.99	2.01
+24h G1/58 BI	259.64	2.00	2.05
+24h G1/74 BI	272.01	1.99	2.15
+24h G1/75 BI	233.29	2.01	1.94
+24h NC BI	247.81	2.01	1.98
+24h LF BI	207.62	2.01	1.56

Table A7: siRNA knockdown samples 3d - 7d batch 1.

Sample Name	Concentration (ng/µL)	260:280 Ratio	260:230 Ratio
Batch I			
-3d P21/19 BI	286.73	2.00	2.08
-3d P21/20BI	219.72	2.00	1.98
-3d P21/21 BI	122.64	1.95	1.81
-3dG1/58 BI	240.17	2.00	2.16
-3d G1/74 BI	270.30	1.99	2.11
-3d G1/75 BI	223.49	2.00	1.98
-3d NC BI	263.91	2.00	1.84
-3d LF BI	261.74	2.01	1.86
+3d P21/19 BI	272.79	2.01	1.82
+3d P21/20BI	229.52	2.01	1.80
+3d P21/21 BI	153.61	2.02	1.66
+3d G1/58 BI	269.70	2.00	1.84
+3d G1/74 BI	230.68	2.00	1.95
+3d G1/75 BI	191.97	1.99	1.79
+3d NC BI	243.62	2.01	2.11
+3d LF BI	238.25	2.02	1.75
-7d P21/19 BI	216.95	2.00	1.87
-7d P21/20BI	239.92	2.01	2.09
-7d P21/21 BI	134.13	1.99	1.90
-7d G1/58 BI	239.40	2.02	1.94
-7d G1/74 BI	237.18	2.02	1.85
-7d G1/75 BI	274.71	2.03	2.00
-7d NC BI	262.49	1.99	2.04
-7d LF BI	304.40	2.03	1.86
+7d P21/19 BI	306.09	2.02	2.10
+7d P21/20BI	159.96	2.01	2.08
+7d P21/21 BI	60.40	1.82	1.63
+7d G1/58 BI	172.28	2.02	1.92
+7d G1/74 BI	88.29	1.85	1.68
+7d G1/75 BI	116.79	1.95	1.55
+7d NC BI	191.23	2.00	2.01
+7d LF BI	178.56	2.02	1.63

Table A8: siRNA knockdown samples 0h - 6h batch II.

Sample Name	Concentration (ng/µL)	260:280 Ratio	260:230 Ratio
Batch II			
-0h P21/19 BII	186.20	2.04	2.62
-0h P21/20BII	246.27	2.03	1.97
-0h P21/21 BII	255.46	2.04	2.03
-0h G1/58 BII	251.08	2.04	1.87
-0h G1/74 BII	241.61	2.00	2.11
-0h G1/75 BII	233.88	2.03	2.07
-0h NC BII	213.71	2.03	1.62
-0h LF BII	118.08	1.98	2.07
+0h P21/19 BII	253.72	2.04	1.37
+0h P21/20BII	241.66	2.04	2.06
+0h P21/21 BII	261.40	2.04	2.07
+0h G1/58 BII	243.64	2.02	2.12
+0h G1/74 BII	230.70	2.02	2.17
+0h G1/75 BII	231.67	2.05	2.13
+0h NC BII	247.31	2.03	2.03
+0h LF BII	235.66	2.02	2.07
-6h P21/19 BII	242.63	2.01	1.95
-6h P21/20BII	223.56	2.03	2.03
-6h P21/21 BII	231.91	2.03	1.93
-6h G1/58 BII	230.31	2.02	2.09
-6h G1/74 BII	232.44	2.04	1.99
-6h G1/75 BII	228.85	2.03	1.77
-6h NC BII	252.08	2.02	2.01
-6h LF BII	232.76	2.03	2.06
+6h P21/19 BII	223.21	2.03	2.17
+6h P21/20BII	241.13	2.05	2.06
+6h P21/21 BII	243.74	2.03	2.13
+6h G1/58 BII	220.74	2.03	1.74
+6h G1/74 BII	232.32	2.02	2.07
+6h G1/75 BII	208.32	2.02	1.88
+6h NC BII	215.79	2.02	2.03
+6h LF BII	224.65	2.02	1.93

Table A9: siRNA knockdown samples 12h – 24h batch II.

Sample Name	Concentration (ng/µL)	260:280 Ratio	260:230 Ratio
Batch II			
-12h P21/19 BII	360.56	2.02	2.13
-12h P21/20BII	326.73	2.04	2.05
-12h P21/21 BII	315.49	2.03	1.99
-12h G1/58 BII	340.05	2.02	2.11
-12h G1/74 BII	334.05	2.02	2.11
-12h G1/75 BII	321.88	2.02	2.09
-12h NC BII	359.47	2.03	2.12
-12h LF BII	367.90	2.02	2.13
+12h P21/19 BII	369.12	2.01	1.82
+12h P21/20BII	364.70	2.04	2.13
+12h P21/21 BII	339.02	2.02	2.06
+12h G1/58 BII	373.06	2.04	1.79
+12h G1/74 BII	321.70	2.03	2.07
+12h G1/75 BII	344.00	2.02	2.08
+12h NC BII	362.57	2.03	2.10
+12h LF BII	358.32	2.04	1.38
-24h P21/19 BII	372.41	2.02	2.09
-24h P21/20BII	367.78	2.05	2.13
-24h P21/21 BII	357.70	2.02	2.03
-24h G1/58 BII	315.72	2.03	2.15
-24h G1/74 BII	366.17	2.03	2.09
-24h G1/75 BII	340.61	2.04	2.14
-24h NC BII	358.60	2.02	2.14
-24h LF BII	381.55	2.05	2.11
+24h P21/19 BII	405.12	2.05	2.03
+24h P21/20BII	372.88	2.03	2.04
+24h P21/21 BII	365.44	2.04	2.06
+24h G1/58 BII	395.46	2.04	1.92
+24h G1/74 BII	401.33	2.03	1.90
+24h G1/75 BII	357.64	2.03	1.57
+24h NC BII	400.12	2.00	2.07
+24h LF BII	379.91	2.05	

Table A10: siRNA knockdown samples 3d – 7d batch II.

Sample Name	Concentration (ng/µL)	260:280 Ratio	260:230 Ratio
Batch II			
-3d P21/19 BII	436.50	2.00	2.07
-3d P21/20 BII	361.08	2.06	1.93
-3d P21/21 BII	274.74	2.03	2.12
-3d G1/58 BII	388.42	2.03	2.08
-3d G1/74 BII	352.19	2.03	2.10
-3d G1/75 BII	348.17	2.04	2.05
-3d NC BII	376.18	2.02	2.08
-3d LF BII	408.21	2.06	2.02
+3d P21/19 BII	432.13	2.01	2.05
+3d P21/20BII	384.77	2.04	2.12
+3d P21/21 BII	301.91	2.02	2.07
+3d G1/58 BII	401.51	2.03	2.07
+3d G1/74 BII	413.93	2.02	2.08
+3d G1/75 BII	397.49	2.01	2.12
+3d NC BII	395.94	2.03	2.16
+3d LF BII	366.77	2.03	1.92
-7d P21/19 BII	498.94	2.05	2.13
-7d P21/20BII	406.55	2.04	2.12
-7d P21/21 BII	351.66	2.04	1.86
-7d G1/58 BII	533.86	2.05	1.88
-7d G1/74 BII	401.50	2.03	2.17
-7d G1/75 BII	407.25	2.04	2.02
-7d NC BII	446.50	2.03	2.12
-7d LF BII	402.19	2.04	2.13
+7d P21/19 BII	495.41	2.04	1.67
+7d P21/20BII	370.43	2.05	1.99
+7d P21/21 BII	187.00	2.01	1.92
+7d G1/58 BII	351.16	2.03	2.16
+7d G1/74 BII	268.96	2.01	1.95
+7d G1/75 BII	245.39	2.01	2.11
+7d NC BII	462.97	2.02	2.06
+7d LF BII	351.44	2.03	2.02

Table A11: siRNA knockdown samples 0h – 6h batch III.

Sample Name	Concentration (ng/µL)	260:280 Ratio	260:230 Ratio
Batch III			
-0h P21/19 BIII	121.76	1.99	1.03
-0h P21/20BIII	114.63	1.93	1.80
-0h P21/21 BIII	108.92	1.97	2.01
-0h G1/58 BIII	119.20	1.96	2.00
-0h G1/74 BIII	126.43	1.99	1.82
-0h G1/75 BIII	116.02	1.95	1.50
-0h NC BIII	138.30	1.97	2.03
-0h LF BIII	126.04	1.96	1.82
+0h P21/19 BIII	120.65	1.96	1.91
+0h P21/20BIII	117.52	1.99	1.82
+0h P21/21 BIII	122.38	1.96	1.97
+0h G1/58 BIII	112.29	1.96	1.75
+0h G1/74 BIII	120.59	1.99	1.84
+0h G1/75 BIII	111.93	1.93	1.97
+0h NC BIII	100.87	1.95	1.97
+0h LF BIII	115.14	1.96	1.78
-6h P21/19 BIII	120.12	1.96	1.89
-6h P21/20BIII	117.12	1.93	1.77
-6h P21/21 BIII	120.43	1.95	1.82
-6h G1/58 BIII	110.46	1.93	1.23
-6h G1/74 BIII	102.11	1.94	1.72
-6h G1/75 BIII	99.68	1.92	1.62
-6h NC BIII	103.08	1.96	1.75
-6h LF BIII	113.43	2.00	1.89
+6h P21/19 BIII	91.77	1.95	1.35
+6h P21/20BIII	100.42	1.98	1.29
+6h P21/21 BIII	108.01	1.96	1.97
+6h G1/58 BIII	78.88	1.94	0.93
+6h G1/74 BIII	99.84	1.98	1.55
+6h G1/75 BIII	89.08	1.93	1.63
+6h NC BIII	107.51	1.90	1.58
+6h LF BIII	102.18	1.91	1.92

Table 12: siRNA knockdown samples 12h – 24h batch III.

Sample Name	Concentration (ng/µL)	260:280 Ratio	260:230 Ratio
Batch III			
-12h P21/19 BIII	163.19	2.04	1.19
-12h P21/20BIII	123.88	1.96	1.67
-12h P21/21 BIII	126.83	2.00	1.59
-12h G1/58 BIII	148.11	2.00	1.74
-12h G1/74 BIII	154.98	1.99	2.04
-12h G1/75 BIII	136.41	2.00	2.10
-12h NC BIII	146.18	2.02	0.89
-12h LF BIII	155.08	2.02	1.87
+12h P21/19 BIII	166.00	2.02	1.94
+12h P21/20BIII	149.57	2.00	1.99
+12h P21/21 BIII	132.62	1.97	1.11
+12h G1/58 BIII	145.07	2.02	1.86
+12h G1/74 BIII	157.93	2.00	1.76
+12h G1/75 BIII	136.18	1.99	1.92
+12h NC BIII	157.95	2.04	1.30
+12h LF BIII	158.98	2.00	1.83
-24h P21/19 BIII	163.58	2.02	1.80
-24h P21/20BIII	125.32	2.04	0.26
-24h P21/21 BIII	131.60	1.98	1.84
-24h G1/58 BIII	144.10	2.00	1.99
-24h G1/74 BIII	141.17	2.00	1.92
-24h G1/75 BIII	137.11	1.99	1.74
-24h NC BIII	160.69	2.01	1.87
-24h LF BIII	149.10	2.02	1.31
+24h P21/19 BIII	176.18	2.03	1.11
+24h P21/20BIII	157.00	2.01	2.06
+24h P21/21 BIII	158.75	2.01	2.01
+24h G1/58 BIII	171.18	2.00	2.00
+24h G1/74 BIII	155.18	1.99	1.84
+24h G1/75 BIII	152.95	1.99	2.05
+24h NC BIII	157.84	2.00	2.10
+24h LF BIII	179.75	2.01	2.13

Table A13: siRNA knockdown samples 3d – 7d batch III.

Sample Name	Concentration (ng/µL)	260:280 Ratio	260:230 Ratio
Batch III			
-3d P21/19 BIII	123.76	1.97	1.76
-3d P21/20 BIII	146.41	1.98	1.87
-3d P21/21 BIII	51.31	1.98	1.70
-3d G1/58 BIII	120.75	1.97	1.44
-3d G1/74 BIII	149.55	1.99	1.97
-3d G1/75 BIII	92.67	1.91	1.38
-3d NC BIII	155.15	1.99	1.95
-3d LF BIII	168.68	1.98	1.78
+3d P21/19 BIII	157.23	1.97	1.65
+3d P21/20BIII	125.64	1.92	1.69
+3d P21/21 BIII	45.99	1.94	0.91
+3d G1/58 BIII	136.37	1.97	1.85
+3d G1/74 BIII	157.49	1.97	1.45
+3d G1/75 BIII	122.26	2.02	1.80
+3d NC BIII	130.46	1.96	1.27
+3d LF BIII	143.20	1.99	1.68
-7d P21/19 BIII	171.42	1.99	2.08
-7d P21/20BIII	89.51	1.92	1.81
-7d P21/21 BIII	46.63	1.82	1.47
-7d G1/58 BIII	76.07	1.93	1.18
-7d G1/74 BIII	87.67	2.02	1.62
-7d G1/75 BIII	90.19	1.97	1.10
-7d NC BIII	132.16	2.01	1.79
-7d LF BIII	222.86	2.03	1.96
+7d P21/19 BIII	142.11	1.96	1.72
+7d P21/20BIII	114.57	1.95	1.87
+7d P21/21 BIII	30.19	1.71	0.78
+7d G1/58 BIII	71.62	2.02	0.59
+7d G1/74 BIII	54.30	1.85	1.20
+7d G1/75 BIII	67.80	1.81	1.77
+7d NC BIII	81.79	1.88	1.50
+7d LF BIII	87.43	1.88	1.56

Appendix 2: Roche Universal Probe Library Primers/Probe Sets for Genes Investigated

Table A14: Roche Universal Probe Library primers/probe sets.

Target Gene (Symbol)	Accession Number	Function	Primer Sequences	Probe Number	Amplicon Sequence
Oncogene					
Erythroblastic leukemia viral oncogene homolog 2 (NeuT)	NM_017003	Involved in mitogenesis	F – ACTGGGACCAGAACTCATCG R – TGGGGGTCCCTTCAAAGT	22	5'-ACTGGGACCAGAACT CATCGGAGCAGGGGCCT CCACCAAGTAACTTTGA AGGGACCCCCA – 3'
Senescent Marker Genes					
Mitogen-activated protein kinase 14 (Variant 1) (MAPK14/P38)	NM_001315	Involved in stress related transcription, cell cycle regulation, and genotoxic stress	F – CTGTTGGACGTTTTTACACCTG R – CCATGAGATGGGTCACCAG	65	5' – CTGTTGGACGTTTTT ACACCTGCAAGGTCTCT GGAGGAATTCAATGATG TGTATCTGGTGACCCATC TCATGG – 3'
Cyclin-dependent kinase inhibitor 1A (p21)	NM_000389	Functions as a regulator of cell cycle progression at G1	F - TCACTGTCTTGTACCCTTGTGC R – GGCGTTTGGAGTGGTAGAAA	32	5' – TCACTGTCTTGTACC CTTGTGCCTCGCTCAGGG GAGCAGGCTGAAGGGTC CCCAGGTGGACCTGGAG ACTCTCAGGGTCGAAAA CGGCGGCAGACCAGCAT GACAGATTTCTACCACTC CAAACGCC – 3'
Tumour protein 53 (p53)	NM_000546	Regulates genes that induce cell cycle arrest, apoptosis, senescence, DNA repair, or changes in metabolism	F - AGGCCTTGGAACTCAAGGAT R - GGTAGACTGACCCTTTTTGGAC	83	5' – AGGCCTTGGAACTCA AGGATGCCCAGGCTGGG AAGGAGCCAGGGGGGA GCAGGGCTCACTCCAGC CACCTGAAGTCCAAAAA GGGTCAGTCTACC – 3'
Phosphatase and tensin homolog (PTEN)	NM_000314	Functions as a tumour suppressor by negatively regulating PIP3 and AKT/PKB signalling pathway	F – GCTACCTGTTAAAGAATCATCTGGA R – CTGGCAGACCACAAACTGAG	59	5' – GCTACCTGTTAAAGA ATCATCTGGATTATAGA CCAGTGGCACTGTTGTTT CACAAGATGATGTTTGA AACTATTCCAATGTTCAG TGGCGGAACTTGCAATC CTCAGTTTGTGGTCTGCC AG – 3'
Pituitary tumour-transforming gene 1 (PTTG1)	NM_004219	Transforming and tumouri-genic activity as well as stimulation of basic fibroblast growth factor expression	F – GCCTCTCATGATCCTTGACG R – TGCTTGAAGGAGACTGCAAC	22	5' – GCCTCTCATGATCCT TGACGAGGAGAGAGAGC TTGAAAAGCTGTTTCAG CTGGGCCCCCCTTCACCT GTGAAGATGCCCTCTCC ACCATGGGAATCCAATC TGTTGCAGTCTCCTTCAA GCA – 3'
Retinoblastoma (RB1)	NM_000321	Negative regulator of the cell cycle	F – CAGAATAATCACACTGCAGCAGATA R – CACGCGTAGTTGAACCTTTTT	2	5' – CAGAATAATCACAC TGCAGCAGATATGTATC TTTCTCCTGTAAGATCTC CAAAGAAAAAAGGTTCA ACTACGCGTG – 3'

Cell Cycle Genes					
Cyclin B2 (CCNB2)	NM_004701	Cell cycle control from the G2 to M phase	F – GCATTATCATCCTTCTAAGGTAGCA R – AAGTTCCATTTTCCTTGTCCTAGA	38	5' – GCATTATCATCCTTC TAAGGTAGCAGCAGCTG CTTCCTGCTTGTCTCAGA AGGTTCTAGGACAAGGA AAATGGAACTT – 3'
Cyclin D1 (CCND1)	NM_053056	Cell Cycle control from the G1 to S phase	F – TGTCCTACTACCGCCTCACA R – CAGGGCTTCGATCTGCTC	16	5' – TGTCCTACTACCGCC TCACACGCTTCCTCTCCA GAGTGATCAAGTGTGAC CCGGACTGCCTCCGGGC CTGCCAGGAGCAGATCG AAGCCCTG – 3'
Cyclin E1 (CCNE1)	NM_001238	Required for cell cycle G1/S transition	F – CCTCGGATTATTGCACCATC R – TTCCAGACTTCCTCTCTATTTGC	27	5' – CCTCGGATTATTGCA CCATCCAGAGGCTCCCC GCTGCCTGTACTGAGCT GGGCAAATAGAGAGGAA GTCTGGAA – 3'
Other Genes of Interest					
Cytochrome c, somatic (CYCS)	NM_018947	Involved in initiation of apoptosis and cellular respiration	F – TGTGCCAGCGACTAAAAAGA R – CTTGCCTCCCTTTTCAACG	48	5' – TGTGCCAGCGACTA AAAAGAGAATTAAATAT GGGTGATGTTGAGAAAG GCAAGAAGATTTTTATT ATGAAGTGTTCCCAGTG CCACACCGTTGAAAAGG GAGGCAAG – 3'
Beta Actin (ACTB)	NM_001101	Cytoskeletal structural protein	F – ATTGGCAATGAGCGGTTC R – GGATGCCACAGGACTCCAT	11	5' – ATTGGCAATGAGCG GTTCCGCTGCCCTGAGG CACTCTTCCAGCCTTCCT TCCTGGGCATGGAGTCC TGTGGCATCC – 3'
Reference Genes					
TATA box binding protein (TBP)	NM_003194	General RNA polymerase II transcription factor	F – GCTGGCCCATAGTGATCTTT R – CTTCACACGCCAAGAAACAGT	3	5' – GCTGGCCCATAGTG ATCTTTGCAGTGACCCA GCAGCATCACTGTTTCTT GGCGTGTGAAG – 3'
Ubiquitin C (UBC)	NM_021009	Protein degradation	F – CTCACTGGCAAGACCATCAC R – TTGCTTTGACGTTCTCGATG	39	5' – CTCACTGGCAAGAC CATCACCCTTGAGGTGG AGCCCAGTGACACCATC GAGAACGTCAAAGCAA – 3'

Appendix 3: Stealth RNAi™ siRNA Duplex Oligoribonucleotide Sequences

Table A15: Stealth RNAi™ siRNA Duplex oligoribonucleotide sequences.

Target Gene	Accession Number	Function	Primer Name	Primer Sequence	Primer Length
Cyclin Dependent Kinase Inhibitor 1A (p21)	NM_000389	Regulator of cell cycle progression at G1.	CDKN1A – HSS173519	F – GAUGUCCGUCAGAACCC AUGCGGCA	25
				R – UGCCGCAUGGGUUCUGA CGGACAUC	25
			CDKN1A – HSS173520	F – UGAGCCGCGACUGUGAU GCGCUAAU	25
				R – AUUAGCGCAUCACAGUC GCGGCUCA	25
			CDKN1A – HSS173521	F – UCCAAACGCCGGCUGAU CUUCUCCA	25
				R – UGGAGAAGAUCAGCCGG CCUUUGGA	25
Pituitary Tumour-Transforming Gene 1 (PTTG1)	NM_004219	Transforming and tumourigenic activities, as well as stimulation of basic fibroblast growth factor expression.	PTTG1 – HSS167058	F – AGGCACCCGUGUGGUUG CUAAGGAU	25
				R – AUCCUUAGCAACCACAC GGGUGCCU	25
			PTTG1 – HSS190074	F – CAGCCUUACCUAAAGCU ACUAGAAA	25
				R – UUUCUAGUAGCUUUAGG UAAGGCUG	25
			PTTG1 – HSS190075	F – CACCUGUUUGCUGUGAC AUAGAUAU	25
				R – AUAUCUAUGUCACAGCA AACAGGUG	25

Appendix 4: mRNA Efficiency Graphs of P21 siRNA Oligoribonucleotides in Knockdown MCF7/NeuT Samples over a Seven Day Dox Incubation Period

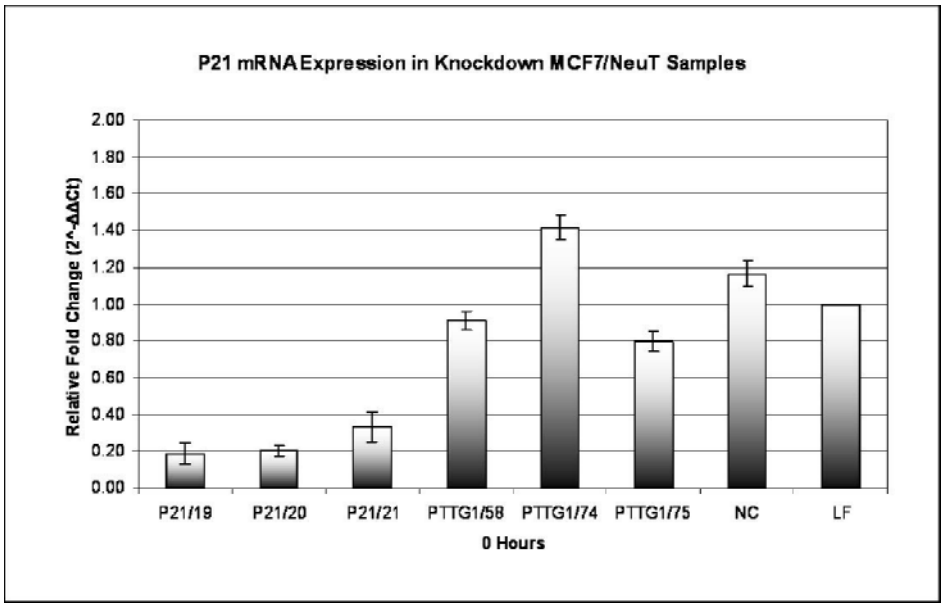

Figure A1: P21 mRNA expression in knockdown MCF7/NeuT samples at 0h dox incubation. P21 siRNA oligoribonucleotides showed an average of 80% knockdown efficiency (samples P21/19 – P21/21). Other samples showed P21 expression relative to each other at much higher levels. 2^-ΔΔCt values represent an average of 3 independent experiments. NC – non-sense oligoribonucleotide); LF – transfection agent.

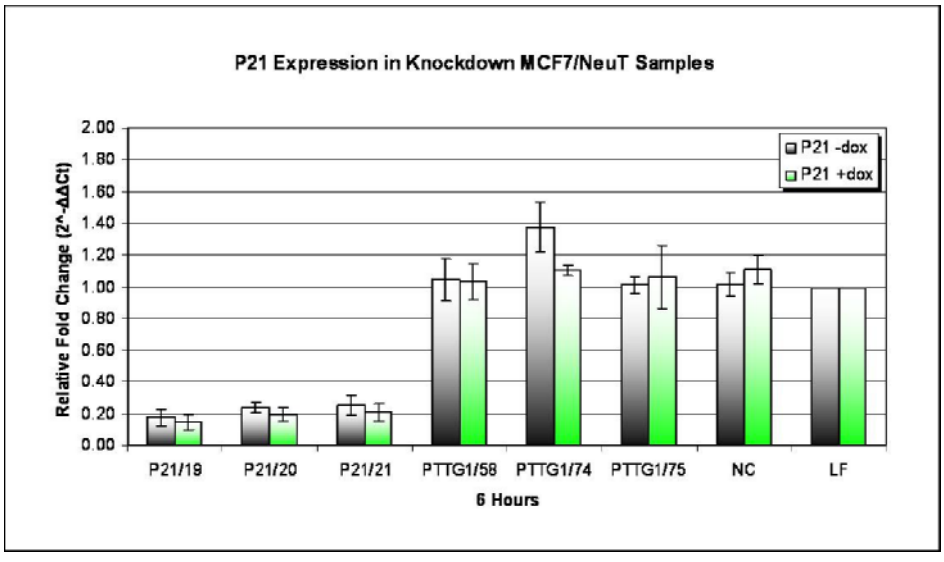

Figure A2: P21 mRNA expression in knockdown MCF7/NeuT samples at 6h dox incubation. P21 siRNA oligoribonucleotides showed an average of 80% knockdown efficiency (samples P21/19 – P21/21). Other samples showed P21 expression relative to each other at much higher levels. 2^-ΔΔCt values represent an average of 3 independent experiments. NC – non-sense oligoribonucleotide); LF – transfection agent.

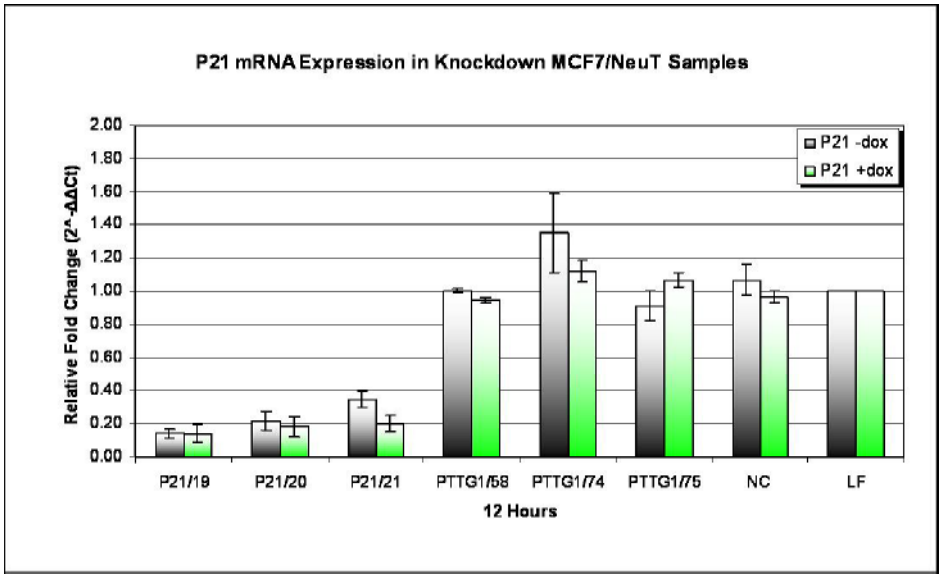

Figure A3: P21 mRNA expression in knockdown MCF7/NeuT samples at 12h dox incubation. P21 siRNA oligoribonucleotides showed an average of 80% knockdown efficiency (samples P21/19 – P21/21). Other samples showed P21 expression relative to each other at much higher levels. 2^-ΔΔCt values represent an average of 3 independent experiments. NC – non-sense oligoribonucleotide); LF – transfection agent.

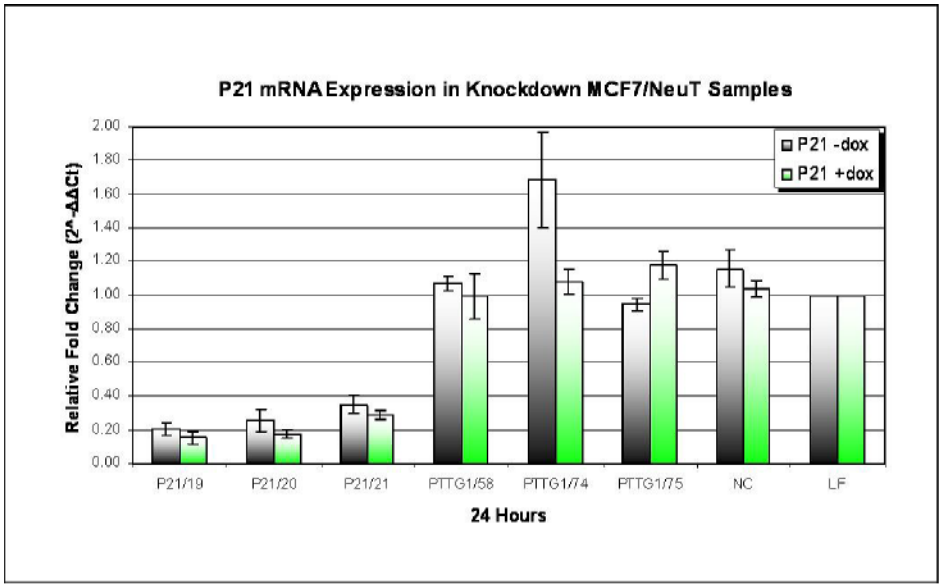

Figure A4: P21 mRNA expression in knockdown MCF7/NeuT samples at 24h dox incubation. P21 siRNA oligoribonucleotides showed an average of 80% knockdown efficiency (samples P21/19 – P21/21). Other samples showed P21 expression relative to each other at much higher levels. 2^-ΔΔCt values represent an average of 3 independent experiments. NC – non-sense oligoribonucleotide); LF – transfection agent.

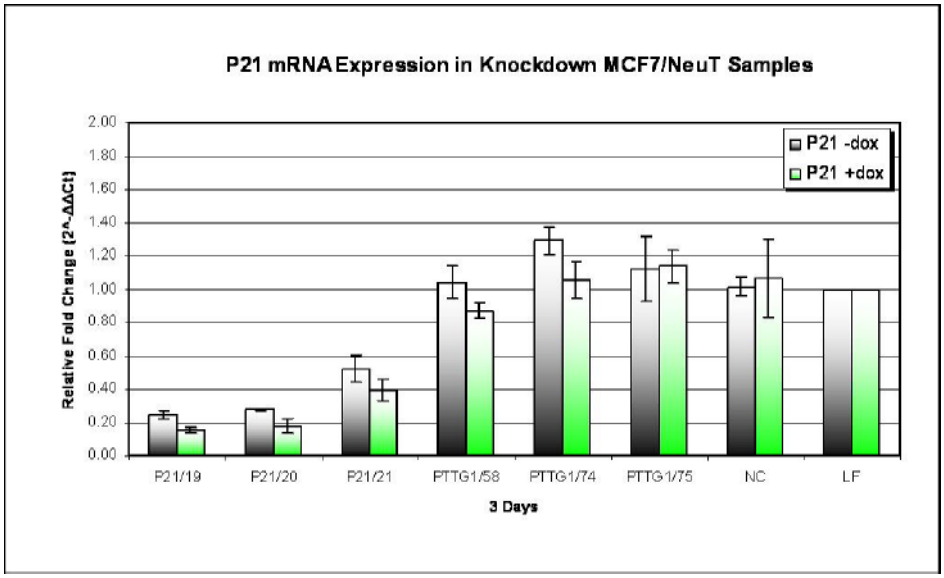

Figure A5: P21 mRNA expression in knockdown MCF7/NeuT samples at 3d dox incubation. P21 siRNA oligoribonucleotides showed an average of 70% knockdown efficiency (samples P21/19 – P21/21). Other samples showed P21 expression relative to each other at much higher levels. 2^-ΔΔCt values represent an average of 3 independent experiments. NC – non-sense oligoribonucleotide); LF – transfection agent.

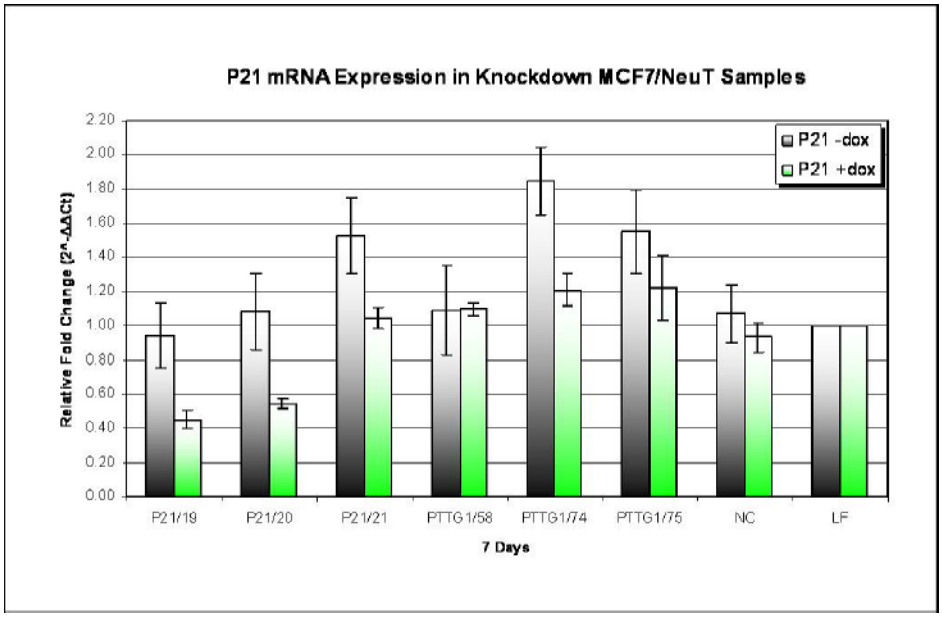

Figure A6: P21 mRNA expression in knockdown MCF7/NeuT samples at 7d dox incubation. P21 siRNA oligoribonucleotides showed an average of 20 - 50% knockdown efficiency (samples P21/19 – P21/21). Other samples showed P21 expression relative to each other at much higher levels. 2^-ΔΔCt values represent an average of 3 independent experiments. NC – non-sense oligoribonucleotide); LF – transfection agent.

Appendix 5: mRNA Efficiency Graphs of PTTG1 siRNA Oligoribonucleotides in Knockdown MCF7/NeuT Samples over a Seven Day Dox Incubation Period

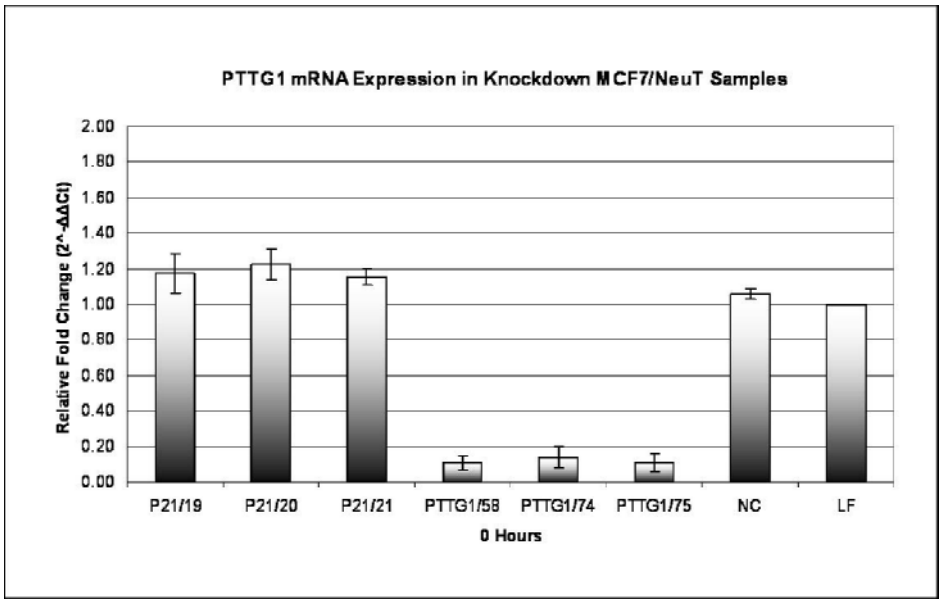

Figure A7: PTTG1 mRNA expression in knockdown MCF7/NeuT samples at 0h dox incubation. PTTG1 siRNA oligoribonucleotides showed an average of 90% knockdown efficiency (samples PTTG1/58 – PTTG1/75). Other samples showed PTTG1 expression relative to each other at much higher levels. 2^-ΔΔCt values represent an average of 3 independent experiments. NC – non-sense oligoribonucleotide); LF – transfection agent.

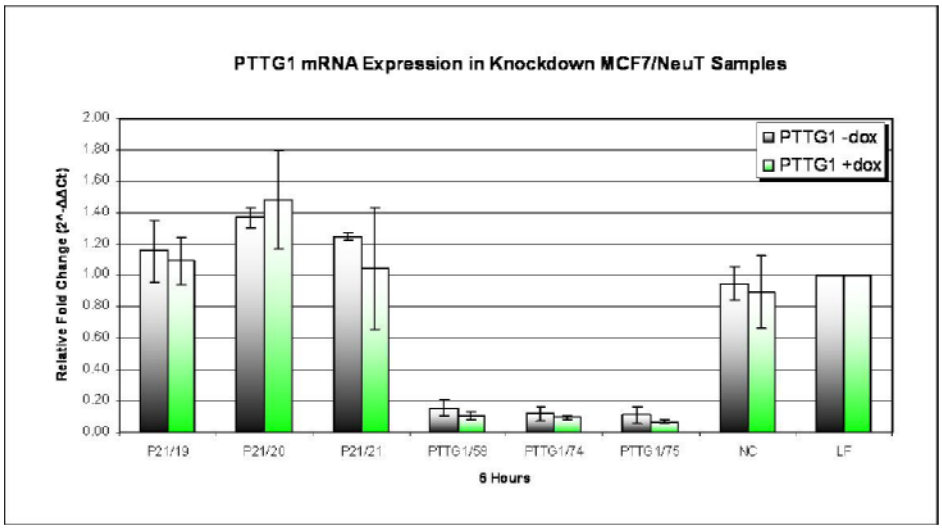

Figure A8: PTTG1 mRNA expression in knockdown MCF7/NeuT samples at 6h dox incubation. PTTG1 siRNA oligoribonucleotides showed an average of 90% knockdown efficiency (samples PTTG1/58 – PTTG1/75). Other samples showed PTTG1 expression relative to each other at much higher levels. 2^-ΔΔCt values represent an average of 3 independent experiments. NC – non-sense oligoribonucleotide); LF – transfection agent.

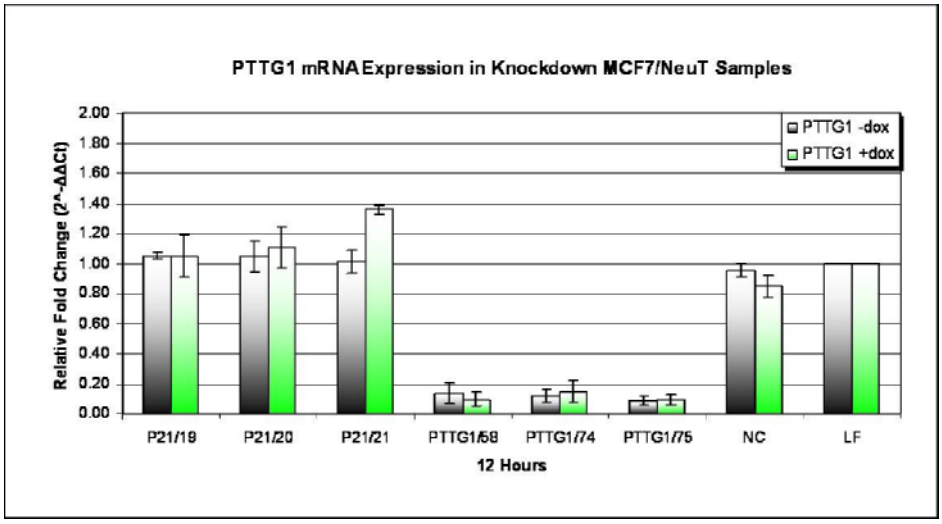

Figure A9: PTTG1 mRNA expression in knockdown MCF7/NeuT samples at 12h dox incubation. PTTG1 siRNA oligoribonucleotides showed an average of 90% knockdown efficiency (samples PTTG1/58 – PTTG1/75). Other samples showed PTTG1 expression relative to each other at much higher levels. 2^-ΔΔCt values represent an average of 3 independent experiments. NC – non-sense oligoribonucleotide); LF – transfection agent.

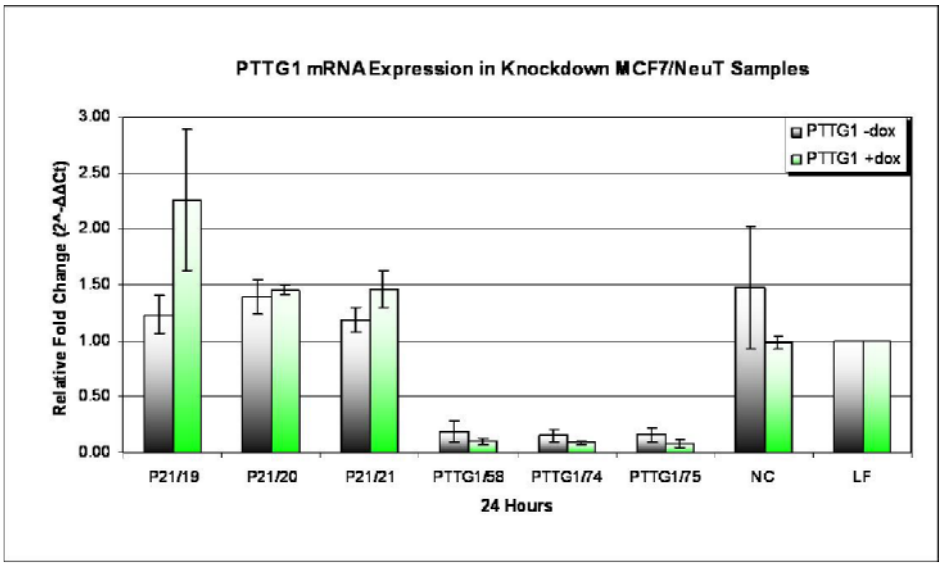

Figure A10: PTTG1 mRNA expression in knockdown MCF7/NeuT samples at 24h dox incubation. PTTG1 siRNA oligoribonucleotides showed an average of 90% knockdown efficiency (samples PTTG1/58 – PTTG1/75). Other samples showed PTTG1 expression relative to each other at much higher levels. 2^-ΔΔCt values represent an average of 3 independent experiments. NC – non-sense oligoribonucleotide); LF – transfection agent.

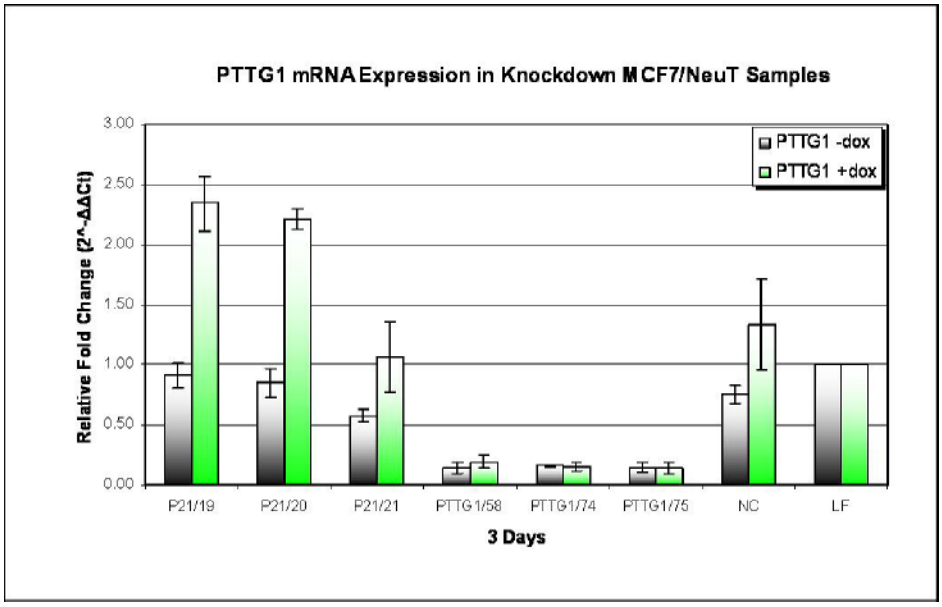

Figure A11: PTTG1 mRNA expression in knockdown MCF7/NeuT samples at 3d dox incubation. PTTG1 siRNA oligoribonucleotides showed an average of 80% knockdown efficiency (samples PTTG1/58 – PTTG1/75). Other samples showed PTTG1 expression relative to each other at much higher levels. 2^-ΔΔCt values represent an average of 3 independent experiments. NC – non-sense oligoribonucleotide); LF – transfection agent.

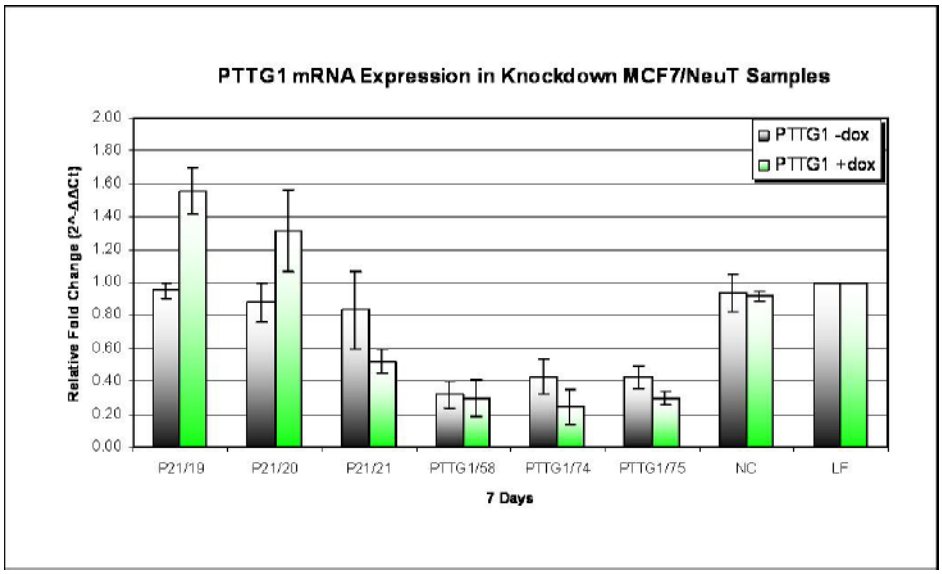

Figure A12: PTTG1 mRNA expression in knockdown MCF7/NeuT samples at 7d dox incubation. PTTG1 siRNA oligoribonucleotides showed an average of 70% knockdown efficiency (samples PTTG1/58 – PTTG1/75). Other samples showed PTTG1 expression relative to each other at much higher levels. 2^-ΔΔCt values represent an average of 3 independent experiments. NC – non-sense oligoribonucleotide); LF – transfection agent.

Appendix 6: mRNA Efficiency Graphs of CYCS siRNA Oligoribonucleotides in Knockdown MCF7/NeuT Samples at 10nM and 30nM Concentrations

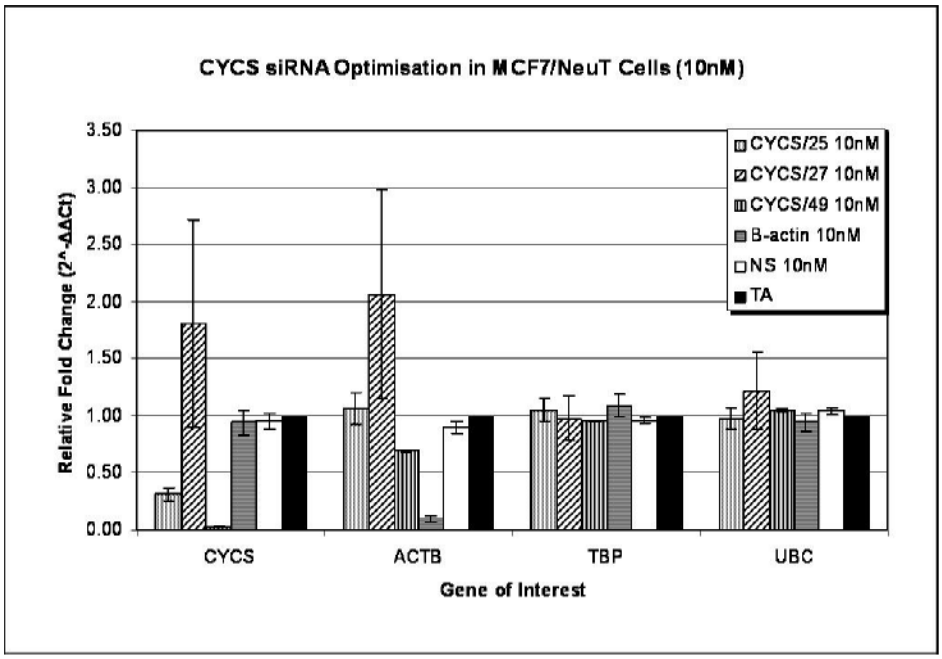

Figure A13: CYCS siRNA optimisation in MCF7/NeuT cells (10nM). Relative fold change values for CYCS (CYCS/25, CYCS/27, CYCS/49), beta-actin (β-actin) and nonsense (NS) siRNA oligoribonucleotides at 10nM final concentrations and transfection agent only (TA) samples. Gene expression was measured for CYCS, β-actin (ACTB) and the reference genes TBP and UBC. CYCS varied across oligoribonucleotides ranging from 90% knockdown efficiency to 60%. ACTB for positive control knockdown efficiency was found to be >80%.

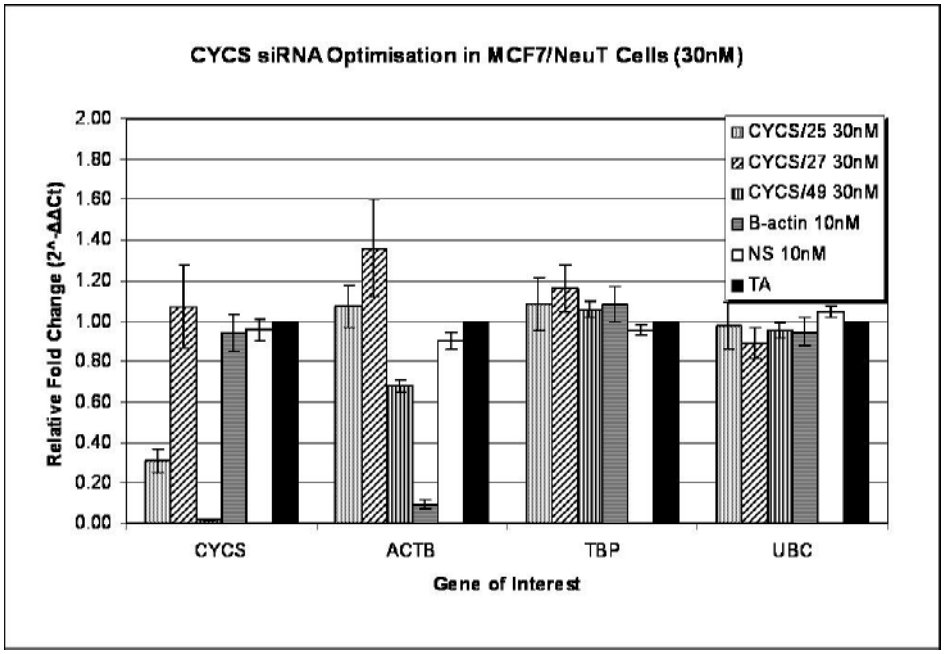

Figure A14: CYCS siRNA optimisation in MCF7/NeuT cells (30nM). Relative fold change values for CYCS (CYCS/25, CYCS/27, CYCS/49), beta-actin (β-actin) and nonsense (NS) siRNA oligoribonucleotides at 30nM final concentrations and transfection agent only (TA) samples. Gene expression was measured for CYCS, β-actin (ACTB) and the reference genes TBP and UBC. CYCS varied across oligoribonucleotides ranging from 90% knockdown efficiency to 70%. ACTB for positive control knockdown efficiency was found to be >80%.

C U R R I C U L U M V I T A E

Lindsey J Maccoux, AMSB

DATE OF BIRTH: **OCTOBER 9TH, 1981**
PLACE OF BIRTH: **GREEN BAY, WISCONSIN USA**
NATIONALITY: **AMERICAN**

EDUCATION:

Technical University of Dortmund, Dortmund, Germany

PhD - Molecular Investigation of ErbB2 Induced Oncogenic Cellular Senescence
October 2006 – *anticipated end date* **December 2009**
Principal research aims to identify eligible biomarkers for reversibility of senescent breast carcinoma cells by investigating intracellular interactions using both qualitative and quantitative methods. Research is carried out at the Institute for Analytical Sciences (ISAS) and the Leibniz Research Centre for Working Environment and Human Factors (IfADo) at the Technical University of Dortmund; Dortmund, Germany.

The University of Manchester, Manchester, England

MSc (Merit) - Immunology and Immunogenetics
September 2005 - September 2006
Dissertation – "Identification of reference genes and analysis of cytokine expression in canine osteoarthritic tissues". Research was carried out at the Manchester Interdisciplinary Biocentre, Manchester and the Faculty of Veterinary Science, University of Liverpool, U.K.

St. Norbert College, De Pere, Wisconsin, U.S.A

BS - Biology Major, Chemistry Minor
August 2000 - May 2004
Emphasis in genetics and molecular biology. Grade point average - 3.10/4.0

AFFILIATIONS:

- American Association for Cancer Research (AACR) Associate Member, November 2009 - present
- Society of Biology (SoB) Associate member, December 2008 - present
- European Association for Cancer Research (EACR) Active member, July 2008 - present
- Royal Society of Chemistry (RSC) Affiliate member, July 2007-present

PUBLICATIONS:

- Petry, I.B., Fieber, E., Schmidt, M., Gehrmann, M., Gebhard, S., Hermes, M., Schormann, W., Selinski, S., Freis, E., Schwender, H., Brulport, M., Ickstadt, K., Rahnenführer, J., Maccoux, L., West, J., Kölbl, H., Schuler, M., Hengstler, J.G. *ERBB2 induces an anti-apoptotic expression pattern of Bcl-2 family members in node negative breast cancer.* Clinical Cancer Research. 2009 [accepted].
- Casdenas, C., Franckenstein, D., Schmidt, M., Gehrmann, M., Hermes, M., Geppert, B., Schormann, W., Maccoux, L., Schumann, A., Wilhelm, C., Freis, E., Ickstadt, K., Rahnenführer, J., Baumback, J.I., Sickmann, A., Hengstler, J.G. *Role of thioredoxin reductase 1 (TXNRD1) and thioredoxin interacting protein (TXNIP) in prognosis of breast cancer*. Cancer Research. 2009 [in press].
- Mariani, M.M., Maccoux, L.J., Matthäus, C., Diem, M., Hengstler, J.G., Deckert, V. *Nuclear membrane lipid fluctuations in senescent epithelial breast cancer cells.* Anal Chem. 2009 [submitted].
- Maccoux, L.J., Mariani, M.M., Matthäus, C., Diem, M., Deckert, V., Hengstler, J.G. *Single cell analysis of senescent breast cancer carcinoma cells using confocal Raman micro-spectroscopy*. Proceedings from the 100th Annual Meeting for the American Association for Cancer Research. American Association for Cancer Research [Supplement]. 2009. April: Vol. 50.
- Maccoux, L.J., Hermes, M., Mariani, M., Manz, A., Franzke, J., Hengstler, J., West, J. *Cell-cell communications in a breast cancer senescence model*. Proceedings from the 20th Meeting of the European Association for Cancer Research. European Journal of Cancer [Supplement]. 2008. Jul: 6(9).
- Maccoux, L.J., Salway, F., Day, P.J.R., Clements, D.N. *Expression profiling of select cytokines in canine osteoarthritis tissues*. Vet Immunol Immunopath. 2007. Jul 15; 118(1-2):59-67.
- Maccoux, L.J., Clements, D.N., Salway, F., Day, P.J.R. *Identification of New Reference Genes for the Normalisation of Canine Osteoarthritic Joint Tissue Transcripts from Microarray Data*. BMC Mol Biol. 2007. Jul 25; 8(1):62.

PRESENTATIONS AND POSTERS:

- Maccoux, L.J. *Oncogenic-induced senescence via the tyrosine kinase receptor ErbB2* [presentation]. Invited speaker to the University of Manchester and the Paterson Institute for Cancer Research. Manchester, UK. October 2009.
- Maccoux, L.J., Mariani, M.M., Matthäus, C., Diem, M., Deckert, V., Hengstler, J.G. *Single cell analysis of senescent breast cancer carcinoma cells using confocal Raman micro-spectroscopy* [poster]. The 100th Annual Meeting for the American Association for Cancer Research. Denver, Colorado, USA. April 2009.
- Maccoux, L.J., Hermes, M., Mariani, M.M., Brulport, M., Frimat, J.P., Franzke, J., Hengstler, J.G., West, J. *Cell–cell communication in a Breast Cancer Model* [poster]. European Association for Cancer Research 20th biannual conference. Lyon, France. July 2008.
- Maccoux, L.J., Salway, F., Mariani, M., Clements, D.N., Day, P.J.R. *Use of Synthetic Template Oligonucleotides (TOs) for Absolute Quantification of Transcripts in Canine Osteoarthritis* [poster]. qPCR International Symposium 2007. Munich, Germany. March 2007.

COLLABORATIONS:

- Mariani, M.M., Maccoux, L.J., Matthäus, C., Diem, M., Hengstler, J.G., Deckert, V. *Raman Imaging and Multivariate Analysis of Senescent Breast Carcinoma Cells* [poster]. ANAKON 2009. Berlin, Germany. (*Received 2nd place in poster competition).*
- Selinski, S., Freis, E., Krahn, U., Schmidt, M., Gehrmann, M., Hermes, M., Maccoux, L., West, J., Schwender, H., Hengstler, J.G., Ickstadt, K. *Survival Analysis on the Basis of Mutagenes Using Cluster and Promoter Analysis* [talk]. 55th Biometrisches Kolloquium (2009). Hannover, Germany.
- West, J., Kittel, S., Frimat, J.P., Maccoux, L., Michels, A., Franzke, J. *Fluidic Control Using Contrasting Energy Patterns* [poster]. International Symposium on Micro Scale Bioseparations 2008. Berlin, Germany.

ATTENDED CONFERENCES:

- 100th Annual Meeting of the American Association for Cancer Research; Denver, Colorado, USA; April 2009.
- European Association for Cancer Research 20th biannual conference; Lyon, France; July 2008.
- 22nd International Symposium on Micro Scale Bioseparations 2008; Berlin, Germany; March 2008 (*hosted*).
- qPCR International Symposium 2007; Munich, Germany; March 2007.

WORK EXPERIENCE:

Institute for Analytical Sciences (ISAS) Dortmund, Germany, October 2006 - Present
***Scientific Assistant* –** Coordinated laboratory set-up of a new molecular research lab, equipment purchasing, established supplier contacts for consumable ordering and managed laboratory maintenance.

LABORATORY EXPERIENCE:

- Polymerase Chain Reactions (PCR, RT-qPCR)
- Fluorescence Microscopy and Video Imaging
- Gene Silencing (siRNA)
- Genetic Analysis and Interpretation
- Fluorescent-Activated Cell Sorting Analysis and Interpretation
- Immunoblotting and Immunofluorescence
- Tissue Collection

OTHER SKILLS:

- Invited peer reviewer for *BMC Molecular Biology*
- Training of fellow scientists in RT-qPCR and related software techniques.
- Computer skills: MS Office©, SPSS©, GeneDoc, Adobe®Photoshop®, Olympus Fluoview™ imaging software